ENVIRONMENTAL ENGINEERING
ASSOCIATION OF THAILAND

THAI ENVIRONMENTAL ENGINEERING JOURNAL

Vol. 38 No. 3 September – December 2024
ISSN (PRINT) : 1686 - 2961
ISSN (ONLINE) : 2673 - 0359

Thai Environmental Engineering Journal

Owner
Environmental Engineering Association of Thailand

Enquiries 122/4 Soi Rawadee, Rama IV Rd., Phayathai, Phayathai, Bangkok 10400

ENVIRONMENTAL ENGINEERING
ASSOCIATION OF THAILAND

Thai Environmental Engineering Journal

Vol. 38 No. 3 September – December 2024

ISSN (PRINT) : 1686 - 2961
ISSN (ONLINE) : 2673 - 0359

Thai Environmental Engineering Journal Vol. 38 No. 3 (2024) : 1-10
www.eeat.or.th

Environmentally Friendly Manufacturing of Fly Ash Geopolymer Mortar

Thanudkij Chareerat[1], Sarawut Chaungchot[1], Santiphap Bussabin[1], Vatwong Greepala[2] and Krit Sriworamas[1*]

[1]Faculty of Engineering, Ubon Ratchathani University, Ubon Ratchathani 34190, Thailand
[2]Faculty of Science and Engineering, Kasetsart University, Sakon Nakhon 47000, Thailand
[*]E-mail : krit.s@ubu.ac.th

Article History; *Received: 24 July 2024, Accepted: 4 October 2024, Published: 24 December 2024*

Abstract

This research presents the environmentally friendly manufacturing (green manufacturing) of geopolymer mortar, focusing on the unit weight and compressive strength of geopolymer made from Mae Moh fly ash from Lampang Province. Graded sand in a dry condition was used in this investigation. The fly ash/sand ratio was set at 1:2.75. Sodium hydroxide (NaOH) and potassium hydroxide (KOH) solutions were used at concentrations of 2.5, 5, and 7.5 molars (M), respectively. The ratios of Na_2SiO_3/NaOH and Na_2SiO_3/KOH were controlled at 0.5:1, 1:1, and 2:1, respectively. The solution/fly ash ratio was set at 0.6. The temperatures for curing the geopolymer mortar were controlled at 30°C and 60°C, respectively. The compressive strength test of geopolymer mortar was conducted at the ages of 7, 28, and 56 days, respectively. Tap water was used to mix the geopolymer mortar, similar to that used in cement mortar for strength comparison.

The results indicated that the concentration of the alkaline solution can affect the rate of polymerization. Higher concentrations can lead to faster polymerization such as at a NaOH concentration of 7.5 M and a Na_2SiO_3/NaOH ratio of 1:1, a maximum compressive strength of 210 ksc was obtained at 56 days of testing (after 1 day of curing at 60°C). Similarly, at a KOH concentration of 7.5 M and a Na_2SiO_3/KOH ratio of 1:1, a maximum compressive strength of 240 ksc was obtained at 56 days of testing (after 1 day of curing at 60°C). Comparatively, the compressive strength of samples mixed with KOH solution was a bit higher than those mixed with NaOH solution. Furthermore, elevated curing temperatures can accelerate the geopolymerization process, enhancing strength in a shorter time frame. As it was clearly found that heat curing at 60°C provided higher compressive strength than curing at room temperature (30°C). Nevertheless, due to the aspect of environmentally friendly manufacturing of geopolymer mortar, a curing temperature close to room temperature (approximately 30°C) can yield a reasonable compressive strength within the range of 160-220 ksc, when stored in air for duration of 56 days, therefore, lengthening the curing time results in higher strength, as it allows more complete polymerization which contributes to the density and interconnectivity of geopolymer structure.

Keywords : Geopolymer; unit weight; strength; fly ash

Introduction

Geopolymers are materials that resemble cement but are produced from non-fossil fuel raw materials. They utilize materials containing silica and alumina in the form of industrial waste, such as fly ash from coal combustion or blast furnace slag from steel manufacturing. Additionally, alternative natural materials, such as metakaolin or natural pozzolans, are also available. Geopolymers have found applications in various industries, including construction, the production of environmentally friendly building materials, and waste management.

Geopolymers are environmentally friendly due to their use of recycled materials and generates significantly lower CO_2 emissions than traditional cement due to the lower calcination temperatures [1], exhibit superior resistance to chemical attacks, including acids and sulfates, making them ideal for harsh environments [2], and typically demonstrate high compressive strength comparable to or exceeding traditional cement-based materials. Studies have shown that strength can be influenced by factors such as raw material composition, curing temperature, and age [3]. However, challenges and concerns surrounding geopolymers include limited knowledge and research, leading to potential misuse due to inadequate education and training. Additionally, there are questions about their long-term durability and stability, necessitating further investigation. Lastly, while geopolymers are environmentally friendly, high production costs may impede their competitiveness in certain markets.

According to the Cement manufacturing process which significantly contributes to environmental pollution by emitting gases that exacerbate the greenhouse effect (Green House Gas; GHG), totaling 13,500 million tons per year, or approximately 7% of all global emissions. Consequently, there is an effort to reduce the use of Portland cement. This includes the development of concrete with high pozzolan content or the production of cementitious material that entirely eliminates Portland cement. One such alternative is geopolymer material [4-5]. Geopolymer is a type of cementitious material made from pozzolans, such as fly ash and calcined kaolin (metakaolin), which are rich in silica (Si) and alumina (Al). The fundamental principle of geopolymer involves a chemical reaction between silica and alumina to form polymer chains. This reaction is facilitated by a highly alkaline solution. When mixed with an alkali hydroxide solution and sodium silicate solution, and catalyzed with heat or thermal stimulation, a strong cementitious material is produced [6-8]. This material can achieve the same strength as conventional cement. The development of geopolymer not only represents an engineering advancement but also helps mitigate environmental pollution and combat global warming, a critical issue today.

This research, therefore, presents the environmentally friendly manufacturing of geopolymer mortar using Mae Moh fly ash as the primary local raw material. The study investigates the effects of varying concentrations of two types of alkali hydroxide solutions i.e. sodium hydroxide and potassium hydroxide on the unit weight and compressive strength of geopolymer mortar. The mortar was cured at room temperature (30°C) without heat energy consumption and at elevated temperature (60°C) with heat energy consumption.

Methodology

Fly ash from the Mae Moh Power Plant in Lampang Province, characterized by an average particle size of 30.4 microns and a specific gravity (S.G.) of 2.23, was utilized in this study. The Mae Moh fly ash exhibited a brownish-gray coloration and displayed a solid spherical morphology with a smooth surface [9-10]. The chemical composition of the fly ash, as analyzed using X-ray Fluorescence (XRF), revealed that it consists primarily of SiO_2, Al_2O_3, Fe_2O_3, and CaO, which collectively account for approximately 88 percent of its total composition. Furthermore, when focusing specifically on the primary compounds, SiO_2, Al_2O_3, and Fe_2O_3 constitute about 69 percent. Consequently, this fly ash is classified as Class C fly ash according to the ASTM C 618 standards. The detailed chemical composition of Mae Moh fly ash is presented in Table 1.

Table 1 Chemical composition of fly ash analyzed by X-ray fluorescence (XRF)

Chemical composition of fly ash	
Silicon Dioxide, SiO_2 (%)	32.10
Aluminum Oxide, Al_2O_3 (%)	19.90
Iron Oxide, Fe_2O_3 (%)	16.91
Calcium Oxide, CaO (%)	18.75
Magnesium Oxide, MgO (%)	3.47
Sodium Oxide, Na_2O (%)	0.69
Potassium Oxide, K_2O (%)	2.38
Sulfur Trioxide, SO_3 (%)	2.24
Loss On Ignition, LOI (%)	0.07

Test Method

1. Calculation of molarity (molar)

Molarity, often referred to as molar concentration, is a unit that quantitatively expresses the concentration of a solute in a solution. It is defined as the ratio of the number of moles of solute to the volume of the solution in liters (L). Molarity is denoted by the symbol 'M' and is expressed in units of moles per liter (mol/L), as represented by the following formula:

$$\text{Molar (M)} = \frac{\text{Number of moles of solute (mol)}}{\text{Volume of solution (L)}}$$

2. Manufacturing of geopolymer mortar

The mix proportions of the geopolymer are detailed in Tables 2 and 3, respectively. The process for manufacturing geopolymer mortar and procedure for mixing geopolymer mortar samples using a mortar mixer is outlined as follows [11]:

1) Place the measured quantities of fly ash and sand into the mixer, and mix for a duration of 2-3 minutes.
2) Mix the sodium hydroxide solution, as prepared in Table 4, with added water thoroughly for an additional 2 minutes. Subsequently, incorporate the sodium silicate solution and continue mixing for a further 5 minutes.
3) Replace the sodium hydroxide solution with potassium hydroxide solution, and then repeat steps 1 and 2.

3. Casting of geopolymer mortar

1) Pour the fresh geopolymer mortar into the test mold in two layers. The first layer should be approximately 25 mm thick. Subsequently, stir the mixture 16 times within a period of 10 seconds, and then pour the remaining geopolymer mortar into the mold. Repeat the aforementioned process for the second layer.
2) Utilize a steel trowel to remove any excess fresh geopolymer mortar that has overflowed onto the edges of the mold, ensuring that the surface is smooth.

4. Curing and storage method

The cast geopolymer mortar should be wrapped in plastic film and subsequently maintained at room temperature (30°C) for duration of 1 hour. Following this initial period, certain samples of the geopolymer mortar were cured at room temperature (30°C) for an additional 24 hours, while others were subjected to heat in an oven at 60°C for the same duration. After the 24-hour curing period, the geopolymer mortar samples were removed from the molds and stored at room temperature (30°C) until they were tested for compressive strength at 7, 28, and 56 days of age, respectively.

5. Compressive strength test of geopolymer mortar

The compressive strength was evaluated following ASTM C109 standard; compressive strength tests determine the load-bearing capacity of the mortar using a compressive strength testing machine at 7, 28, and 56 days, resulting in a total of 324 samples. These samples were categorized into two groups: 162 samples derived from sodium hydroxide (NaOH) solution (with 81 samples cured at 30°C and 81 samples cured at 60°C) and 162 samples derived from potassium hydroxide (KOH) solution (with 81 samples cured at 30°C and 81 samples cured at 60°C).

Table 2 Mix proportions of geopolymer using sodium hydroxide solution with 1,650 g of sand and 600 g of fly ash

Concentration (M)	Na_2SiO_3 (g)	NaOH (g)	Added water (g)	Na_2SiO_3/NaOH solution ratio	Solution to fly ash ratio
2.5	120	240	69	0.5	0.6
	180	180	71	1	0.6
	240	120	124	2	0.6
5	120	240	98	0.5	0.6
	180	180	97	1	0.6
	240	120	138	2	0.6
7.5	120	240	127	0.5	0.6
	180	180	123	1	0.6
	240	120	153	2	0.6

Table 3 Mix proportions of geopolymer using potassium hydroxide solution with 1,650 g of sand and 600 g of fly ash

Concentration (M)	Na_2SiO_3 (g)	KOH (g)	Added water (g)	Na_2SiO_3/ KOH solution ratio	Solution to fly ash ratio
2.5	120	240	69	0.5	0.6
	180	180	71	1	0.6
	240	120	124	2	0.6
5	120	240	98	0.5	0.6
	180	180	97	1	0.6
	240	120	138	2	0.6
7.5	120	240	127	0.5	0.6
	180	180	123	1	0.6
	240	120	153	2	0.6

Table 4 Weight of substances used in each concentration

Substances	Concentration / solution 1 liter		
	2.5 M	5 M	7.5 M
Sodium hydroxide	100 g	200 g	300 g
Potassium hydroxide	140 g	280 g	420 g

Results and Discussion

1. Unit weight test

Based on the conducted tests, it was found that the ratios of sodium silicate solution to sodium hydroxide solution, as well as the ratios of sodium silicate solution to potassium hydroxide solution, at concentrations of 2.5, 5, and 7.5 M had minimal impact on the unit weight of the geopolymer. In contrast, the variables that significantly influenced the unit weight of the geopolymer were the testing age and the curing temperature. As illustrated in Figure 1, the unit weight measurements taken during the first 7 days indicated an average value of 2.23. However, upon examination at 28 days, the unit weight value decreased slightly to 2.22, with subsequent measurements showing minimal further reduction. Notably, curing at room temperature produced a higher unit weight compared to curing at elevated temperatures of 60 °C. An overall results of this investigation yielded average geopolymer unit weight of 2.22.

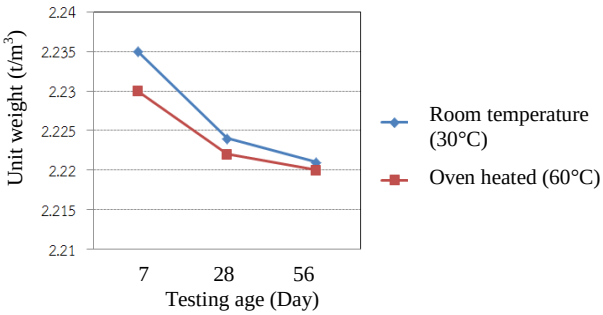

Figure 1 Relationship between unit weight and testing age of geopolymer

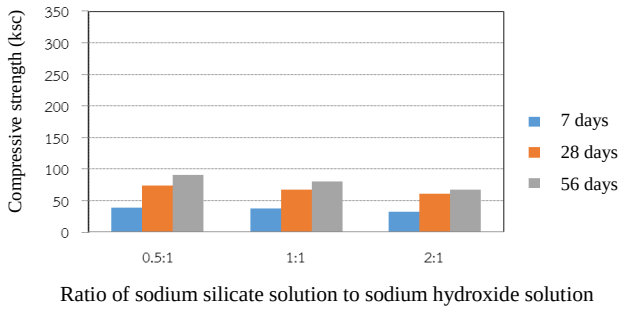

Figure 2 Relationship between compressive strength and the ratio of sodium silicate solution to sodium hydroxide solution cured at 30°C

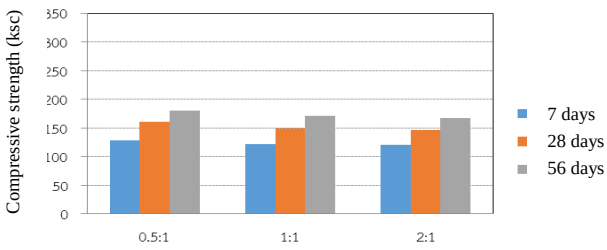

Figure 3 Relationship between compressive strength and the ratio of sodium silicate solution to sodium hydroxide solution cured at 60°C

2. Compressive strength test

2.1 Sodium silicate to sodium hydroxide solution ratio

From the initial seven days of testing, it was observed that the compressive strength values of the ratios 0.5:1 and 1:1 were comparable, both achieving a strength of 40 ksc, while the ratio of 2:1 exhibited the lowest compressive strength at 32 ksc. Further assessment of compressive strength conducted at 28 and 56 days revealed that the 0.5:1 ratio yielded the highest compressive strength at 91 ksc. When comparing the solution ratios of 1:1 and 2:1, both cured at 30°C, as illustrated in Figure 2, it was noted that the trends in compressive strength development remained similar when the geopolymer was subjected to testing at 60°C. Specifically, the 0.5:1 ratio consistently provided the highest compressive strength, while the 2:1 ratio produced the least, as depicted in Figure 3. Consequently, the optimal ratio of the geopolymer synthesized from sodium hydroxide solution was determined to be 0.5:1 to 1:1. This finding aligns with the research conducted by Chindaprasirt et al. (2007) [12], which investigated the fundamental properties of workability and compressive strength of geopolymers derived from high-calcium fly ash. Their study noted that the flow capacity ranged from 105% to 140%, and recommended a ratio of sodium silicate solution to sodium hydroxide solution between 0.67 and 1.0 to achieve satisfactory compressive strength.

2.2 Sodium silicate to potassium hydroxide solution ratio

Development of compressive strength in geopolymer over a period of 7 days, utilizing ratios of 0.5:1, 1:1, and 2:1, revealed a consistent trend in compressive strength development across the different formulations. Further testing conducted at intervals of 28 and 56 days indicated that the geopolymer mixture with a ratio of 1:1 exhibited the highest compressive strength, while the 2:1 ratio resulted in the lowest compressive strength, as illustrated in Figure 4.

Moreover, compressive strength testing of the geopolymer cured at 60°C demonstrated that its performance during the first 7 days surpassed that of samples cured at room temperature (30°C), yielding a difference of approximately 90 ksc. Evaluating the compressive strength values at 28 and 56 days post-curing revealed that the 1:1 geopolymer ratio consistently provided the highest compressive strength. In contrast, the compressive strength values for the 0.5:1 and 2:1 ratios were comparable, as depicted in Figure 5.

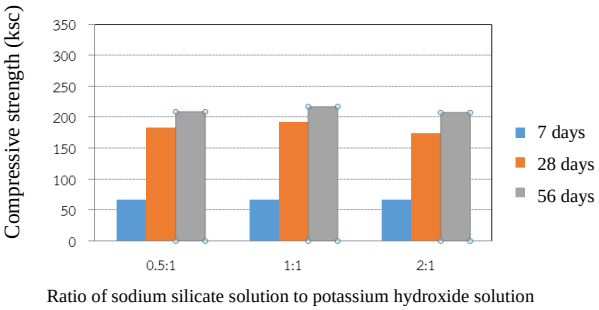

Figure 4 Relationship between compressive strength and the ratio of sodium silicate solution to potassium hydroxide solution cured at 30°C

Therefore, it can be concluded that the optimal ratio for the geopolymer synthesized from potassium hydroxide solution, based on the results obtained during this study, is 1:1. This finding aligns with the research conducted by Hardjito and Tsen (2008) [13], who explored geopolymers synthesized from fly ash using potassium silicate and potassium hydroxide solutions. Their findings indicate that the effectiveness of potassium hydroxide solution as a stimulant for compressive strength is contingent upon the concentration of the solution, similarly to the effects observed with high-concentration sodium hydroxide solutions. Hardjito and Tsen recommended that the ratio of potassium silicate solution to potassium hydroxide solution should be maintained within the range of 0.8 to 1.5 to ensure optimal compressive strength performance.

2.3 Concentration of sodium hydroxide solution

Based on the test results of geopolymers exposed to sodium hydroxide solutions at concentrations of 2.5 M, 5.0 M, and 7.5 M, it was observed that the compressive strength of the geopolymer exhibited direct variation relationship with the concentration of the solution. In compressive strength tests conducted on geopolymers aged for 7 days, the lowest compressive strength was recorded at a concentration of 2.5 M, whereas the highest compressive strength was observed at a concentration of 7.5 M. However, the difference in compressive strength between these concentrations was minimal, amounting to only 5 ksc. Upon evaluating the compressive strength of geopolymers aged 28 days, it was reaffirmed that the solution concentration of 7.5 M yielded the highest compressive strength. Similarly, after testing geopolymers aged 56 days, the concentration of 7.5 M once again resulted in the highest compressive strength, particularly when cured at 30°C, as illustrated in Figure 6. Furthermore, when subjected to heating at 60°C, it was determined that geopolymers tested after 7 days exhibited higher compressive strength across all solution concentrations compared to those cured at 30°C, with the values obtained from samples aged 28 and 56 days corroborating this finding. Notably, the geopolymer produced at a concentration of 7.5 M displayed higher compressive strength when compared to those at concentrations of 2.5 M and 5.0 M, as demonstrated in Figure 7.

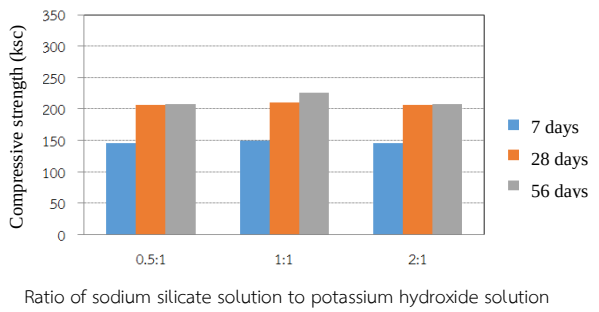

Figure 5 Relationship between compressive strength and the ratio of sodium silicate solution to potassium hydroxide solution cured at 60°C

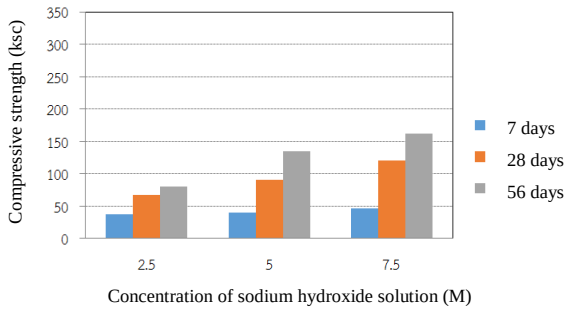

Figure 6 Relationship between compressive strength and concentration of sodium hydroxide solution at 30°C

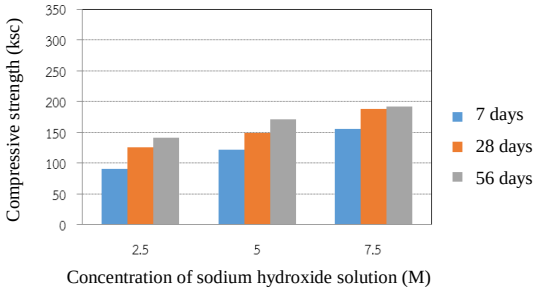

Figure 7 Relationship between compressive strength and concentration of sodium hydroxide solution at 60°C

2.4 Concentration of potassium hydroxide solution

Based on the test results of geopolymer constructed with potassium hydroxide solutions at concentrations of 2.5, 5.0, and 7.5 M, it was observed that the variation in compressive strength over the initial 7 days of testing was minimal in comparison to the concentration of the potassium hydroxide solution. The compressive strength values were similar, averaging approximately 65 ksc. However, during the curing periods of 28 days and 56 days, the trends indicated that compressive strength exhibited a direct variation relationship with increasing concentrations of potassium hydroxide solution, particularly at a concentration of 7.5 M. The sample cured for 56 days at 30 °C achieved a maximum compressive strength of 217 ksc, as illustrated in Figure 8. In contrast, samples cured at a temperature of 60 °C demonstrated consistently superior compressive strength across all concentrations, with the highest compressive strength recorded at 240 ksc, as shown in Figure 9. For comparison purposes, a sodium silicate to sodium hydroxide solution ratio of 1:1 and a solution to fly ash ratio of 0.6 were utilized.

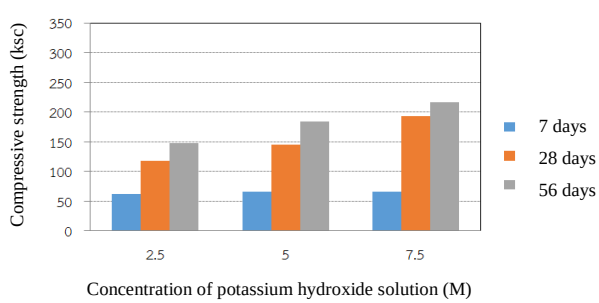

Figure 8 Relationship between compressive strength and concentration of potassium hydroxide solution at 30°C

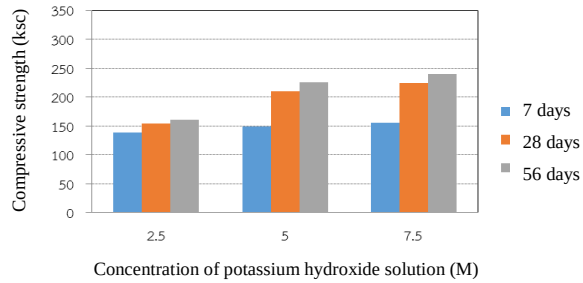

Figure 9 Relationship between compressive strength and concentration of potassium hydroxide solution at 60°C

2.5 Development of compressive strength of geopolymer using sodium hydroxide solution as a catalyst

Based on the testing, it was found that the compressive strength of geopolymer mortar developed with a 2.5 M concentration exhibited the lowest compressive strength, while a sodium hydroxide solution with a concentration of 7.5 M provided the highest compressive strength across all curing durations, as illustrated in Figure 10. The samples exhibiting the highest compressive strength during each curing period are illustrated in Figure 10, which compares the performance of samples with a sodium silicate solution to sodium hydroxide solution ratio of 1.0 and a solution to fly ash ratio of 0.6.

Curing the samples at a temperature of 60°C significantly accelerated the reaction, leading to improved compressive strength compared to curing at 30 °C. Notably, the rate of compressive strength development was most pronounced at 7 days of age when compared to the samples cured at 30°C, with a subsequent decrease in strength gain observed at 28 days testing. After 28 days, the increase in compressive strength was less pronounced, as depicted in Figure 11, which compares samples with a sodium silicate solution to sodium hydroxide solution ratio of 1:1 and a solution to fly ash ratio of 0.6.

2.6 Development of compressive strength of geopolymer using potassium hydroxide solution as a catalyst

Based on evaluations conducted using potassium hydroxide solution as a catalyst, the findings indicate that the development of compressive strength in geopolymer mortar is influenced by the concentration of the catalyst.

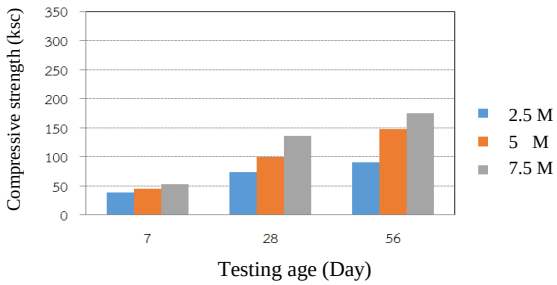

Figure 10 Relationship between compressive strength and testing age of geopolymer using sodium hydroxide solution at curing temperature of 30°C

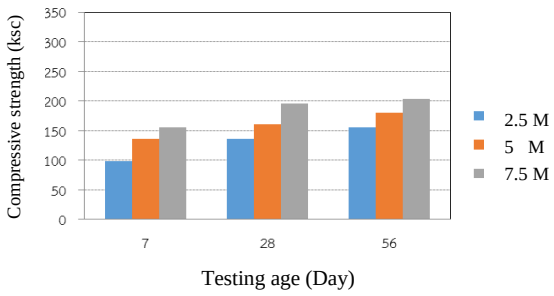

Figure 11 Relationship between compressive strength and testing age of geopolymer using sodium hydroxide solution at curing temperature of 60°C

Specifically, a potassium hydroxide concentration of 2.5 M resulted in the lowest compressive strength, while a concentration of 7.5 M yielded the highest compressive strength. After a testing of 7 days, compressive strength values were found to be quite similar across all concentrations, averaging approximately 61 ksc, as illustrated in Figure 12. These samples were compared using a sodium silicate solution to sodium hydroxide solution ratio of 1.0, along with a solution to fly ash ratio of 0.6.

Curing the samples at 60°C accelerated the chemical reactions, leading to an enhancement in compressive strength compared to the ambient temperature of 30 °C. The rate of compressive strength development was notably higher at 7 days in case of curing at 60°C compared to those cured at 30°C, although this rate experienced a decline when the samples were tested at 28 days. After 28 days, the increase in compressive strength diminished, with the maximum compressive strength reaching 240 ksc. Samples incubated for 56 days at a concentration of 7.5 M demonstrated this improvement, as depicted in Figure 13. The analyses conducted also involved comparing samples based on a sodium silicate solution to sodium hydroxide solution ratio of 1.0 and a solution to fly ash ratio of 0.6.

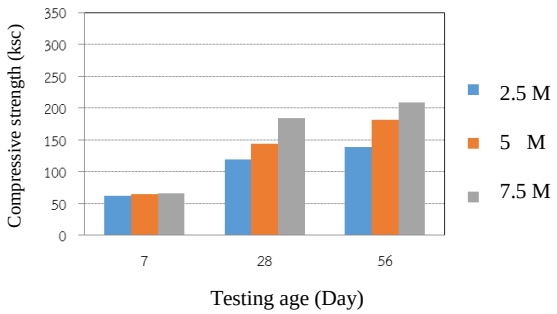

Figure 12 Relationship between compressive strength and testing age of geopolymer using potassium hydroxide solution at curing temperature of 30°C

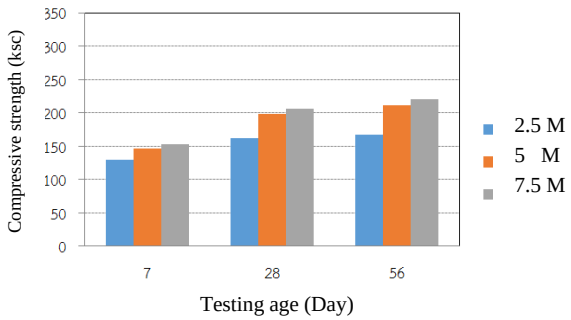

Figure 13 Relationship between compressive strength and testing age of geopolymer using potassium hydroxide solution at curing temperature of 60°C

2.7 Comparison of compressive strength between geopolymer mortars made from sodium hydroxide solution and potassium hydroxide solution and cement mortar

The test results indicated that the compressive strength of geopolymer mortar formulated with sodium hydroxide solution is approximately 10% lower than that of geopolymer mortar produced with potassium hydroxide solution. Furthermore, when comparing the geopolymer mortar with the

highest compressive strength to cement mortar, it was demonstrated that the geopolymer mortar achieved approximately 80% of the maximum compressive strength of the cement mortar. This is illustrated in Figure 14, which presents the comparison of a sodium silicate solution ratio to a sodium hydroxide solution of 0.5, a sodium hydroxide solution concentration of 7.5 M, as well as a sodium silicate to potassium hydroxide solution ratio of 1.0, with a potassium hydroxide solution concentration also set at 7.5 M, yielding the highest compressive strength among the geopolymer samples.

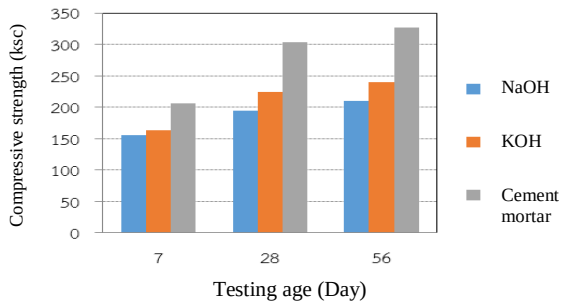

Figure 14 Relationship between compressive strength and testing age of geopolymer and cement mortar

Conclusions

Sodium hydroxide and potassium hydroxide solutions with concentrations of 2.5, 5, and 7.5 M exhibited varying in compressive strengths. The results indicated that compressive strength increased with higher concentrations of the solutions. The optimal compressive strength was achieved with a 1:1 ratio of sodium silicate solution to both sodium hydroxide and potassium hydroxide solutions.

Furthermore, geopolymer constructed using potassium hydroxide solution demonstrated approximately a 10% higher compressive strength compared to those made with sodium hydroxide solution across all tested ages. Additionally, curing at a temperature of 60°C resulted in a more rapid increase in compressive strength than curing at 30°C. Nevertheless, due to the aspect of environmentally friendly manufacturing of geopolymer mortar, a curing temperature close to room temperature (approximately 30°C) can yield a reasonable compressive strength within the range of 160-220 ksc, when stored in air for duration of 56 days.

In conclusion, the manufacturing of fly ash geopolymer mortar employs environmentally friendly practices by managing waste through the utilization of fly ash from the Mae Moh electricity manufacturing Power Plant, which reduces industrial waste. It enhances energy efficiency by activating geopolymer at a low room temperature of 30°C, decreasing energy consumption compared to traditional methods. Additionally, it minimizes environmental impact by using lower concentrations of sodium hydroxide (2.5-5.0 M) instead of the typical 10-15 M [12], thereby reducing chemical hazards. Furthermore, advocating for geopolymer mortar as a sustainable alternative to traditional cement can significantly lower the carbon footprint in construction, promoting more sustainable building practices.

Acknowledgments

The researchers would like to express their gratitude to the Faculty of Engineering, Ubon Ratchathani University on their support of this research.

References

[1] Davidovits, J. 2011. Geopolymer chemistry and applications. Geopolymer Institute.

[2] Duxson, P., et al. 2007. Geopolymer technology: The current state of the art. Journal of Materials Science. 42(9): 3023-3035.

[3] Wang, H., et al. 2021. Mechanical properties of geopolymer composites: A review. Journal of Composites Science. 5(3): 78.

[4] Charin Senawong, Kietsuda Somna and Wichian Charlie. 2010. Compressive strength and bonding strength of geopolymer concrete from fly ash. Burapha Science Journal. 15: 13-22.

[5] Thanakorn Phungernkham. 2010. Study of compressive strength of geopolymer mortar from fly ash mixed with diatomite perlite and natural zeolite. Master of Engineering, Thesis in Civil

Engineering, School of Engineering, Suranaree University of Technology.

[6] Wichian Charlie and Ubonlak Rattanasak. 2009. Study of durability properties of geopolymer materials. From the ash bottom of the stove. Burapha Science Journal. 14(1): 47-55.

[7] Weeraphong Phikunprayong and Wanchai Yodsudjai. 2009. Properties of geopolymer mortar to develop into a repair material. 14th National Civil Engineering Conference, Suranaree University of Technology: 1801-1805.

[8] Thiensak Klapprasit, Samit Songpiriyakit and Chai Jaturapitakkul. 2006. Study of compressive strength of geopolymer paste made from rice husk ash and tree bark ash mixed with coal ash. Academic conference 2nd Annual Concrete, Udon Thani: MAT 53-58.

[9] Prinya Chindaprasirt and Chai Jaturapitakkul. 2004. Cement, pozzolan and concrete. Bangkok: Thai Concrete Association.

[10] Prinya Chindaprasirt and Intharachai Horwichit. 2005. Portland cement mixed with Mae Moh fly ash. Office of Technology for Rural Affairs. Faculty of Engineering, Khon Kaen University.

[11] Prinya Chindaprasirt, Thanudkij Chareerat, Waraporn Kunawanakit and Anuchart Luenansaksiri. 2005. Preliminary study of geopolymer production from Mae Moh fly ash. 1st Annual Concrete Academic Conference, Rayong: 13-18.

[12] Chindaprasirt, P., Chareerat, T. and Sirivivatnanon, V. 2007. Workability and strength of coarse high calcium fly ash geopolymer. Cement and Concrete Composites. 29(3): 224-229.

[13] Hardjito, D. and Tsen, M.Z. 2008. Strength and thermal stability of fly ash based geopolymer mortar. The 3rd International Conference - ACF/VCA. 144-150.

Thai Environmental Engineering Journal Vol. 38 No. 3 (2024) : 11-21
www.eeat.or.th

Synthesis of Cassava Rhizome Biochar for Methomyl Adsorption

Lalita Kamolklang[1], Pariyaporn Seekhumlek[1], Anusara Kaeokan[1] and Apichon Watcharenwong[1*]

[1]School of Environmental Engineering, Institute of Engineering,
Suranaree University of Technology, Nakhon Ratchasima 30000, Thailand
[*]E-mail : w.apichon@sut.ac.th

Article History; *Received: 31 May 2024, Accepted: 5 October 2024, Published: 24 December 2024*

Abstract

This research aims to study the synthesis of biochar from cassava rhizomes and the factors involved in the adsorption of methomyl. Methomyl is a carbamate pesticide. The factors of interest in the synthesis of biochar include the pyrolysis temperatures of 300, 400, and 500 °C and the pyrolysis time of 2.5 hours under nitrogen gas conditions, and the obtained biochar was modified with phosphoric acid to increase the efficiency of adsorption. The synthesized biochar was examined using various techniques, including CHN/O, BET, SEM, FTIR, and XTM. The factors of interest in the adsorption study include contact time, agitation speed, and pH value. The study found that the temperature and duration of pyrolysis affect biochar quality. The selected biochar was obtained at 500 °C for 2.5 hours with the highest %C of 78.149 and the lowest H/C of 0.026, similar to other research studies. The biochar is of high quality, has a stable C ratio, and a low H/C. A higher carbon content results in more stable biochar. Modifying biochar with phosphoric acid results in an increase in its physical and chemical properties. The specific surface area from BET measurement and the average pore diameter increased from 2.29 to 3.39 m^2/g and 1.57 to 6.54 Å, respectively. For methomyl adsorption experiments, it was found that equilibrium was reached after 180 minutes. The rotational speed and pH value affected the adsorption efficiency. The optimum condition for methomyl adsorption was an agitation speed of 200 rpm because it achieved the highest adsorption efficiency of 19.7%. Further agitation speed experiments revealed that turbulence is critical in controlling the solid-liquid mass transfer mechanism. The pH condition that resulted in the best adsorption was pH 3, with an efficiency of 27.90% and the highest adsorption capacity (qe) at 2.79 mg/g.

Keywords : biochar; cassava rhizomes; methomyl; pesticides; phosphoric acid

Introduction

Currently, the agricultural sector uses pesticides in farming, accumulating pesticides in the environment. When pesticide accumulation exceeds saturation, it will cause desorption from the soil. Pesticides are washed away by the leaching process of rain into natural water sources [1]. Pesticides contaminating natural water sources can accumulate in the food chain of living organisms in these water sources. Methomyl, a class I (restricted-use pesticide) according to the US EPA, is harmful to mammals, fish, and aquatic invertebrates. The high water solubility (57.9 g/L at 25 °C) [2] of methomyl and its low sorption affinity to soil contribute to a high likelihood of detecting methomyl in surface and groundwater [3]. This results in an increased risk to human health [4]. Methomyl has neurotoxic effects with symptoms such as headache, dizziness, and abnormal muscle function [5]. Exposure to methomyl can cause difficulty breathing and, in high doses, respiratory arrest [6], nausea, vomiting, and abdominal pain [7]. Methomyl has been found in groundwater and surface water at 10 µg/L and 30 µg/L, respectively. The standards for soil and surface water pesticides should not exceed 0.1 µg/L, as regulated by the EU and US EPA [3]. However, the amount of methomyl detected is still higher than the standard.

This research focuses on methomyl treatment. Previous research studies have used various technologies to treat methomyl, such as adsorption, photodegradation, and advanced oxidation processes. Adsorption is widely used to remove pesticides because it is easy to apply and inexpensive [3]. Biochar is a carbon-rich product used as an adsorbent to remove contaminants from water supplies due to its physical and chemical properties. Biochar production is also relatively low-cost, as most of the starting materials are waste products from the industrial and agricultural sectors, leading to interest in synthesizing biochar from biomass. Biochar is a product of the carbonization of biomass, characterized by a porous structure. Biochar has properties that help improve soil quality [8], sequester carbon in the soil [9], and reduce greenhouse gas emissions [10]. Biochar is therefore a material with the potential to promote sustainability in agriculture and environmental management. In this research, the starting raw material for producing biochar is cassava rhizome because cassava is one of the economic crops of Thailand. In the study by Aup-Ngoen in 2020, it was found that cassava rhizomes have the highest percentage of carbon content compared to durian peel, pineapple peel, and corncob, making it a suitable starting material for producing biochar [11]. Adsorption of atrazine and imidacloprid using phosphoric acid-modified biochar from agricultural waste showed maximum adsorption efficiencies of 70.7% for atrazine and 77.8% for imidacloprid, respectively. The phosphoric acid treatment increased the adsorption of both pesticides [12].

Therefore, the objective is to study factors in biochar synthesis from cassava rhizomes and investigate the factors involved in the adsorption of methomyl using biochar derived from cassava rhizomes.

Methodology

Preparation and modification of biochars

Preparation of biochars**:** 10g of cassava rhizomes were pyrolysis at temperatures of 300, 400, and 500 °C for 2.5 hours with a temperature increasing rate of 5°C/minute under nitrogen gas conditions.

Modification of biochar: The size of the biochar was controlled by grinding it into powder form and analyzing the particle size using a laser scattering particle size distribution analyzer. The average particle size was 54 µm. And then 10 g were immersed in 100 mL 14% H_3PO_4 solution for 24 hours at 25°C, to enhance its surface area and introduce functional groups such as P=O and P-OOH, which improve the adsorption of pollutants [13]. After that, the phosphoric-modified biochars were washed with distilled water until the pH of the supernatants was stable. Subsequently, the supernatants were discarded, and the biochars were oven-dried overnight at 105°C [14].

Characterization of biochars

The elemental analyzer measured the total elemental composition, such as carbon, hydrogen, nitrogen, and oxygen. Brunauer–Emmett–Teller (BET) was used to detect specific

surface areas of biochars. Fourier transform infrared (FTIR) spectra of biochars were conducted by an FTIR instrument. The morphology of the biochar was determined via scanning electron microscopy (SEM) and Synchrotron X-ray tomographic microscopy (XTM) at beamline 1.2W was operated at 1.2GeV, 150 mA in Synchrotron Light Research Institute (SLRI) were characterized the porosity by Octopus Analysis software and rendered in 3D tomographic reconstruction by using Drishti software. A laser scattering particle size distribution analyzer was used to measure the size and particle distribution of the material. Point of zero charge with salt addition technique To determine the charge on the surface of biochar.

Adsorption experiments

Varying methomyl pH solutions (3, 5, 7, 9, and 11), the pH values in the study were all adjusted with HCL solution and NaOH solution, and varying agitation speeds (100, 150, 200, and 250 rpm) were also investigated in separate experiments. Batch experiments were conducted using an orbital shaker at an agitation speed of 200 rpm at room temperature. To an Erlenmeyer flask 250 ml filled with 10 mg/L methomyl (aq), Volume 100 ml, a specific mass of biochar (1 g/L) was added. Equilibrium studies were performed by shaking the suspension containing biochar and methomyl in a particular time interval, up to a maximum of 360 min. The samples were collected at 2 mL, poured into the vials at the specified time, and filtered through a 0.45-µm Nylon filter before methomyl analysis. Methomyl removal efficiencies were measured in triplicates following a specific protocol for each condition. The filtrate was analyzed for pesticide concentrations using high-pressure liquid chromatography (HPLC) techniques. The analysis was performed using an Agilent 1260 Infinity II HPLC system (Agilent Technologies), equipped with a C18 column (Agilent ZORBAX Eclipse Plus, 4.6 × 250 mm, 5 µm particle size). The mobile phase consisted of 65% acetonitrile and 35% DI water, and the flow rate was set at 0.5 mL/min. Detection was performed at a wavelength of 234 nm. [15]. The experimental data were analyzed using Microsoft Excel. All experiments were conducted in triplicates, and the results were expressed as mean values with standard deviations. In the adsorption experiments, the effect of pH (ranging from 3 to 11) on methomyl removal efficiency was analyzed. Statistical significance was assessed using one-way ANOVA at a significance level of $p < 0.05$ to determine the differences in adsorption efficiencies across the different experimental conditions.

Results and Discussion

Characterization of biochars

Table 1 shows that the physical characteristics of biochar produced at 300°C are somewhat brownish, resembling wood, which suggests incomplete combustion. In contrast, biochar produced at 400°C and 500°C is entirely black, indicating complete combustion. Therefore, only biochar produced at 400°C and 500°C was selected for CHN/O analysis to determine its composition.

The Biochar synthesized at a temperature of 500 °C for 2.5 hours exhibited the highest carbon content at 78.149%, with an H/C ratio of 0.026, consistent with other studies that indicate the significant influence of pyrolysis temperature on biochar's elemental composition. Higher pyrolysis temperatures increase the carbon concentration in biochar while reducing hydrogen and nitrogen levels, enhancing the chemical stability of the biochar. This makes it well-suited for agricultural and environmental applications, such as soil improvement and pollutant adsorption. Furthermore, as the H/C ratio decreases, the aromatic structure of the biochar increases, leading to greater stability and improved pollutant adsorption capacity [16].

Then, the selected biochar was treated with phosphoric acid. From Table 2, the modification of phosphoric acid could increase the specific surface area of biochar produced from cassava rhizome, which was proven by BET analysis. Although the change in specific surface area was small, the biochar modified with phosphoric acid showed a higher average pore diameter, similar to Peng's study [13].

Table 1 Elemental compositions of Biochar obtained from the different temperatures

Photo/ Sample Biochar		% C	% H	% N	Ratio H/C
	300 °C / 2.5 hr.	N/A			
	400 °C / 2.5 hr.	75.132	3.7878	1.7910	0.0504
	500 °C / 2.5 hr.	78.149	2.0398	0.6919	0.0261
Abbreviation: NA = not available.					

Table 2 Physiochemical characteristics of biochars from BET analysis

Sample	Surface Area (m^2/g)	Average pore diameter (Å)	Total pore volume (cc /g)
Biochar CA	2.29	157.40	0.0176
Biochar+ H_3PO_4	3.39	654.4	0.0133

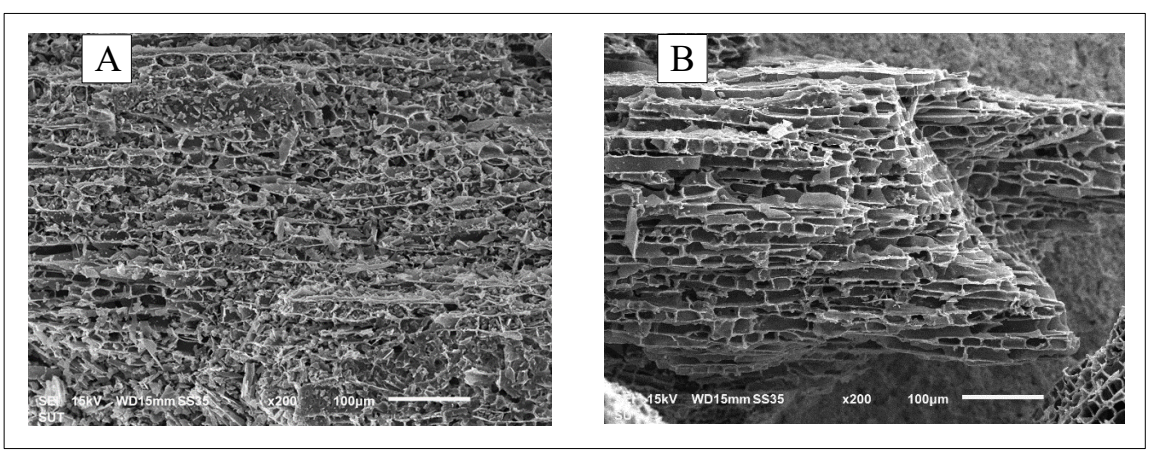

Figure 1 SEM images of (A) Biochars CA.
(B) BiocharCA + H_3PO_4.

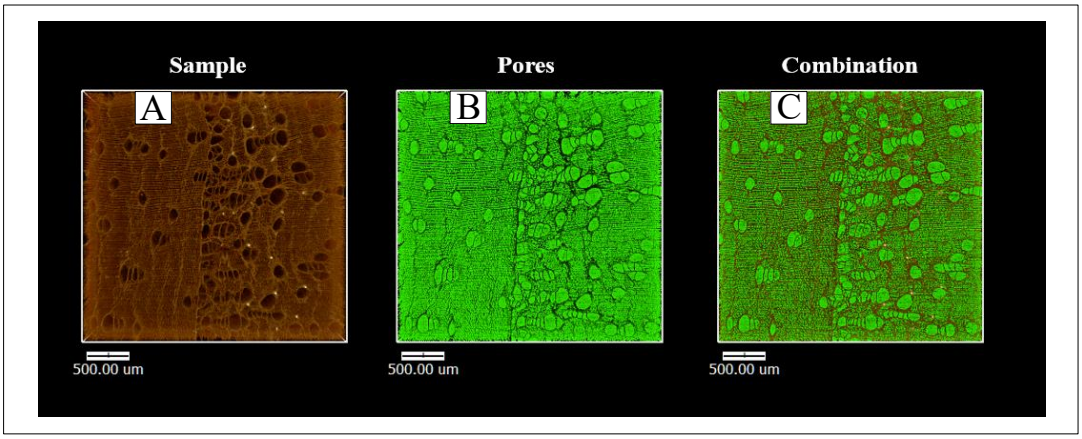

Figure 2 Results of the X-ray Tomographic Microscopy (XTM) technique of the synthesized biochar cassava rhizomes 500°C/2.5 hr.

From Figure 1, This SEM image reveals significant changes in the structure after treatment with phosphoric acid (H_3PO_4). The porous structure becomes apparent, and the surface appears more collapsed or compacted, which may be due to the corrosive effect of phosphoric acid, which may cause some of the mesopores to collapse. The structure in Image B shows that although the micropores are increased (resulting in increased surface area), the larger pores may be partially blocked or their volume reduced. The 3D X-ray characteristics and porosity (%) of biochar were studied using the X-ray Tomographic Microscopy (XTM) technique from Synchrotron Light Research Institute (SLRI). XTM results in Figure 2 show a 3D X-ray image in which Figure 2A shows only biochar solid structure (brown color), Figure 2B shows only the pore in the biochar sample, and Figure 2C shows both biochar solid structure combined with pore in structure. From XTM measurement, a porosity of 28% was obtained, which means that the remaining 72% was solid biochar.

From Table 2, The BET analysis supports these visual observations, showing that the surface area increased after modification (from 2.29 m^2/g to 3.39 m^2/g), while the total pore volume decreased (from 0.0176 cc/g to 0.0133 cc/g). This increase in surface area is likely due to the creation of more micropores, while the reduction in pore volume and the larger pore diameter (from 157.4 Å to 654.4 Å) suggest that some of the mesopores were collapsed or blocked during the treatment. The chemical nature of H_3PO_4 treatment can explain this phenomenon. The acid not only reaches the surface of the biochar but also introduces new functional groups, especially in micropores. While these micropores increase the surface area, larger mesopores' collapse or partial blockage reduces the overall pore volume.

Additionally, the increase in average pore diameter may result from structural changes like the selective expansion or merging of particular pores during the acid treatment. Other studies report similar effects. For example, Peng et al. (2017) found that H_3PO_4 modification of biochar increased surface area by promoting microporosity while reducing pore volume due to structural collapse of mesopores [13]. Similarly, Chen et al. (2018) observed a significant increase in surface area after H_3PO_4 treatment, despite lower pore volume, due to the creation of additional functional groups that enhance adsorption properties [17]. In conclusion, H_3PO_4 treatment increases the surface area by enhancing micropore development, even though mesopores may collapse or become blocked, resulting in reduced pore volume but improved adsorption efficiency.

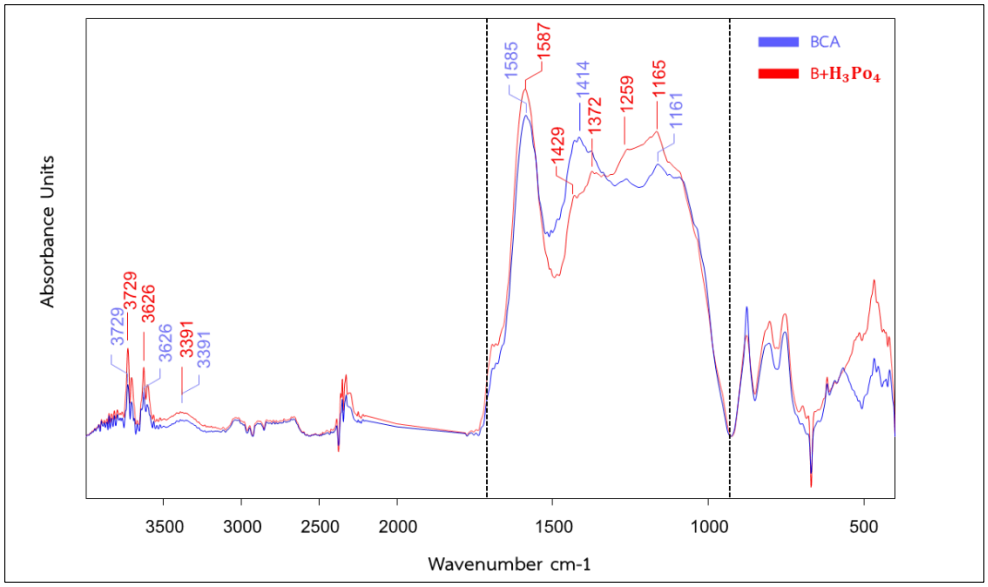

Figure 3 FTIR spectra of BiocharCA. and BiocharCA + H_3PO_4.

The results of the Fourier transform infrared spectrophotometer (FTIR) are shown in Figure 3. A peak at 3729–3391 cm^{-1} This range corresponds to the stretching vibrations of -OH groups, indicating the presence of hydroxyl groups due to moisture or water content in the samples. The higher intensity in the B-H_3PO_4 sample suggests a more significant presence of hydroxyl groups compared to the untreated BCA sample [18]. A peak at 1587–1429 cm^{-1} This region is associated with C=C stretching vibrations in aromatic rings characteristic of carbonized structures. The B-H_3PO_4 sample shows a more vigorous intensity, indicating enhanced aromatic carbon structures due to H_3PO_4 treatment [19]. A peak at 1372–1269 cm^{-1} The peaks in this range can be attributed to C-H bending vibrations in methylene groups and C-O stretching vibrations in esters. The stronger absorption in the B-H_3PO_4 sample reflects the formation of new chemical bonds in the modified biochar structure. A peak at 1165–1101 cm^{-1} This region corresponds to P=O stretching vibrations, which indicate the presence of phosphate groups introduced by the H_3PO_4 treatment. The distinct absorption in B-H_3PO_4 highlights the incorporation of phosphorus into the biochar structure [13]. The FTIR analysis shows significant structural changes in the biochar after treatment with phosphoric acid. The B-H_3PO_4 sample exhibits increased phosphate (-P=O) groups, enhanced aromatic carbon structures (C=C), and more pronounced hydroxyl (-OH) groups. These changes result from crosslinking and new bond formation facilitated by the H_3PO_4 modification process, which strengthens the carbon skeleton and alters the biochar's functional groups [20]. Phosphoric acid treatment shows an increase in the formation of P=O, P=OOH groups, similar to Peng's studies [13], where P=O, P-OOH groups were detected after treatment with phosphoric acid. Research has studied the size of biochar for adsorption. It was found that small biochar had increased adsorption. Therefore, biochar is crushed before use [21]. The size and distribution were then measured using a laser scattering particle size distribution analyzer. For the particle size distribution analysis using laser scattering, it was found that the particle size distribution of biochar was in the range of 10–300 μm, and the average particle size was 54 μm, as shown in Figure 4.

By studying the pH value at zero surface charge, points of zero charge of the adsorbent are shown in Figure 5, where the value refers to the pH at which the sum of the surface charges of the adsorbent is equal to zero. When the pH value of the solution is lower than the value, the surface of the adsorbent will display a positive charge. When the pH value of the solution is higher than the value, it will cause the surface of the adsorbent to display a

negative charge [22]. The results of this study found that the point of zero charge of biochar from cassava rhizomes is 6.05, meaning that at pH of 6.05, the surface charge of cassava rhizome biochar is zero, and the of cassava rhizome biochar modified with phosphoric acid is 5.15 shown in Figure 6B.

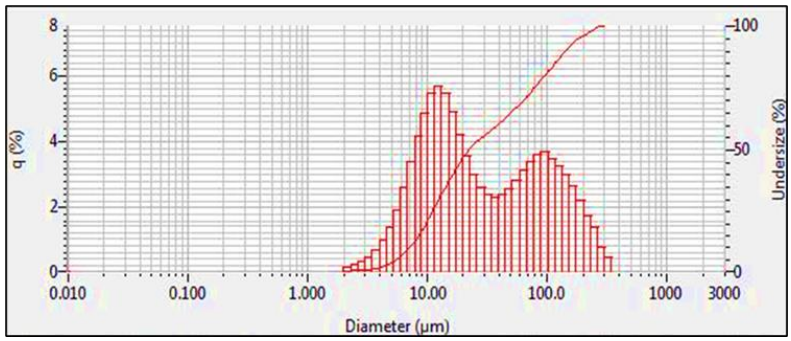

Figure 4 Measurement of size and distribution of biochar particles

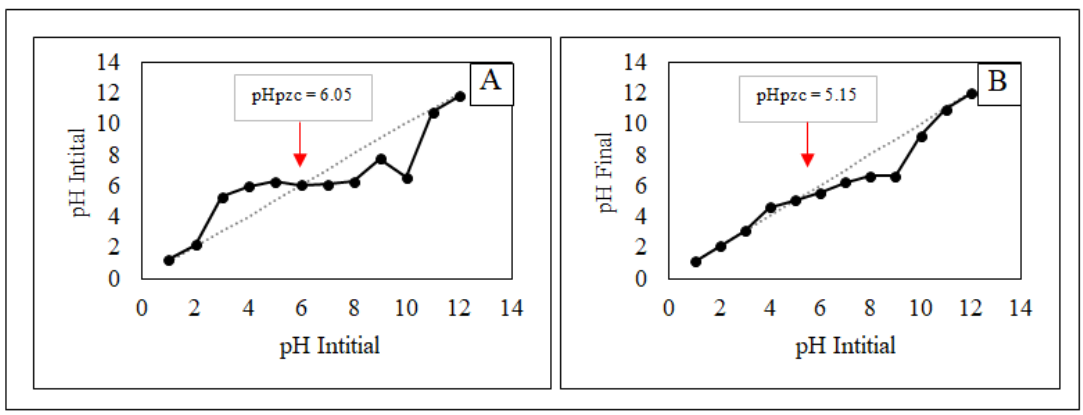

Figure 5 Points of Zero Charge (pH_{pzc}) of biochar.
(A) biochar from cassava rhizomes (B) biochar from cassava rhizomes modified with phosphoric acid

Adsorption Experiment

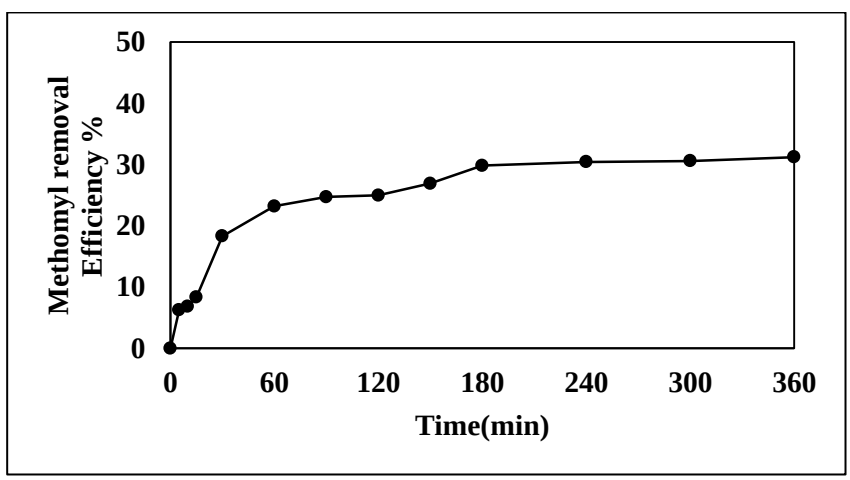

Figure 6 Effect of the contact time Initial concentration methomyl 10 mg/l, biochar from cassava rhizomes modified with phosphoric acid 1 g, Initial pH 6.20, agitation speed 200 rpm.

The ability to adsorb methomyl by biochar from cassava rhizomes modified with phosphoric acid increases with increasing contact time, and the adsorption rate increases rapidly during the first 180 minutes, as shown in Figure 6. However, over time, the adsorption rate caused by the movement of methomyl molecules in the adsorbent particles begins to slow until equilibrium is reached at a contact time of 180 minutes. The adsorption capacity is most remarkable from 180 to 360 minutes, during which the adsorption rate equals the desorption speed. This study found that during the contact period of 180 minutes, the efficiency was 29.84%.

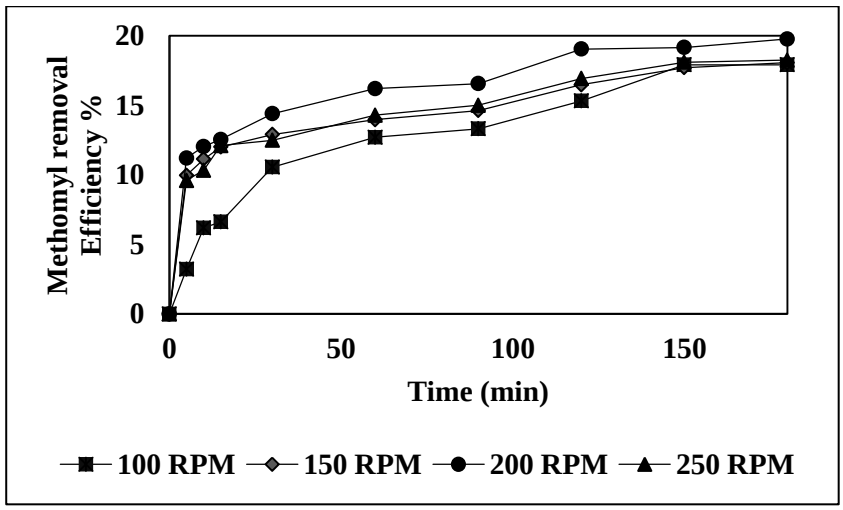

Figure 7 Effect of the agitation speed Initial concentration methomyl 10 mg/l, biochar from cassava rhizomes modified with phosphoric acid 1 g, Initial pH 6.00, agitation speed 200 rpm.

Figure 7 shows that when the agitation speed was increased, the methomyl adsorption efficiency by biochar was increased. However, when the speed is increased to more than 200 rpm, the adsorption efficiency decreases. The effect of turbulence is one of the critical factors that are important in controlling the solid-liquid mass transfer mechanism [23]. Figure 8 shows At pH 3, the biochar demonstrates the highest adsorption capacity (qe) at 2.79 mg/g, indicating that in acidic conditions, biochar is highly effective at adsorbing methomyl. As pH increases, qe decreases. At pH 5, it drops to 2.46 mg/g, and by pH 11, it reaches 2.05 mg/g. This decline in qe is consistent with the fact that methomyl molecules become less available for adsorption due to increased hydrolysis in basic conditions. In addition, pH significantly affected methomyl removal efficiency, with the highest removal at pH 11 (50.81%). This was significantly different from the removal rates at pH 3–9, which ranged from 20.55% to 27.90% ($p < 0.05$). The higher efficiency at pH 11 is attributed to base-catalyzed hydrolysis, where methomyl breaks down into less toxic by-products, rather than just adsorbing onto the biochar. This aligns with previous studies on methomyl degradation in alkaline conditions [22]. At pH 3, the adsorption efficiency was the highest (27.90%), likely due to stronger electrostatic interactions between the biochar and methomyl under acidic conditions. In contrast, neutral and slightly basic pH levels (7–9) showed lower efficiency due to reduced electrostatic attraction as methomyl becomes less charged. Post-hoc tests confirmed a significant difference between pH 3 and pH 11 ($p < 0.05$), supporting the idea that both adsorption and hydrolysis play key roles in methomyl removal at different pH levels. In summary, lower pH favors adsorption, while higher pH promotes degradation, consistent with the behavior of similar compounds [24]. Optimizing pH can therefore maximize methomyl removal depending on the desired mechanism. At pH 3, the biochar demonstrates the highest adsorption capacity (qe) at 2.79 mg/g, indicating that in acidic conditions, biochar is

highly effective at adsorbing methomyl. As pH increases, qe decreases. At pH 5, it drops to 2.46 mg/g, and by pH 11, it reaches 2.05 mg/g. In the research by Fathy, N. A., Attia, A. A., & Hegazi, B. (2016), the adsorption capacity of carbon xerogel was found to be 15.52 mg/g. Generally, carbon xerogel has a higher surface area and a more developed porous structure, which is the reason for its higher adsorption capacity [25]. This decline in qe is consistent with the fact that methomyl molecules become less available for adsorption due to increased hydrolysis in basic conditions. Methomyl, a carbamate pesticide, undergoes rapid decomposition in alkaline conditions due to base-catalyzed hydrolysis. When the pH exceeds its pKa of 9.7, hydroxide ions (OH^-) attack the carbamate group in methomyl, accelerating its breakdown into simpler compounds and leading to its degradation into products like methomyl oxime and methylcarbamic acid [24]. This is consistent with findings from research of Wang, Z. et al. (2022), which show accelerated decomposition in basic environments due to nucleophilic attacks on carbamate structures, and Akl, M. A. et al. (2016), who demonstrated that in the pH range of 2-8, methomyl is relatively stable. In contrast, when the pH increased to 10, the residual methomyl content was only 12% of the original value. Moreover, at pH values as high as 12, methomyl was completely degraded into other compounds, which means that methomyl is relatively degraded in the alkaline solution. Therefore, the effect of pH on the adsorption capacity was investigated in the range of pH 2-8 [26].

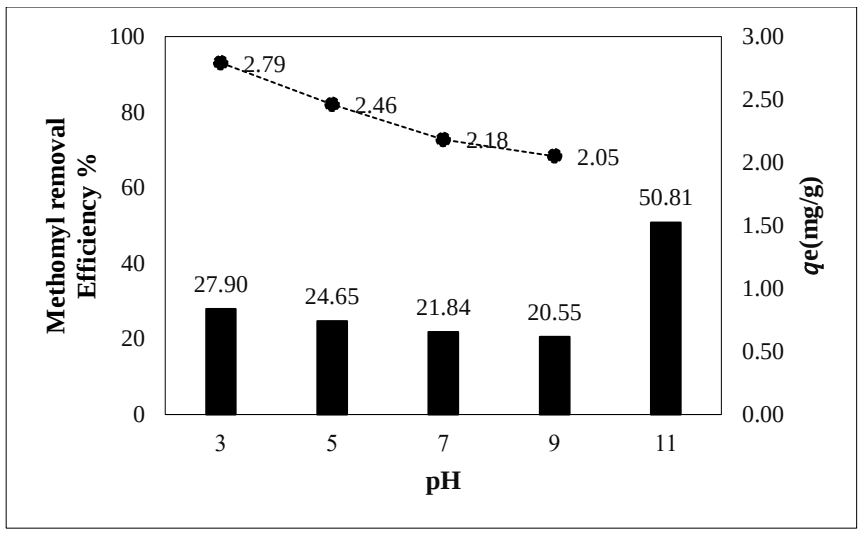

Figure 8 Effect of pH on methomyl removal. Initial concentration methomyl 10 mg/l, biochar from cassava rhizomes modified with phosphoric acid 1 g, agitation speed 200 rpm.

Conclusions

In this study, biochar was successfully synthesized from cassava rhizomes, with the optimal conditions being pyrolysis at 500°C for 2.5 hours. This condition produced biochar with a high carbon content of 78.149% and a low H/C ratio of 0.026, indicating its high stability. Biochar's stability is primarily attributed to its high carbon content and low H/C ratio, essential for applications requiring long-term carbon sequestration and enhanced material properties. Biochar was modified using phosphoric acid to improve its physical and chemical characteristics. The modification increased the specific surface area from 2.29 m^2/g to 3.39 m^2/g and the average pore diameter from 1.57 Å to 6.54 Å, enhancing its porosity and adsorption capacity. The XTM measurements revealed a porosity of 28%, with the remaining 72% as solid biochar. The phosphoric acid treatment also introduced new functional groups, including P=O and P-OOH, as confirmed by FTIR analysis. These chemical modifications are critical for enhancing the biochar's reactivity and adsorption performance. The adsorption experiments

demonstrated that the biochar modified with phosphoric acid exhibited a significant adsorption capacity, particularly between 180 and 360 minutes, where equilibrium between adsorption and desorption was observed. Key factors influencing adsorption efficiency were agitation speed and pH, with optimal adsorption occurring at a stirring speed of 200 rpm. In acidic conditions (pH 3), the removal was 27.90%, attributed to strong electrostatic interactions between the biochar and methomyl. Neutral to slightly basic pH levels (7–9) showed lower efficiency due to reduced electrostatic attraction. This study demonstrates the potential of cassava rhizome biochar, particularly when modified with phosphoric acid, as an efficient and eco-friendly adsorbent for pesticide removal from aqueous solutions. Its high stability, porosity, and surface functionality make it a promising candidate for environmental remediation. Future research should explore the scalability of this method for industrial applications and further investigate the biochar's performance in actual environmental conditions. Additionally, the study could be expanded to include adsorption isotherms and kinetic models to better understand the adsorption mechanisms at varying pollutant concentrations.

Acknowledgements

This work was supported by (i) Suranaree University of Technology (SUT), (ii) Thailand Science Research and Innovation (TSRI), and (iii) National Science, Research and Innovation Fund (NSRF) - Grant no. 179270.

References

[1] Zhao, X., Ouyang, W., Hao, F., Lin, C., Wang, F., Han, S. and Geng, X. 2013. Properties comparison of biochars from corn straw with different pretreatment and sorption behaviour of atrazine. Bioresource Technology, 147: 338-344.

[2] Van Scoy, A.R., Yue, M., Deng, X. and Tjeerdema, R.S. 2013. Environmental fate and toxicology of methomyl. Reviews of Environmental Contamination and Toxicology, 93-109.

[3] Srikhaow, A., Chaengsawang, W., Kiatsiriroat, T., Kajitvichyanukul, P. and Smith, S.M. 2022. Adsorption kinetics of imidacloprid, acetamiprid and methomyl pesticides in aqueous solution onto eucalyptus woodchip derived biochar. Minerals, 12(5): 528.

[4] Baron, R.L. 1991. Carbamate insecticides. In W.J. Hayes, Jr. and E.R. Laws, Jr. (eds.). Handbook of Pesticide Toxicology. Vol. 3: 1125-1189. Academic Press, San Diego.

[5] Ahmad, M.F., Ahmad, F.A., Alsayegh, A.A., Zeyaullah, M., AlShahrani, A.M., Muzammil, K. and Hussain, S. 2024. Pesticides Impacts on Human Health and the Environment with Their Mechanisms of Action and Possible Countermeasures. Heliyon. 10: e29128.

[6] Gupta, R.C., Malik, J.K. and Milatovic, D. 2011. Organophosphate and carbamate pesticides. In Reproductive and Developmental Toxicology. 471-486. Academic Press.

[7] Salazar-Flores, J., Pacheco-Moisés, F.P., Ortiz, G.G., Torres-Jasso, J.H., Romero-Rentería, O., Briones-Torres, A.L. and Torres-Sánchez, E.D. 2020. Occupational exposure to organophosphorus and carbamates in farmers in La Cienega, Jalisco, Mexico: Oxidative stress and membrane fluidity markers. Journal of Occupational Medicine and Toxicology. 15: 1-11.

[8] Lehmann, J. and Joseph, S. 2015. Biochar for Environmental Management: Science, Technology and Implementation. Routledge.

[9] Woolf, D., Amonette, J.E., Street-Perrott, F.A., Lehmann, J. and Joseph, S. 2010. Sustainable biochar to mitigate global climate change. Nature Communications. 1(1): 56.

[10] Song, X., Pan, G., Zhang, C., Zhang, L. and Wang, H. 2016. Effects of biochar application on fluxes of three biogenic greenhouse gases: A meta-analysis. Ecosystem Health and Sustainability. 2(2): e01202.

[11] Aup-Ngoen, K. and Noipitak, M. 2020. Effect of carbon-rich biochar on mechanical properties of PLA-biochar

composites. Sustainable Chemistry and Pharmacy, 15: 100204.
[12] Mandal, A., Singh, N. and Purakayastha, T.J. 2017. Characterization of pesticide sorption behaviour of slow pyrolysis biochars as low cost adsorbent for atrazine and imidacloprid removal. Science of the Total Environment, 577: 376-385.
[13] Peng, H., Gao, P., Chu, G., Pan, B., Peng, J. and Xing, B. 2017. Enhanced adsorption of Cu (II) and Cd (II) by phosphoric acid-modified biochars. Environmental Pollution, 229: 846-853.
[14] Chen, T., Luo, L., Deng, S., Shi, G., Zhang, S., Zhang, Y., ... and Wei, L. 2018. Sorption of tetracycline on H3PO4 modified biochar derived from rice straw and swine manure. Bioresource Technology, 267: 431-437.
[15] Phrommeerit, A. and Muangsookthikarn, W. 1995. Measurement of methomyl levels in deceased blood using High Performance Liquid Chromatography. Chiang Mai Medical Technology Journal, 28(2), May.
[16] Mimmo, T., Panzacchi, P., Baratieri, M., Davies, C.A. and Tonon, G. 2014. Effect of pyrolysis temperature on miscanthus (Miscanthus×giganteus) biochar physical, chemical and functional properties. Biomass and Bioenergy, 62: 149-157.
[17] Chu, G., Zhao, J., Huang, Y., Zhou, D., Liu, Y., Wu, M. and Steinberg, C.E. 2018. Phosphoric acid pretreatment enhances the specific surface areas of biochars by generation of micropores. Environmental Pollution, 240: 1-9.
[18] Salami, A., Vilppo, T., Pitkänen, S., Weisell, J., Raninen, K., Vepsäläinen, J. and Lappalainen, R. 2020. Cost-effective FTIR and 1H NMR spectrometry used to screen valuable molecules extracted from selected West African trees by a sustainable biochar process. Scientific African, 8: e00315.
[19] Abdullah, N., Taib, R.M., Aziz, N.S.M., Omar, M.R. and Disa, N.M. 2023. Banana pseudo-stem biochar derived from slow and fast pyrolysis process. Heliyon, 9(1): e12940.
[20] Jagtoyen, M. and Derbyshire, F. 1998. Activated carbons from yellow poplar and white oak by H3PO4 activation. Carbon, 36(7-8): 1085-1097.
[21] Zheng, W., Guo, M., Chow, T., Bennett, D.N. and Rajagopalan, N. 2010. Sorption properties of greenwaste biochar for two triazine pesticides. Journal of Hazardous Materials, 181(1-3): 121-126.
[22] Yang, G.P., Zhao, Y.H., Lu, X.L. and Gao, X.C. 2005. Adsorption of methomyl on marine sediments. Colloids and Surfaces A: Physicochemical and Engineering Aspects, 264(1-3): 179-186.
[23] Agarwal, S., Sadeghi, N., Tyagi, I., Gupta, V.K. and Fakhri, A. 2016. Adsorption of toxic carbamate pesticide oxamyl from liquid phase by newly synthesized and characterized graphene quantum dots nanomaterials. Journal of Colloid and Interface Science, 478: 430-438.
[24] Wang, Z., Zhang, Q., Wang, G., Wang, W. and Wang, Q. 2022. Hydrolysis mechanism of carbamate methomyl by a novel esterase PestE: a QM/MM approach. International Journal of Molecular Sciences, 24(1): 433.
[25] Fathy, N.A., Attia, A.A. and Hegazi, B. 2016. Nanostructured activated carbon xerogels for removal of methomyl pesticide. Desalination and Water Treatment, 57(21): 9957-9970.
[26] Akl, M.A., Youssef, A.F.M., Hassan, A.H. and Maher, H. 2016. Synthesis, characterization and evaluation of peanut shells-derived activated carbons for removal of methomyl from aqueous solutions. J Environ Anal Toxicol, 6(352): 2161-0525.

Thai Environmental Engineering Journal Vol. 38 No. 3 (2024) : 23-34
www.eeat.or.th

Characterizing Particle Number Size Distributions and Source Contribution for Public Elementary School Classrooms in Bangkok

Hnin Phyu Phyu Aung[1*] and Win Trivitayanurak[1,2]

[1]Department of Environmental Engineering, Faculty of Engineering, Chulalongkorn University, Bangkok 10330, Thailand
[2]Professor Aroon Sorathesn Center of Excellence in Environmental Engineering, Faculty of Engineering, Chulalongkorn University, Bangkok 10330, Thailand
[*]E-mail : hninphyu2693@gmail.com

Article History; *Received: 31 May 2024, Accepted: 16 October 2024, Published: 24 December 2024*

Abstract

This study provides crucial information on indoor air pollution in public elementary schools in Bangkok, highlighting the substantial impact it has on the health and learning conditions of students, particularly in view of the city's rapidly urban expansion. The research examines particle size distributions (PSD) in four urban schools using the scanning mobility particle sizers (SMPS) and the optical particle sizers (OPS) to cover particle size range of 10 nm to 10 microns. Measurement covered class hours on weekdays and experiments on the weekends. Throughout the study, outdoor particle number concentration (PNC) was significantly higher than indoor levels. On weekdays, the indoor 1-hour mean PNC at Site S4 reached 23,182 cm^{-3} as a highest level among others, classified as a High PNC level according to WHO good practice guidelines. This suggests substantial internal sources, inadequate ventilation, and the impact of nearby traffic and school activities. Similarly, during weekend measurements, Sites S1 and S3 also reached High PNC levels, with concentrations of 27,663 cm^{-3} and 29,534 cm^{-3}, respectively. Peaks in PNC were directly linked to the use of cleaning products containing volatile chemicals, underlining the pronounced impact of these activities on indoor air quality. The weekday indoor particle number size distribution (PNSD) exhibited a single-mode distribution, significantly influenced by routine class activities and student movements. Over the weekend, the indoor PNSD across all sites showed fluctuations corresponding to various experimental setups involving changes in ventilation and cleaning activities. This study underscores the necessity of strategic indoor air quality management in schools, aiming to reduce exposure to high PNCs, improve indoor air quality in classrooms, and provide better educational settings for children in increasingly urbanized regions. Effective strategies might include enhanced ventilation, controlled cleaning practices, and real-time monitoring of PNC and PNSD to maintain a healthy educational environment.

Keywords : indoor air quality; particle size distribution; ultrafine particle; urban schools; air pollution mitigation; environmental health

Introduction

The rapid expansion of cities like Bangkok brings numerous social and economic benefits but also creates environmental challenges. Among these, air pollution poses a substantial threat affecting the health of millions of people. For the context of urban schools, the combination of pollution from external sources and insufficient ventilation in public schools has become crucial [1]. In addition, the World Health Organization (WHO) emphasizes the importance of indoor air quality since it connects to several public health issues [2]. As per guidance of United Nations Sustainable Development Goals (UN SDGs), namely intending to contribute to the well-being (Goal 3), education quality (Goal 4), and sustainability (Goal 11) of urban areas, inside school air quality management activities plays critical role. Among the air quality issues, fine particulate matter still remains for a challenge; on top of that, ultrafine particles (UFPs) deserve a spotlight. Due to the ability of UFPs in evading the immune system, it can lead to serious respiratory diseases [3]. Up to now, the lack of comprehensive guidelines regarding UFPs highlights a significant lapse in our efforts to combat air pollution, especially in small rooms like school classrooms. Since significant amounts of time are spent by students and teachers inside classrooms, the pollutants in the air might disrupt health and learning capabilities [4]. To provide the baseline information to support decisions to tackle UFPs in Bangkok's public elementary school classrooms, first we must determine the concentration of these particles.

Understanding the conditions that lead to poor indoor air quality is essential for establishing effective risk-mitigation measures, especially the schools that require immediate action. Even though studies on indoor particle number size distribution. in schools have been conducted in various locations like Hanoi, Vietnam [5], Brisbane, Queensland, Australia [6], China [7], and Korea [8], no previous data has been recorded for Bangkok's schools hence there is lacking of such data relavant to distinct meteorological, infrastructural, and urban development patterns of Bangkok.

In Bangkok, most previous research and monitoring infrastructure have focused on ambient air quality while there has been a lack of studies investigating the air quality within school buildings. The present study therefore aimed to provide critical indoor pollution data in Bangkok's public elementary schools. By means of identifying sources of indoor pollution, assessing the influence of outdoor air quality, and analyzing the impact of environmental conditions on particle levels, the results could favor not only to illuminate the current state of classroom air quality but also to support decisions for actionable strategies to ameliorate. Our study could eventually contribute to healthier and supportive learning environments for vulnerable children of Bangkok in line with aforementioned SDGs.

Methodology

Sampling Sites: The study was conducted in Pathumwan District, a central business district in Bangkok. Four elementary schools, namely, Wat Chaimongkol School (S1), Wat Pathum Wanaram School (S2), Wat Daung Khae School (S3), and Suan Lumphini School (S4), were chosen based on their varied urbanization features and proximity to high-traffic roads as shown in Figure 1. The classrooms chosen for the study are kindergarten level equipped with air conditioner to keep cool and allow closed room condition especially during high $PM_{2.5}$ days. These rooms are also equipped with air treatment devices donated to the schools. The devices operate by releasing atomized water particles containing hydroxyl radicals to eradicate viruses and bacteria. Site S1, S2, and S3, each have an air treatment device installed on the ceiling. Site S4 has the same technology with a different setup, an air conditioner integrated with the disinfecting particle generating device.

Instrumentation: The Scanning Mobility Particle Sizers (SMPS) TSI 3910 was used to measure particle size distribution covering a size range of 10 nm to 420 nm across 13 size channels. Secondly, Optical Particle Sizers (OPS): The TSI 3330 measured particles within the 300 nm to 10,000 nm range. Next, TESTO 440 Flow Meter was positioned near the classroom door to measure the air flow into or out of the classroom [9]. An airthinX sensor for

measuring temperature, pressure, humidity, $PM_{2.5}$ and PM_{10} was installed inside the classroom and employed for the outdoor measurement simultaneously [10]. All instruments used in this study are demonstrated in Figure 2.

Measurement conditions: Measurements were conducted inside and outside the classrooms simultaneously. Figure 3 depicts the measurement spots which are similar for all sites. The study included weekdays and weekends measurements under two different settings. During weekdays, we conducted measurement during regular school hours to capture the typical air quality conditions without any intervention. However, weekend measurements were conducted during the same hours without any class activities but with varying experimental conditions to examine air quality under varying influencing factors, namely, air conditioning, electric ceiling fan, ventilation (windows and doors opening), cleaning activity, and, finally, the use of air treatment system. Table 1 tabulates the 12 experimental setups conducted to investigate the effects of influencing factors on indoor air quality.

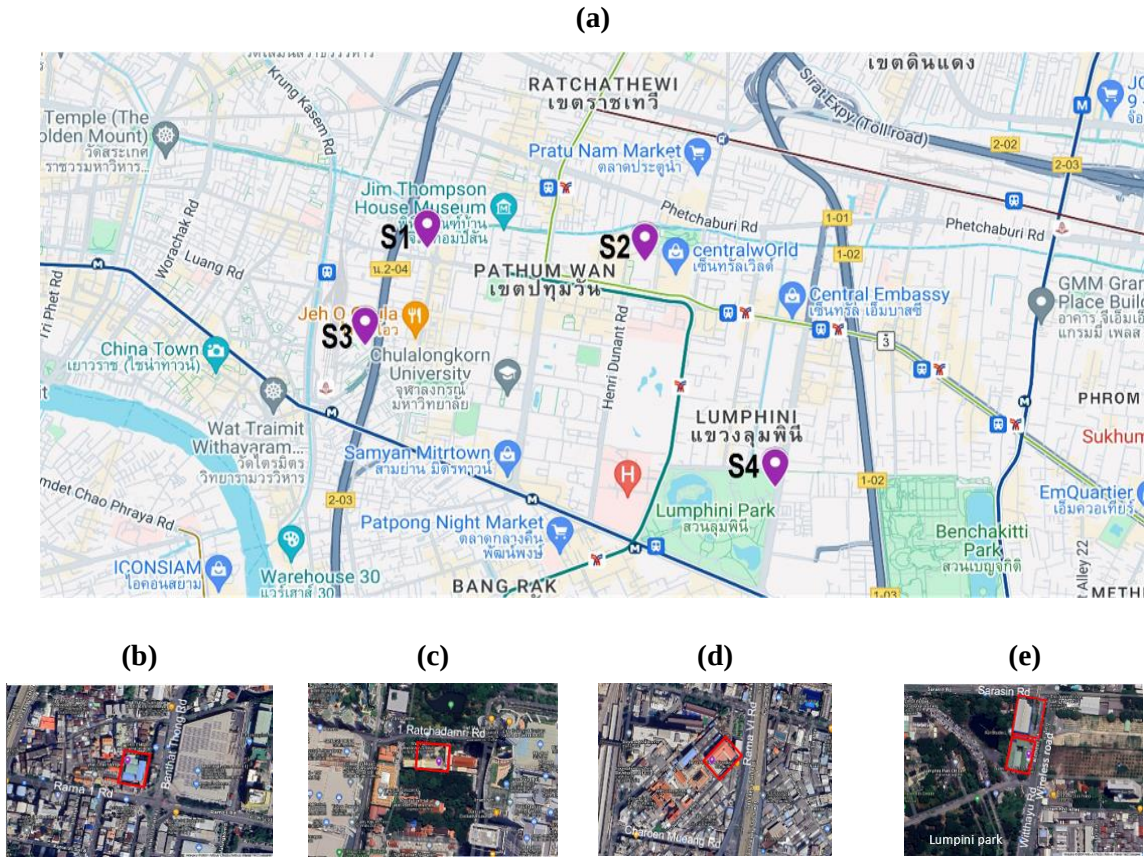

Figure 1 Map of sampling sites (a) overview map, (b) S1-Wat Chaimongkol School, (c) S2-Wat Pathum Wanaram School, (d) S3-Wat Daung Khae School, and (e) S4-Suan Lumphini School. The red inserts indicate school buildings and the placemarks identify the classroom location

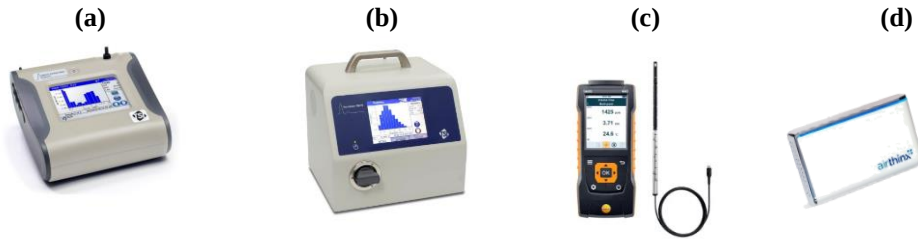

Figure 2 Instruments used for the onsite measurements: (a) Scanning Mobility Particle Sizer (SMPS, Model 3910 TSI), (b) Optical Particle Sizer (OPS, Model 3330 TSI), (c) an air flow meter (TESTO 440) and (d) AirthinX sensor

Figure 3 Measurement setup for a) outside and b) inside of the classrooms

Table 1 Experimental setup for weekend measurements

Condition	Fan	Air condition	Window and door	Cleaning	Air treatment
C1	On	Off	Open	No	On
C2a	Off	Off	Open	No	On
C2b	Off	Off	Open	Yes	On
C3	On	Off	Open	No	Off
C4a	Off	Off	Open	No	Off
C4b	Off	Off	Open	Yes	Off
C5	On	On	Closed	No	Off
C6a	Off	On	Closed	No	Off
C6b	Off	On	Closed	Yes	Off
C7	On	On	Closed	No	On
C8a	Off	On	Closed	No	On
C8b	Off	On	Closed	Yes	On

Results and Discussion

Classroom weekday measurement results

The 1-hour average of outdoor particle number concentration (PNC) in the weekdays revealed 11.46 x 10^3 #/cm^3, 9.86 x 10^3 #/cm^3, 17.59 x 10^3 #/cm^3, and 13.33 x 10^3 #/cm^3, at sites S1, S2, S3, and S4, respectively. And then, the 1-hour mean of indoor PNC was 10.22 x 10^3 #/cm^3, 16.14 x 10^3 #/cm^3, 18.71 x 10^3 #/cm^3, and 23.18 x 10^3 #/cm^3 in each respective site. According to the WHO global air quality guideline, the indoor PNC at site S4 exceeded the high PNC level of 20,000 #/cm^{-3} for 1-hour mean value. This high PNC can be a result of students having lunch in the classroom followed by cleaning activities with some use of cleaning products; unlike other sites where students went

for lunch outside the classrooms. Table 2 shows the statistics of outdoor and indoor total PNC in each school during the weekday measurement. The weekend results are not shown as the experiments do not represent actual PNC that students usually are exposed to. The correlation analysis of indoor and outdoor PNC during the weekdays was conducted and moderate correlations were observed in S1, S3 and S4 with the coefficients, R^2 of 0.47, 0.31 and 0.66, respectively. However, S2 revealed low correlation (R^2 = 0.04) because the outdoor measurement was in a building corridor with walls and doors that may lead to accumulation unlike measurement in open corridors at other sites.

Distinct patterns in particle number size distributions (PNSD) were influenced by both interior activities and outdoor environmental conditions [11]. The time-series PNSD of the weekday classroom of the four sites exhibit similar features thus only that of S1 is presented in Figure 4. The indoor PNSD features a stable one-mode size distribution which is related to the fact that classroom windows were closed throughout the operating hours. An abrupt change of indoor PNSD at midday is consequential of movement of all students leaving for lunch and re-entering afterwards thus the exchange of outdoor air. In contrast, the outdoor PNSD exhibits greater variability. The peak in the morning is related to the morning traffic rush hours. Then the PNSD progressively diminished as atmospheric conditions becoming more unstable with increasing solar radiation and traffic congestion ease up during the midday and afternoon periods [12]. The identified difference and relatedness of the indoor and outdoor PNSD underscore the necessity for focused indoor air quality management, particularly in periods of heightened activity that may result in intermittent deterioration of air quality. The characteristics of the PNSD can be depicted as multi-modal lognormal particle number size distribution plots as shown in Figure 5. Since the PNSD exhibits one mode for most of time with only some occasion of two modes, only two selected instances are shown. The plots in Figure 5 are accompanied by Table 3 presenting the parameters of the size distribution, namely, number concentrations (N) in #/cm3, geometric mean ($\overline{D}_{pg}$) in nm, and geometric standard deviation ($\boldsymbol{\sigma}_g$) in nm.

Table 2 Summarizing statistics of outdoor and indoor 1-hour averaged total PNC in each school during weekday measurement

Schools	Measurement condition	Descriptive statistics for total PNC (x 10^3 #/cm^3)					
		Mean ± Std.Dev	Minimum	25th Percentile	Median	75th Percentile	Maximum
S1	Indoor	10.2 ± 3.57	6.02	6.31	9.78	13.7	22
	Outdoor	11.4 ± 3.30	3.69	7.55	10.8	15.4	36.8
S2	Indoor	15.7 ±9.72	6.84	7.31	11.5	28.1	47.1
	Outdoor	10.1 ± 3.94	3.74	6.96	8.95	11.7	33.7
S3	Indoor	18.7 ± 3.58	4.82	13.2	3.58	21.5	31.8
	Outdoor	17.6 ± 8.18	5.83	10.6	8.18	20.4	66.2
S4	Indoor	21.7 ± 7.27	10.5	14.4	19.4	25.1	56.9
	Outdoor	14.0 ± 5.33	7.5	8.17	12.6	17.7	40.1

Std.Dev = standard deviation.

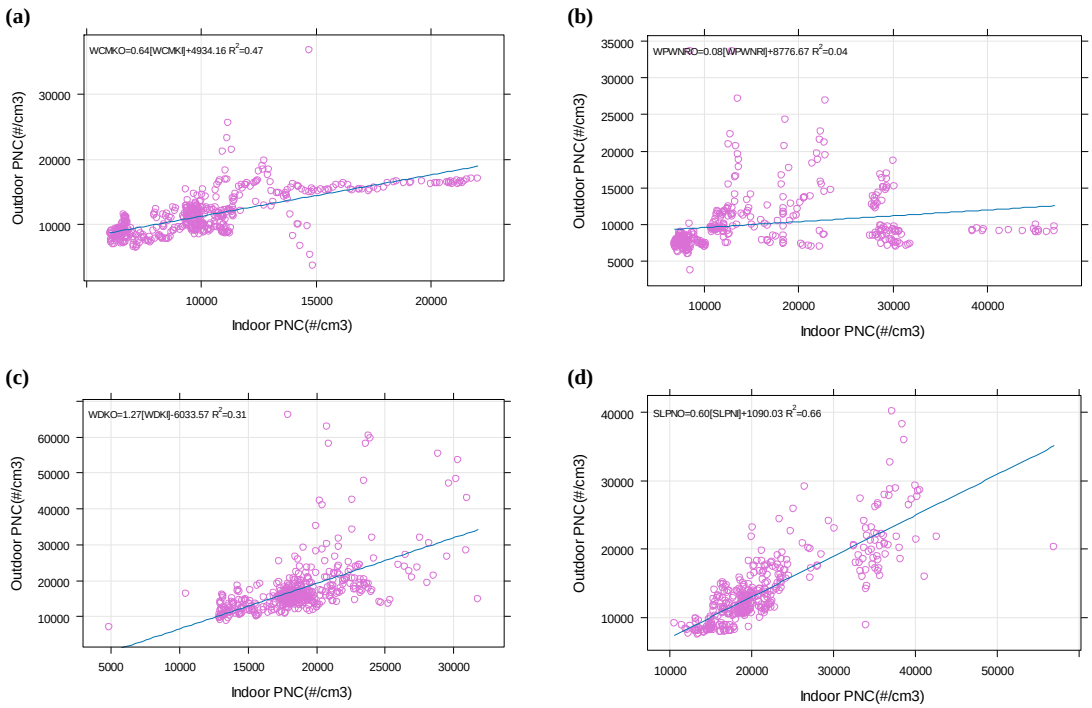

Figure 4 Scatter plot of linear regression analysis of weekday outdoor and indoor PNC in (a) S1, (b) S2, (c) S3 and (d) S4, respectively

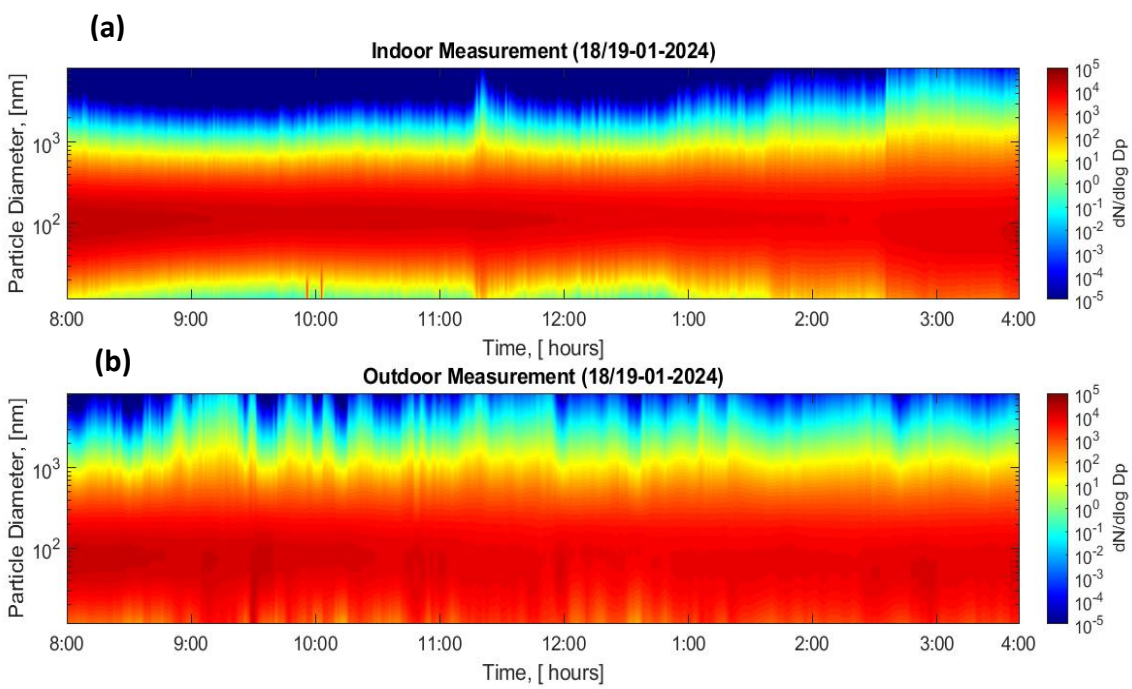

Figure 5 Particle number size distribution time series during weekday measurement for a) indoor and b) outdoor

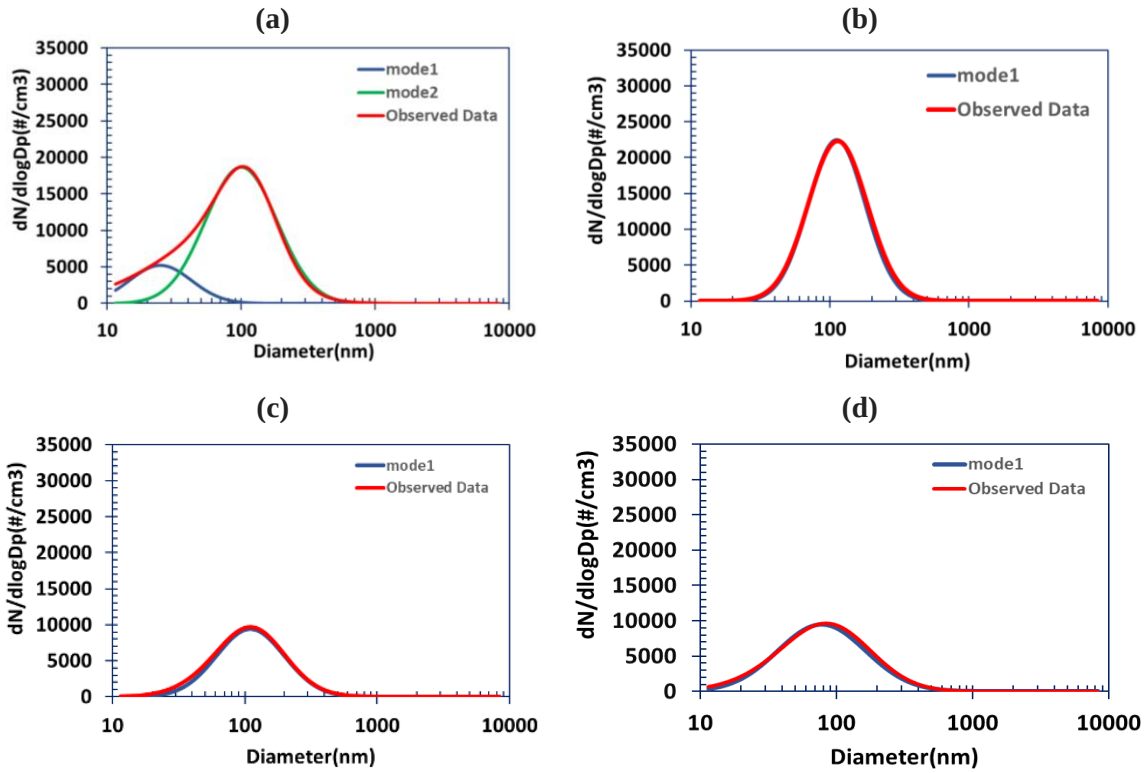

Figure 6 Multi-modal number size distribution plots of the weekday measurement for S1 for selected hours. a) outdoor 9-10 am, b) indoor 9-10 am, c) outdoor 2-3 pm, and d) indoor 2-3 pm. The lines are fitted mode 1 (blue), fitted mode 2 (green) and measured (red)

Table 3 Multi-modal number size distribution parameters of the weekday measurement for S1 for selected hours (1)9-10 am and (2)2-3 pm

	Fitted mode 1			Fitted mode 2		
	N (#/cm^3)	Dpg (nm)	$\sigma_{g\ (nm)}$	N (#/cm^3)	Dpg (nm)	$\sigma_{g\ (nm)}$
Out (1)	3000	23	1.7	12,000	100	1.9
In (1)	_	_	_	11,500	112	1.6
Out (2)	_	_	_	7,700	78	2.1
In (2)	_	_	_	6,500	110	1.8

As shown in Table 3, the existence of two separate modes indicates a combination of fresh emissions and aged particles from various sources in an outdoor environment. The lower concentration and smaller size of Mode 1 might be possible because of recently emitted particles from nearby traffic or other sources [13]. On the other hand, the bigger particles and greater concentration of Mode 2 are suggestive of aged particles that have grown in size over time after being emitted from sources such as transportation. Upon comparing the indoor PNSD with the outdoor PNSD at the same time as shown in Table 3, indoor shows that distributions center at bigger diameters and are narrower; this would be due to aging of outdoor particles. Even though the ventilation of the classroom is most of the time prevented with closed doors and windows, the indoor PNSD showed a sustained and stable distribution that

can be due to introduction of outdoor particles into the room at the beginning of the day together with the air purification device that generates disinfecting particles which operated throughout the operating hours [14].

Figure 7 shows the analysis of indoor/outdoor (I/O) hourly particle concentration ratios at four sites for weekday measurement. Particularly at sites S2 and S4, the ratios are consistently higher than 1. The elevated I/O ratio at site S2 may be attributed to its location situated far from the main road, implying a lower impact from outdoor vehicular emissions. The fact that there is less exposure to external contaminants in this setting indicates that interior sources or activities may have a greater impact on indoor air quality [14]. As for the site S4, the reason could be a combination of factors that the indoor purification system here differs from rest of the sites and also the fact that the road adjacent to the school (Wireless Road) is relatively less busy than the main road (Rama 4 road).

Weekend experiment results

The 1-hour average of outdoor particle number concentration (PNC) in the weekend analysis was 11,000 #/cm^3, 6,380 #/cm^3, 16,586 #/cm^3, and 11,627 #/cm^3 in S1, S2, S3 and S4, respectively. And then, the 1-hour mean of indoor PNC was 27,663 #/cm^3, 6,167 #/cm^3, 29,534 #/cm^3, and 13,977 #/cm^3, in each respective site. Although all outdoor PNC results showed the low PNC situation when comparing the WHO good practice for PNC [2], the indoor PNC of S1 and S3 revealed as the high PNC (>20,000 #/cm^3) during the cleaning activities.

The experiment was conducted during the weekend as tabulated in Table 1. The time-series PNSD are shown in Figure 8 for site S1. The indoor PNSD features fluctuation caused by the changing experimental setups while the outdoor PNSD exhibits similar features as that of the weekdays. Major change of the indoor PNSD can be seen at midday as the setup changes from open windows and doors to closed windows and doors. Obvious hotspots on the contour coincide with the cleaning activity with the use of cleaning agents containing volatile chemicals. The period right after cleaning also shows lingering particles undergoing microphysical growth. The PNSD of the interesting period with cleaning, namely, C4 and C6, are chosen to display the multi-modal size distribution in Figure 9 and the size distribution characteristics are presented in Table 4. The contrast between the indoor two-mode and the outdoor single-mode during cleaning activities highlights the influence of cleaning activities such as spraying cleaning agents and the use of volatile chemical products in mopping the floor.

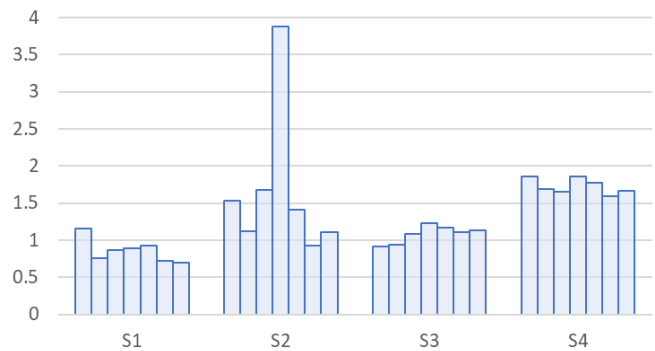

Figure 7 Weekday I/O ratios. Each bar presents hourly average value

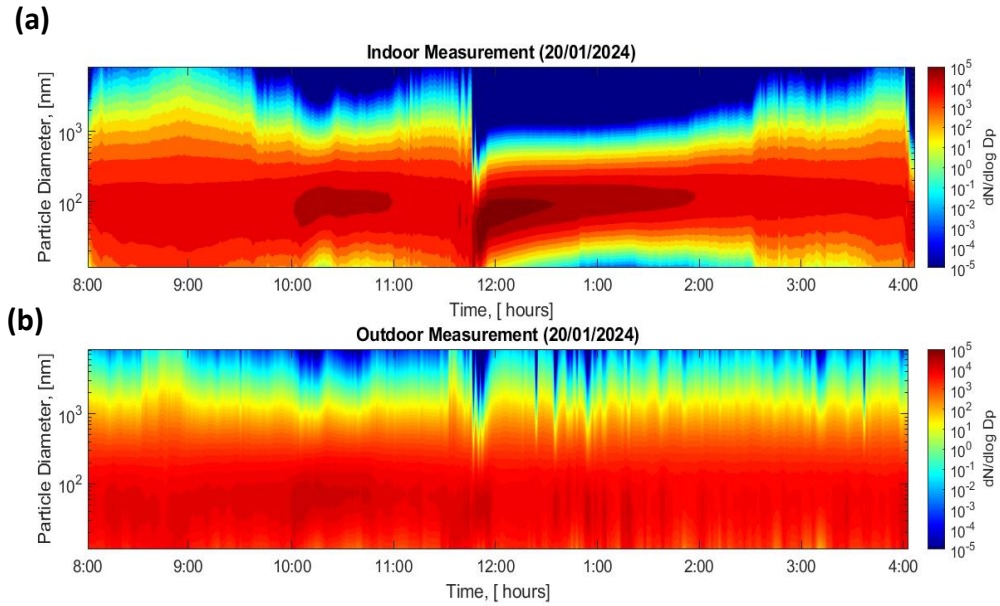

Figure 8 Particle number size distribution time series during weekend measurement for a) indoor and b) outdoor

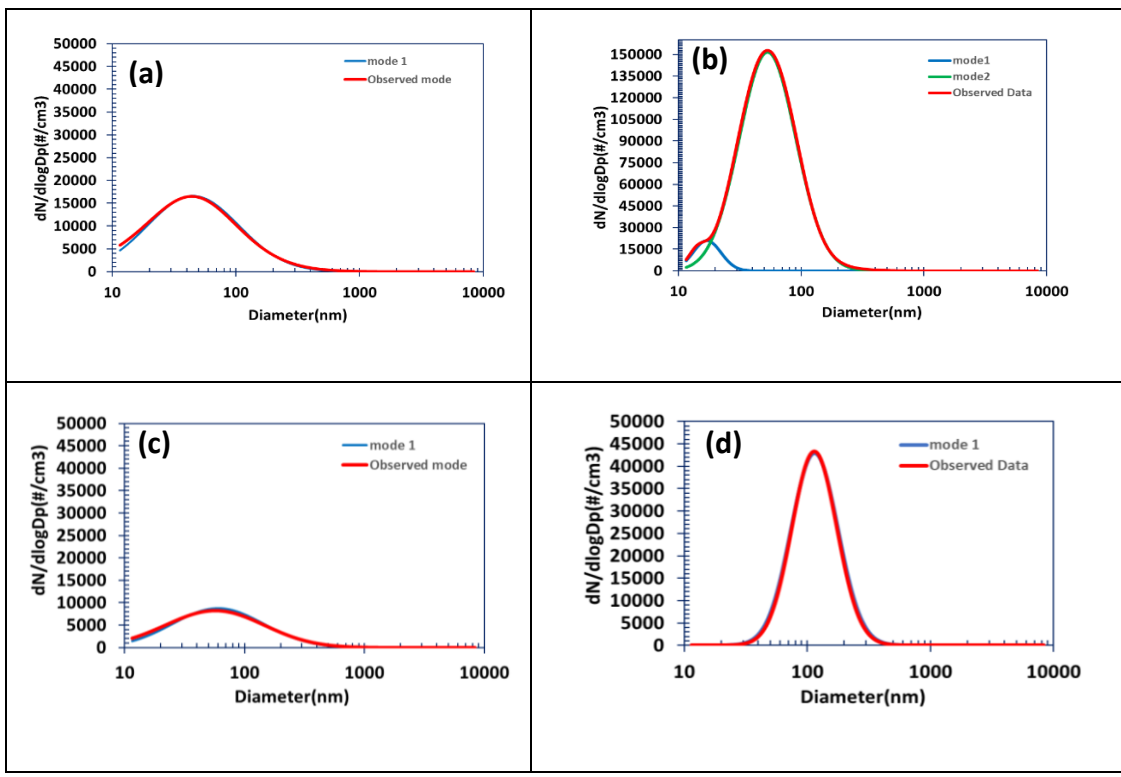

Figure 9 Multi-modal number size distribution plots of the weekend measurement for S1 for selected hours. a) outdoor 11:30-12:00 pm, b) indoor11:30-12:00 pm, c) outdoor 1:30-2:00 pm, and d) indoor 1:30-2:00 pm. The lines are fitted mode 1 (blue), fitted mode 2 (green) and measured (red)

The selected periods presented in Table 4 also highlight the difference between the open-window (C4b) and close window (C6b) conditions. It is speculated that open-window condition allows free flow of outdoor air that replenishes and supplies air with oxidation capacity thus the more likelihood of reactions of volatile organic compounds (VOCs) to become lower volatility products and secondary particles. The C6b condition shows lower number concentration and larger diameter population that may be explained by a combination of lower oxidation with the lack of outside air and the presence of the air purifying particles leading to coagulation growth. Nevertheless,[3] (1-hour average) that the WHO guideline specifies as high PNC condition.

When studying the particle number levels in classrooms under various cleaning and ventilation conditions, it was observed that stations S1 and S2 had the highest particle counts during C4b cleaning periods. The increase in pollutant levels can be due to the open windows, [15] which enable external air pollutants to enter. However, in C5, even though the cleaning process was finished, and the window was closed with the AC running, a higher level of particle number was still found. This indicates that the particles and precursor gas that linger in the indoor air and later contained by shutting down ventilation can lead to heighten concentrations. On the other hand, the particle number levels at station S4 reached their highest point in the morning, at the same time as the processes for opening windows. This provides evidence that natural ventilation has an important influence on the levels of particles indoors. The results highlight the complex connection between cleaning activities, HVAC system performance, and natural ventilation in affecting the indoor air quality in school environments [16]. Figure 10 presents the indoor/outdoor (I/O) hourly particle concentration ratios at four sites for weekend measurement. The ratios for S1 and S3 peak at condition C5 as discussed above. The reasoning why the peaking pattern of sites S1 and S3 were not replicated at sites S2 and S4 remains unclear and will need more in-depth investigation in future works.

Table 4 Multi-modal number size distribution parameters of the weekend measurement for S1 for selected condition

	Fitted mode 1			Fitted mode 2		
	N (#/cm^3)	**Dpg (nm)**	**$\sigma_{g\ (nm)}$**	**N (#/cm^3)**	**Dpg (nm)**	**$\sigma_{g\ (nm)}$**
Out -C4b	_	_	_	10500	45	2.3
In – C4b	6000	17	1.3	87500	53	1.7
Out- C6b	_	_	_	5700	97	1.5
In – C6b	_	_	_	20500	115	1.6

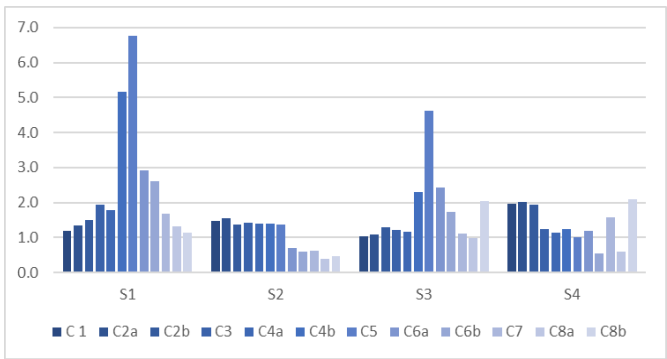

Figure 10 Weekend I/O ratios. Each bar presents the average value of each experiment condition

Conclusions

A comprehensive investigation of hourly average PNC from four schools in Bangkok central business district during regular weekday schedules indicated significant variation related to outdoor concentrations. The size distributions were observed to be unimodal for most of the study period. The particle number size distributions inside classrooms show connection to the outdoor particles that are influenced majorly by traffic emissions and size growth. The experiments conducted in the study indicated that cleaning activity indoors can cause surge of PNC likely due to cleaning agents. One school site revealed an average of the 1-hour mean PNC exceeding the high PNC level recommended by WHO. The results emphasize the need for intervention to improve air quality to safeguard the well-being of young children, particularly during periods of high indoor activity and cleaning procedures. This research helps establish the baseline information about ultrafine particles for future urban environmental policy, therefore preparing the way for sustainable school settings in increasingly urbanizing areas.

Acknowledgements

The author thanks the official staff from the Department of Environmental Engineering, Chulalongkorn University for their kind assistance during sampling. We thank the Sustainable Environment Platform of Chulalongkorn University for this collaboration. My gratitude goes to EnviGit for providing cusense.net data and Innovative Instruments Co., Ltd. for providing the SMPS and OPS instruments and their kind assistance. The author would like to thank the school authorities for their participation.

References

[1] Jareemit, D., J. Liu, and M. Srivanit, 2023. Modeling the effects of urban form on ventilation patterns and traffic-related $PM_{2.5}$ pollution in a central business area of Bangkok. Building and Environment. 244: 110756.

[2] WHO. 2021. WHO global air quality guidelines. Particulate matter ($PM_{2.5}$ and PM_{10}), ozone, nitrogen dioxide, sulfur dioxide and carbon monoxide. Geneva: World Health Organization.

[3] Mata, T. M., Martins, A. A., Calheiros, C. S. C., Villanueva, F., Alonso-Cuevilla, N. P., Gabriel, M. F. and Silva, G. V. 2022. Indoor Air Quality: A Review of Cleaning Technologies. Environments, 9(9), 118.

[4] Son, Y.-S. 2023. A review on indoor and outdoor factors affecting the level of particulate matter in classrooms of elementary schools. Journal of Building Engineering, 75: 106957.

[5] Tran, D.-H., Nguyen, M.-P., Dang, N.-M. and Pham, T.-T. 2022. Characterization of Size-Resolved Particles And chemical Composition at two Elementary Schools Inhanoi, EM International Journal. Vol 41, (Issue 3,): p. Page No.(837-852)

[6] Guo, H., Morawska, L., He, Congrong, Zhang, Y., Ayoko, Go, and Cao, M. 2010. Characterization of particle number concentrations and $PM_{2.5}$ in a school: influence of outdoor air pollution on indoor. air. Environmental Science and Pollution Research. 17(6): 1268-1278.

[7] Zhou, Y., Shao, Y., Yuan, Y., Liu, J., Zou, X., Bai, P., Zhan, M., Zhang, P., Vlaanderen, J., Vermeulen, R., Downward, G.S. 2020. Personal black carbon and ultrafine particles exposures among high school students in urban China. Environmental Pollution. 265: 114825.

[8] Heo, S., Kim, D.Y., Kwoun, Y., Lee, T.J. and Jo, Y.M.. 2021. Characterization and source identification of fine dust in Seoul elementary school classrooms. Journal of Hazardous Materials. 414: 125531.

[9] TESTO. Air velocity & IAQ measuring instrument. Available from: https://www.testo.com.

[10] Aethair IAQ, T.S. Aethair IAQ, Techanical Specification. Available from: https://aethair.io/products/iaq.

[11] Kalaiarasan, G., Kumar, P., Tomson, M., Zavala-Reyes, J. C., Porter, A. E., Young, G., Sephton, M. A., Abubakar-Waziri, H., Pain, C. C., Adcock, I. M.,

Mumby, S., Dilliway, C., Fang, F., Arcucci, R. and Chung, K. F. 2024. Particle Number Size Distribution in Three Different Microenvironments of London. Atmosphere, 15(1), 45. https://doi.org/10.3390/atmos15010045.

[12] Sadrizadeh, S., Yao, R., Yuan, F., Awbi, H.B., Bahnfleth, W., Bi, Y., Cao, G., Croitoru, C., de Dear, R., Haghighat, F., Kumar, P., Malayeri, M., Nasiri, F., Ruud, M., Sadeghian, P., Wargocki, P., Xiong, J., Yu, W. and Li, B. 2022. Indoor air quality and health in schools: A critical review for developing the roadmap for the future school environment. Journal of Building Engineering. 57. 104908. 10.1016/j.jobe.2022.104908.

[13] Riley, W.J., McKone, T.E., Lai., A.C.K. and Nazaroff, W.W. 2002. Indoor Particulate Matter of Outdoor Origin: Importance of Size-Dependent Removal Mechanisms. Environmental Science & Technology. 36(2): 200-207.

[14] Lee, W.-C., Catalano, P.J., Yoo, J.Y., Park, C.J. and Koutrakis, P. 2015. Validation and Application of the Mass Balance Model To Determine the Effectiveness of Portable Air Purifiers in Removing Ultrafine and Submicrometer Particles in an Apartment. Environmental Science & Technology. 49(16): 9592-9599.

[15] Jung, C., Samanoudy, G.E. and Alqassimi, N. 2023. Assessing the impact of ventilation systems on indoor air quality: a mock-up experiment in Dubai. Frontiers in Built Environment. 9.

[16] Mata, T. M., Martins, A. A., Calheiros, C. S. C., Villanueva, F., Alonso-Cuevilla, N. P., Gabriel, M. F. and Silva, G. V. 2022. Indoor Air Quality: A Review of Cleaning Technologies. Environments. 9: 118.

Thai Environmental Engineering Journal Vol. 38 No. 3 (2024) : 35-44
www.eeat.or.th

Sustainable Tourism Management Using Waste Minimization Approach: A Case Study of an Elephant Park in Chiang Mai

Palita Kunchorn[1] and Alice Sharp[2*]

[1]Environmental Science Research Center, Faculty of Science, Chiang Mai University, Mueang Chiang Mai, Chiang Mai 50200, Thailand
[2]Department of Biology, Faculty of Science, Chiang Mai University, Mueang Chiang Mai, Chiang Mai 50200, Thailand
[*]E-mail : alice.sharp@cmu.ac.th

Article History; *Received: 27 May 2024, Accepted: 12 November 2024, Published: 24 December 2024*

Abstract

Elephant Park is one of the famous tourist destinations in many districts of Chiang Mai. The growth of tourism in elephant parks has a positive effect on national and local economies. However, tourist activities create solid waste, food waste, and elephant dung. Without proper waste management, environmental issues may arise. Therefore, this research aims to study the current solid waste situation in the elephant park, develop a solid waste management strategy using a waste minimization approach, and implement pilot activities. One of the elephant parks in Chiang Mai was used as a case study. Several methodological approaches have been used in this research, including surveying the elephant park, interviewing stakeholders, collecting solid waste, identifying waste characteristics and streams, improving compost quality from elephant dung, and developing waste separation points. Descriptive statistics and content analysis were used to analyze the data. Finally, all data will be used to construct a sustainable solid waste management strategy for the elephant park. The results showed that the elephant park produces an average waste of 10.84 kg per day from tourist activity. These wastes could be classified into four types, namely organic waste (27.16%), recyclable waste (15.36%), general waste (55.77%), and hazardous waste (1.71%), respectively. A person at the elephant park produces an average of waste at 0.03 kg/day. Waste minimization activities for the two major categories were proposed. It includes waste separation points for recyclables and improvement of compost quality from elephant dung. In addition, all people in the elephant park need to sort their waste correctly before disposal to make it easier to manage and help reduce the amount of waste that goes to landfill. In the future, the researcher recommends conducting follow-up assessments after implementing the management strategy.

Keywords : solid waste; elephant park; waste management; elephant dung

Introduction

Solid waste management is one of the challenging issues in many countries, particularly in developing countries. Developing economic systems, tourism, and urban community expansion in these countries have increased the amount of solid waste generated. The assessment of solid waste management in Thailand by the Pollution Control Department found that in 2023 [1], 26.95 million tons of solid waste were generated from various sources. Compared to 2022, solid waste increased by 5 percent (25.70 million tons), with 27.7 percent of the total solid waste generated improperly eliminated. When considering Chiang Mai province, it was found that it produced up to 1,475 tons of solid waste daily in 2023. Improper waste management, specifically open dumps and burning, can lead to other environmental problems, such as wastewater and groundwater contamination. Even proper management technologies, like landfills, can increase the emission of greenhouse gases. Landfill management can produce landfill gases that include CH_4, CO_2, CO, H_2S, N_2, NH_3,

O_2, and water vapour [2], contributing to the global climate change problem. According to the United States Environmental Protection Agency (USEPA) [3], waste disposal methods by bulk and landfill contribute to the third-largest methane emissions of human-caused methane emissions. Methane gas has a Global Warming Potential (GWP) 28 times greater than carbon dioxide [4].

Thailand's tourism industry is experiencing high growth and is crucial to the country's economy and social system, serving as a significant source of income [5]. In 2023, the Ministry of Tourism and Sports reported that Thailand welcomed approximately 28 million international tourists, generating revenue of 1.2 trillion Bath, a figure expected to rise in the future. However, tourism also significantly contributes to waste generation [e.g., 6-7]. However, tourism is also a significant contributor to waste generation. Proper management of tourism-related waste can alleviate the burden on local government organizations tasked with waste management and contribute to more effective conservation of natural resources and the environment.

Chiang Mai boasts majestic mountains, lush forests, cascading waterfalls, and abundant natural resources. Its captivating blend of stunning scenery and unique art and culture continuously attracts both Thai and foreign tourists. Among its famous tourist attractions are the elephant parks scattered across many districts. These parks offer a variety of activities, including elephant shows, painting, bamboo rafting, ox-cart riding, and more. The growth of tourism in these elephant parks has positively impacted both national and local economies. A study by Kontogeorgopoulos (2009) [8] shows how wildlife tourism, particularly in elephant parks, contributes significantly to the local economy in northern Thailand. However, without proper environmental management, including the handling of solid waste, elephant dung, and other wastes, there is a risk of environmental degradation and related issues. Research by Salangam et al. (2019) [9] highlights the urgent need for effective waste management practices to mitigate environmental impacts in elephant parks, emphasizing the importance of implementing better practices to avoid long-term environmental harm.

To address these challenges, adopting a waste minimization approach is imperative. This strategy focuses on reducing waste produced by individuals, businesses, and society rather than focusing solely on waste disposal or management after it'cams produced. The main principles of waste minimization are source reduction, reuse, recycling, composting and education and awareness. Waste minimization aims to shift society towards a more sustainable, resource-efficient approach to consumption and waste management, ultimately reducing the environmental impacts of waste generation and disposal.

Amidst this backdrop, the importance of adopting a waste minimization approach becomes evident. Hence, this research aims to investigate the current solid waste situation within the elephant park, develop a solid waste management strategy utilizing a waste minimization approach, and implement pilot activities in environmentally friendly tourist destinations by integrating the concept of minimizing waste into management in the study area. One of the Elephant Parks in Chiang Mai was used as a case study. The sustainable tourism management scheme aims to avoid environmental problems, especially the waste generated from the activities of the elephant park and tourists visiting. Furthermore, this research aligns with Thailand's 20-year National Strategy [10], which underscores the imperative of developing sustainable tourism practices and curbing greenhouse gas emissions.

Methodology

In this research, several methodological approaches have been employed to study the current solid waste situation at one of the elephant parks in Chiang Mai province. This park provides various tourist activities, including elephant shows, elephant rides, ox-cart rides, and bamboo rafting, as well as amenities such as parking, restaurants, and shops. The research aims to develop a solid waste management strategy using a waste minimization approach and to implement pilot activities. Data analysis was conducted using descriptive statistics and content analysis. The research process is outlined in the flow chart presented in Figure 1.

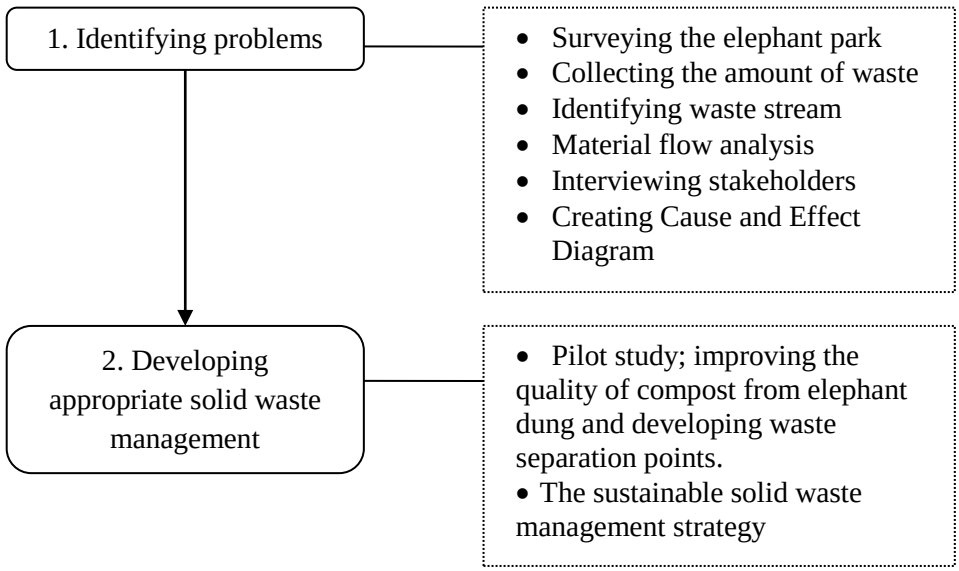

Figure 1 Research Framework

Identifying Problems

To identify the problems regarding solid waste management in the elephant park, the researchers conducted a site survey and interviewed the owner, manager, assistant manager and head cook to understand how they manage solid waste. After that, the researchers collected data on the amount and composition of waste generated from tourism activities at various locations within the elephant park, including an office, a restaurant, toilets, a shop, and all trash cans, for seven days in January 2023. This data was used to calculate the average waste weight per day (kg/day) and per person (kg/person). The average daily waste weight was calculated by dividing the total waste collected over seven days by the number of collection days. Additionally, the average waste generated per tourist was determined by dividing the total waste weight over the seven-day period by the total number of tourists during that time. Finally, all collected data were used to create a waste stream and cause-and-effect diagrams using STAN version 2.7.101."

Developing an Appropriate Solid Waste Management Strategy

Waste stream and Cause-and-Effect Diagrams were utilized for decision-making and to develop a sustainable solid waste management strategy, employing a waste minimization approach and implementing pilot activities. These activities included enhancing compost quality from elephant dung and establishing waste separation points. In the elephant dung compost experiments, researchers mixed elephant dung with other waste materials, such as cattle dung and food waste, to improve compost quality. Compost quality will be analyzed using the following parameters: nitrogen, phosphorus, potassium, amount of organic matter, complete decomposition, carbon-to-nitrogen ratio, sodium, and pH by the Institute of Product Quality and Standardization, Maejo University. Additionally, three waste separation points were established within the elephant park. Waste bins of different colors were provided for proper segregation: red for hazardous waste, blue for general waste, green for food waste, and yellow for recyclables. Finally, recommendations will be provided to the park owner on the most effective solid waste management strategy.

Results and Discussion

The Current Solid Waste Situation

The cause-and-effect diagram in Figure 2, developed through surveys and interviews with stakeholders, identifies key waste management issues at the elephant park. The root causes of the problem can be divided into four main categories: management practices, types of waste

generated, lack of waste separation points, and human factors. Currently, waste management at the park lacks systematic organization. A significant volume of food scraps and elephant dung must be dealt with daily, and proper waste separation points are lacking. Additionally, the insufficient knowledge and understanding of waste separation among staff and visitors exacerbate the problem. This is further complicated by language barriers, as many employees do not speak Thai, and tourists come from diverse cultural backgrounds, making it challenging to educate individuals on proper waste management practices. These underlying causes contribute to the accumulation of mixed waste destined for landfills.

The identification of management practices, types of waste, lack of separation points, and human factors as root causes of waste management issues aligns with broader trends observed in ecotourism. Pham Phu et al. (2019) [11] similarly identified inefficient management practices as a major factor contributing to poor waste handling in ecotourism destinations. Nayono S. & Nayono S.E. (2021) [12] emphasized the need for structured waste management frameworks that address both infrastructural shortcomings and the educational needs of staff and tourists. These findings reinforce the necessity of comprehensive strategies that integrate improved waste collection infrastructure with education and training programs, particularly in contexts like elephant parks, where large volumes of organic waste are generated.

According to the waste material flow shown in Figure 3, solid waste at the elephant park can be divided into two main categories: waste generated from human activities and waste generated by elephants. The total amount of solid waste that must be managed daily is 2,393.84 kg. The largest portion of this waste is elephant dung. As herbivores, elephants consume a diet primarily consisting of ripe bananas, leaves, bamboo, tree bark, and other fruits. They spend up to 18 hours a day eating and typically consume 100–200 kilograms of food daily. For example, a female elephant weighing 3,000 kg will eat around 168 kg/day, while a 4,000-kg bull will consume 192 kg/day. Given that elephants only digest about 40% of their food, they produce approximately 50–60 kg of dung daily [13]. With 47 elephants in the park, this amounts to around 2,350 kg of dung per day, making it the primary waste that the park must manage.

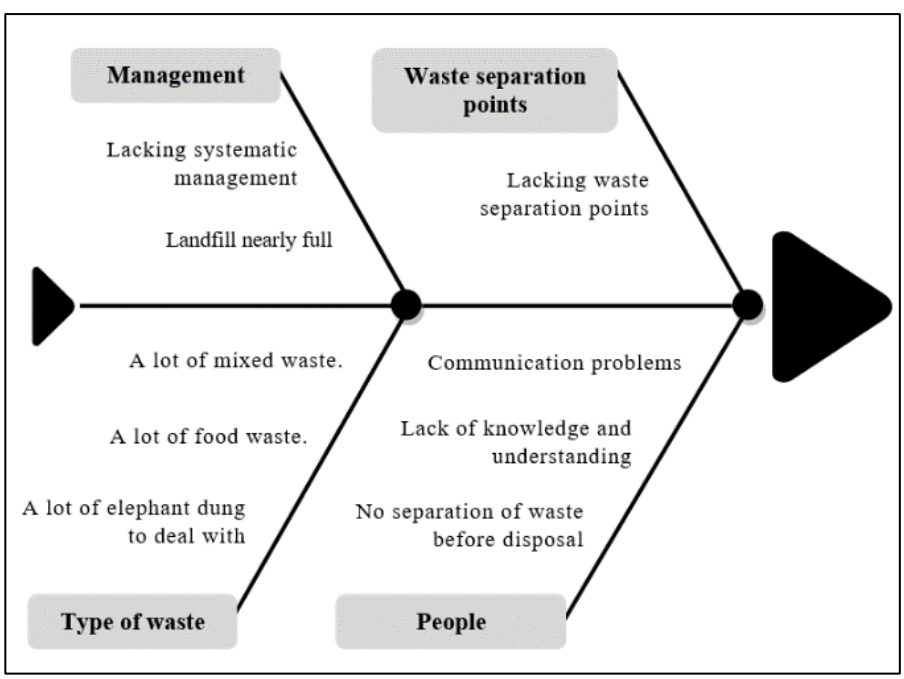

Figure 2 Cause and Effect Diagram of the Waste Management Problem in the Elephant Park

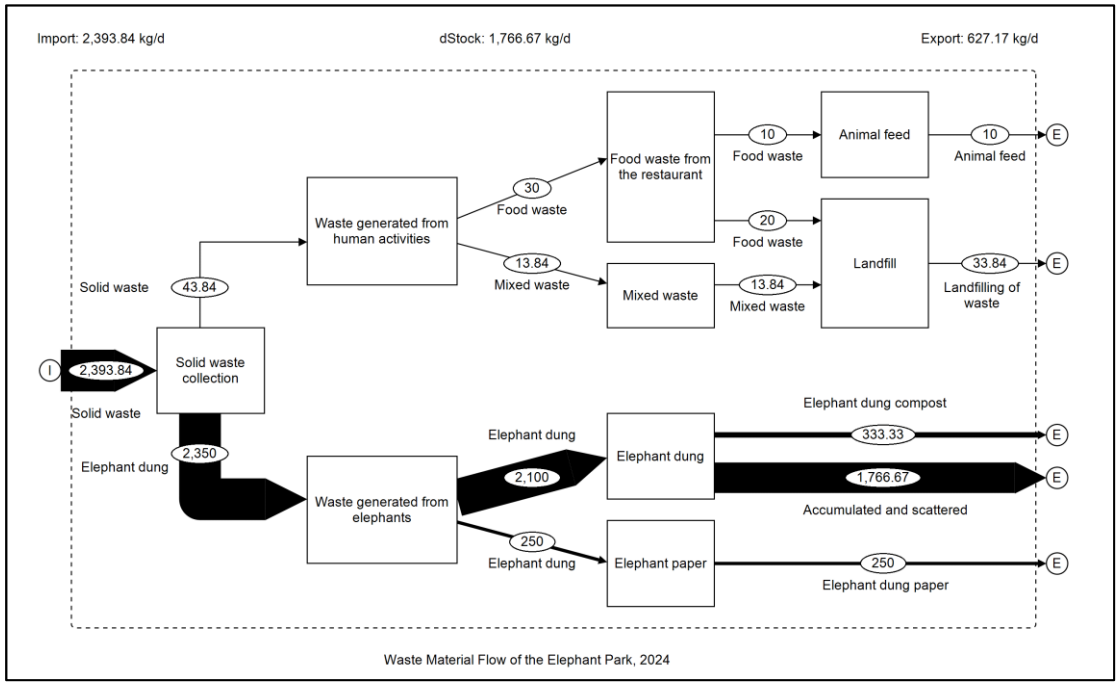

Figure 3 Waste Material Flow of the Elephant Park

In our initial survey and interview with the manager, it was revealed that approximately 250 kg of elephant dung per day is used to produce dung paper, while another 333.33 kg is utilized for composting, though this is done by dumping the dung in an open field without any treatment. Upon examination of the compost quality by the Institute of Product Quality and Standardization at Maejo University, it was found that many parameters, such as nitrogen, phosphorus, and organic matter, were below the standards set by the Department of Agriculture [14]. Thus, improvements are needed to enhance the quality of the compost and add value to the products derived from elephant dung. Details of these experiments are provided in Section 3, "Improving the Quality of Elephant Dung Compost."

The waste data indicate that tourism activities within the park generate an average of 10.84 kg of solid waste per day. This figure does not include the approximately 2,350 kg/day of elephant dung, 30 kg/day of food waste from the restaurant, or 3 kg/day of recyclable office waste. These findings are consistent with those of Pham Phu et al. (2019) [15], who found that ecotourism sites tend to generate a significant amount of waste, often exceeding regular household waste per capita due to the high concentration of visitors in limited areas. Tourists in natural parks typically contribute a substantial amount of both organic and general waste, with a growing trend in plastic consumption and disposal.

The waste composition is classified into four categories: organic waste (27.16%), recycling waste (15.36%), general waste (55.77%), and hazardous waste (1.71%). Organic waste, which includes leaves and food waste, accounts for 27.16%. Recycling waste consists of glass (14.77%), aluminum (0.33%), and metal cans (0.26%). General waste, which makes up the largest portion, includes non-recyclable plastics (23.99%), paper (26.37%), and other materials (5.41%). Hazardous waste consists mainly of masks (1.45%) and batteries (0.26%). Similar patterns were observed by Nayono S. & Nayano S.E. (2021) [12], who found that rural tourism destinations often generate a high percentage of non-recyclable general waste, largely due to insufficient waste separation practices. Our study supports this argument but adds the layer of quantifying waste generation per person, which averages 0.03 kg/day. While this figure seems low, the cumulative effect over time is considerable, particularly during high tourist seasons, echoing Nayono's observations of waste accumulation.

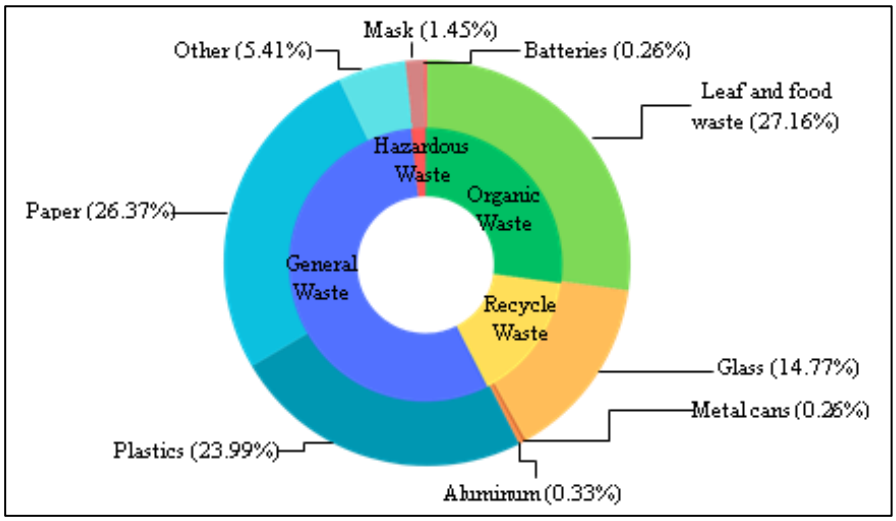

Figure 4 Waste Composition

One of the unique contributions of this study is its focus on elephant parks, a distinct context within waste management in ecotourism. Elephant parks have a different waste profile compared to typical tourism sites due to the large amount of organic waste, including elephant dung and plant matter, which make up 27.16% of the total waste. This highlights the need to design waste management strategies that are tailored to the specific requirements of such destinations. By focusing on waste issues in an elephant park, this study not only adds to the body of knowledge on waste management in ecotourism but also offers a specialized approach to addressing waste in wildlife tourism environments.

The Solid Waste Management Strategy

The solid waste management strategy for the elephant park has been developed through a comprehensive process involving surveys, waste data analysis, interviews, and the utilization of waste flow and cause-and-effect diagrams. This strategy aims to effectively address the waste management challenges identified in the park. The following recommendations are proposed:

1. Constructing systematic management:
   - The cleaning staff will assume responsibility for daily waste collection, categorizing waste by type.
   - Food waste will be repurposed as animal feed and compost, while elephant dung will be used in paper production.
   - Water and ice waste will be repurposed for watering plants.
2. Establishing appropriate waste separation points:
   - Five types of waste bins are proposed: general waste, recycling waste, food waste, water and ice waste, and hazardous waste.
   - The hazardous waste bin will be located at the Elephant Park office for proper disposal by municipal authorities.
   - Waste separation points should have clear signs indicating the type of waste to encourage people to segregate waste properly.
3. Educating both employees and tourists about waste separation to enhance understanding and awareness:
   - Interesting projects will be implemented to educate employees and tourists about waste separation practices.
   - Media campaigns will be established to promote waste segregation among employees and tourists.
4. Improving the quality of elephant dung compost:
   - Elephant dung will be used as raw material for compost processing, and the resulting products will be sold to mediators. However, efforts should be made to improve the quality of elephant dung composting and

shorten the fermentation time. This will help reduce the accumulated dung and ensure the production of products that meet market demand.

5. Converting the accumulated elephant dung to biogas:
   - Due to the limitations of composting and the necessity of adding additional materials to improve quality, resulting in increased production costs, the authors suggest using accumulated elephant dung as raw material for biogas processing to convert dung to energy. This is an effective method for reducing the main organic waste in the elephant park.

Implementing proper waste separation will lead to increased recycling rates and a reduction in general waste. Organic waste will be utilized as animal feed, compost, and for biogas production. Recyclable materials, including glass, paper, plastic, metal cans, and aluminum, will be sold to waste buyers, generating additional income for the park. Hazardous waste disposal will be managed appropriately by the subdistrict administrative organization.

The expected outcome of implementing this waste management strategy is a significant reduction in the amount of general waste sent to landfills, estimated at up to 33.25 kg/day (from 33.84 kg/day to 0.59 kg/day). Figure 5 illustrates the predicted waste volume when managed effectively, highlighting the potential for the elephant park to become a model ecotourism destination for waste reduction in the future.

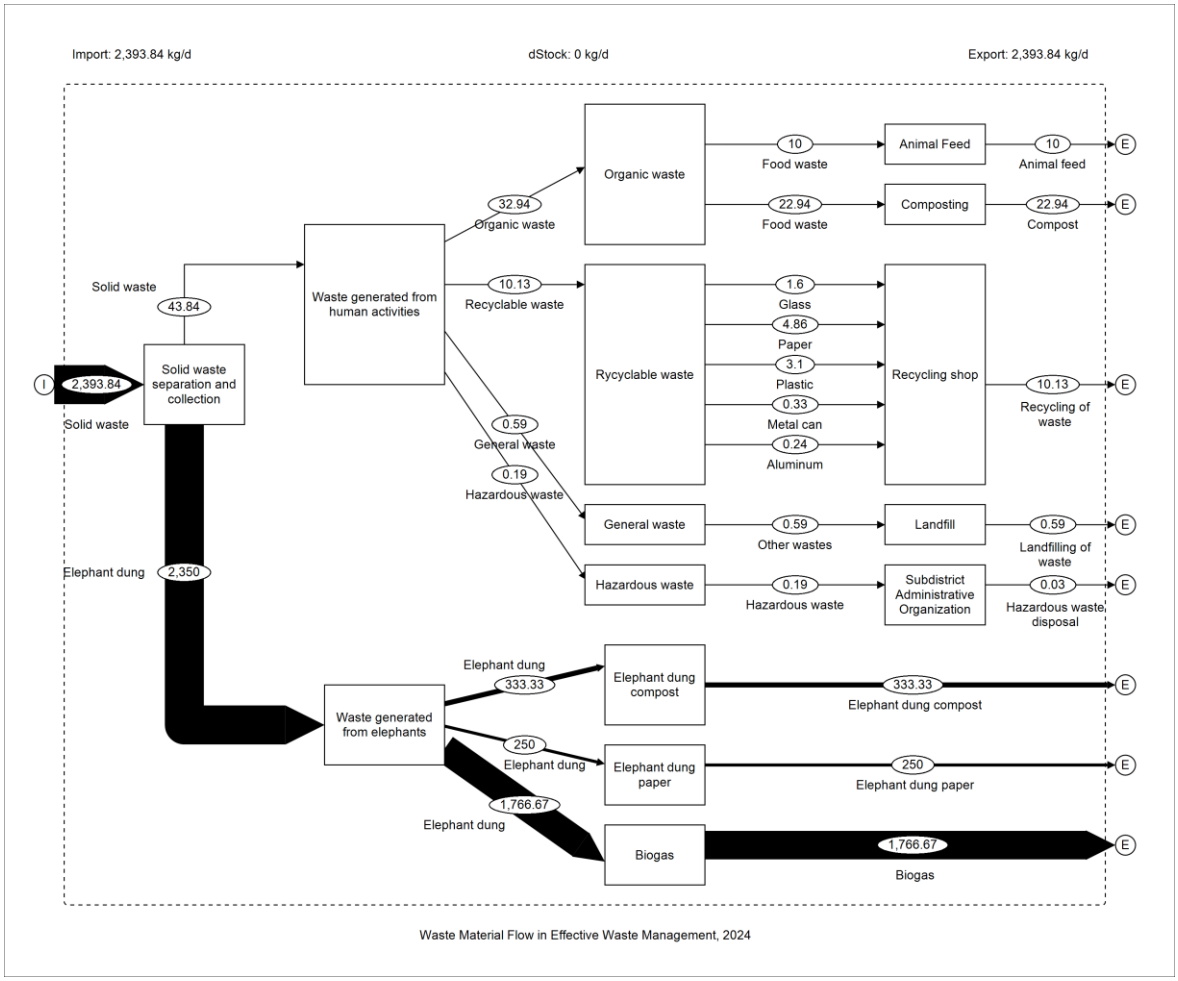

Figure 5 Waste Material Flow in Effective Waste Management in the Elephant Park

Improving the Quality of Elephant Dung Compost

This study aimed to improve the quality of elephant dung compost by incorporating organic waste from the elephant park, reducing the overall amount of organic waste generated in the elephant park. Elephant dung, cattle dung and food waste were used in this experiment in different ratios, as shown in Table 1. There are four treatments, namely the control (based on the quality inspection results of the elephant park), Formula 1, 2 and 3. Each treatment was replicated three times. In addition, phosphate rock and P.D.1 (microbial activators for composting produced by the Land Development Department) were added to all treatments. Compost piles were turned every week to enhance oxygen circulation within the pile. The composting process continued until the compost reached a dark brown or black colour, the internal temperature of the pile decreased, and it emitted a soil-like smell. Samples were sent to the Institute of Product Quality and Standardization, Maejo University, to assess the compost's quality. The experimental results are presented in Table 2.

The findings indicate that composts from all formulations (F1, F2, and F3) still show nitrogen, phosphorus, and organic matter levels below the standards set by the Department of Agriculture (as shown in Table 2). These results reflect common challenges faced in composting practices, particularly when handling large volumes of organic waste, such as elephant dung. Similar limitations in compost quality have been documented in studies, such as by Ayilara et al. (2020) [16], who found that nutrient imbalances, time constraints, and pathogen management often impede compost quality in agricultural settings. These factors are particularly problematic in systems dealing with high quantities of organic waste, such as those generated by wildlife tourism facilities. In our study, the limitations in elephant dung composting can be attributed to the complex nature of the raw materials, which require careful management of moisture, aeration, and nutrient balance. These challenges are consistent with findings by Azim et al. (2017), who emphasized that achieving optimal composting results requires precise control over raw material ratios and environmental conditions [17]. Future improvements in the composting process could benefit from a more controlled environment and additional raw materials. Incorporating nutrient-rich materials, such as Napier Grass and bat guano, into the composting process could be a potential solution to improve nutrient content. Studies have shown that Napier Grass, due to its high nitrogen content, can significantly enhance compost quality when used in combination with other organic materials [18]. Similarly, bat guano has been widely recognized for its high phosphorus content, which not only accelerates the decomposition process but also enhances the overall nutrient profile of the compost [19]. These materials are therefore recommended for future studies aiming to optimize compost nutrient levels and shorten fermentation times. Our study contributes to the existing body of literature by applying these composting principles in the unique context of an elephant park, where organic waste is predominantly composed of elephant dung. This focus on wildlife tourism sites adds an important dimension to the current understanding of composting challenges in ecotourism destinations. By integrating locally available, high-nutrient materials into the composting process, we aim to provide a sustainable waste management solution for elephant parks, thus advancing the field of waste management in ecotourism.

Table 1 Proportion of Elephant Dung, Cattle Dung, and Food Waste in Each Treatment

Treatment	Proportion		
	Elephant dung	**Cattle dung**	**Food waste**
Control	Based on the results of the quality inspection of the Elephant Park		
Formula 1 (F1)	0.5	0.5	-
Formula 2 (F2)	0.8	0.1	0.1
Formula 3 (F3)	0.8	0.15	0.05

Table 2 The Quality of the Elephant Dung Compost by the Institute of Product Quality and Standardization, Maejo University

Parameters	Standard value	Unit	Mean ± SD			
			Control	F1	F2	F3
Total Nitrogen	≥1.0	% by weight	0.70	0.57±0.09	0.68±0.08	0.61±0.01
Phosphorus (P_2O_5)	≥0.5	% by weight	0.06	0.31±0.03	0.24±0.05	0.23±0.06
Potassium (K_2O)	≥0.5	% by weight	0.81	1.42±0.47	0.95±0.20	0.79±0.18
Organic Matter	≥20	% by weight	14.47	17.14 ±0.41	15.75±0.68	17.76±3.12
Germination Index	>80	%	99.72	100.52±0.25	97.83±1.15	90.53±7.79
C/N Ratio	≤20:1	-	12.00	18.00±2.16	13.33±1.25	17.00±2.65
Sodium	≤1	% by weight	0.01	0.07±0.02	0.10±0.02	0.21±0.27
pH	5.5-8.5	-	6.58	6.66±0.15	7.42±0.02	7.54±0.04

Conclusions

This study devised a comprehensive solid waste management strategy for an elephant park in Chiang Mai by employing a waste minimization approach. Key findings indicate that the park generates significant waste, primarily from tourist activities and elephant dung. By implementing pilot activities, including composting elephant dung and establishing waste separation points, the research demonstrated practical methods to reduce the environmental impact of the park. The research identified challenges in current waste management practices, including the lack of systematic waste separation and the need for better education among staff and tourists. Composting experiments revealed that improving the quality of elephant dung compost is crucial for enhancing its usability, though further improvements in compost quality are necessary. Based on these findings, practical recommendations include continuing to improve compost quality, educating park employees and tourists on waste segregation, and exploring alternative uses for elephant dung, such as biogas production. Future research should focus on assessing the long-term impact of these strategies and collecting seasonal data to refine waste management practices. Implementing these recommendations could position the elephant park as a model for sustainable tourism and waste reduction.

Acknowledgements

The authors are thankful for the financial support from the faculty of Science at Chiang Mai University and the Development and Promotion of Science and Technology Talents Project scholarship.

References

[1] Pollution Control Department (PCD). 2023. Information on the country's solid waste situation. Available from: https://thaimsw.pcd.go.th/report_country.php?year=2566.

[2] Osra, F. A., Ozcan, H. K., Alzahrani, J. S. and Alsoufi, M.S. 2021. Municipal solid waste characterization and landfill gas generation in kakia landfill, Makkah. Sustainability. 13(3): 1462.

[3] United States Environmental Protection Agency (USEPA). 2023. Basic Information about Landfill Gas. Available from: https://www.epa.gov/lmop/basic-information-about-landfill-gas.

[4] Intergovernmental Panel on Climate Change (IPCC). 2014. Synthesis Report. Climate Change 2014: The Physical Science Basis. Contribution of Working Groups I, II and III to the Fifth Assessment Report of the Intergovernmental Panel on Climate Change.

[5] Sriarkarin, S., and Lee, C.H. 2008. Integrating multiple attributes for sustainable development in a national park. Tourism Management Perspectives. 28: 113-125.
[6] Obersteiner, G., Gollnow, S. and Eriksson, M. 2021. Carbon footprint reduction potential of waste management strategies in tourism. Environmental Development. 39: 100617.
[7] Sakcharoen, T., Niyommaneerat, W., Faiyue, B. and Silalertruksa, T. 2023. Low-carbon municipal solid waste management using bio-based solutions and community participation: The case study of cultural tourism destination in Nan, Thailand. Heliyon. 9(11).
[8] Kontogeorgopoulos, N. 2009. Wildlife tourism in semi-captive settings: A case study of elephant camps in northern Thailand. Current Issues in Tourism. 12(5-6): 429-449.
[9] Salangam, A., Phimyon, J., Kessada, P., Phuengphai, P., Thanomsit, C., Jamnongkan, T., Tongnunui, S. and Wattanakornsiri, A. 2019. Solid Waste Quantity, Composition and Characteristic, and Its Current Management at Elephant Study Center (Surin, Thailand). Naresuan University Journal: Science and Technology (NUJST). 27(2): 48-57.
[10] Office of the National Economic and Social Development Council (NESDC). 2021. Thailand's 20-year National Strategy (2018-2037).
[11] Pham Phu, S. T., Fujiwara, T., Hoang, M. G., Pham, V. D., and Tran, M. T. 2019. Waste separation at source and recycling potential of the hotel industry in Hoi An city, Vietnam. Journal of Material Cycles and Waste Management. 21: 23-34.
[12] Nayono, S. and Nayono, S. E. 2021. Mapping the Problems, Stakeholders, and Potential Solutions of Solid Waste Management in a New-Emergence Tourist Area: A Case Study in Nglanggeran, Gunungsewu UNESCO Global Geopark. In IOP Conference Series: Earth and Environmental Science. 832(1): 012066.
[13] Schliesinger, J. 2015. Elephants in Thailand vol 1: Mahouts and their cultures today. Booksmango.
[14] Announcement of the Department of Agriculture subject Criteria for organic fertilizers, B.E. 2557. Available from: https://www.doa.go.th/ard/wp-content/uploads/2019/11/FEDOA11.pdf.
[15] Pham Phu, S. T., Fujiwara, T., Hoang Minh, G. and Pham Van, D. 2019. Solid waste management practice in a tourism destination–The status and challenges: A case study in Hoi An City, Vietnam. Waste management & research. 37(11): 1077-1088.
[16] Ayilara, M. S., Olanrewaju, O. S., Babalola, O. O. and Odeyemi, O. 2020. Waste management through composting: Challenges and potentials. Sustainability. 12(11): 4456.
[17] Azim, K., Soudi, B., Boukhari, S., Perissol, C., Roussos, S. and Thami Alami, I. 2018. Composting parameters and compost quality: a literature review. Organic agriculture. 8: 141-158.
[18] Pakwan, C., Jampeetong, A. and Brix, H. 2020. Interactive effects of N form and P concentration on growth and tissue composition of hybrid Napier grass (Pennisetum purpureum× Pennisetum americanum). Plants. 9(8): 1003.
[19] Palita, S. K., Panigrahi, R. and Panda, D. 2021. Potentiality of bat guano as organic manure for improvement of growth and photosynthetic response in crop plants. Proceedings of the National Academy of Sciences, India Section B: Biological Sciences. 91(1): 185-193.

Thai Environmental Engineering Journal Vol. 38 No. 3 (2024) : 45-54
www.eeat.or.th

Workplace Environment and Health Effects of Ribbed Smoked Sheet Factory: A Case Study of Thung Yai Rubber Fund Cooperative

Supandee Maneelok[1], Peerapol Juntaro[2], Rattatammanoon Ainthong[2], Peerapol Kaoien[3] and Nantaporn Noosai[4*]

[1]Department of Occupational Health and Safety, Faculty of Health and Sports Science, Thaksin University, Phatthalung 93210, Thailand
[2]Department of Occupational Health and Safety, Faculty of Health and Sports Science, Thaksin University, Phatthalung 93210, Thailand
[3]Siam General Technology Co., Ltd., Trang 92140, Thailand
[4]Department of Civil and Environmental Engineering, Faculty of Engineering, Prince of Songkla University, Hat Yai, Songkhla 90112, Thailand
[*]E-mail : nantaporn.no@psu.ac.th

Article History; *Received: 27 May 2024, Accepted: 2 December 2024, Published: 24 December 2024*

Abstract

This study investigates environmental conditions and their impact on worker health within the Thung Yai Rubber Fund Cooperative, specifically focusing on the Ribbed Smoke Sheet factory. Working area temperature and wind velocity were systematically monitored at two locations using digital thermometers and anemometers, respectively. Air quality parameters, including total dust, carbon dioxide (CO_2), and oxygen (O_2) levels, were assessed using real-time monitoring equipment. A qualitative approach was adopted to evaluate adverse health effects experienced by workers, employing standardized questionnaires and comprehensive interviews. The results revealed significant health implications among workers exposed to total dust and an inappropriate working environment over the last three months. Specifically, 53.8% of workers experienced nose congestion and stuffy nose; 46.2% experienced a runny nose; 30.8% experienced sore eyes, itchy eyes, body rash, and body itching; 15.4% experienced red eyes; 38.5% experienced sore throat, coughing, mucus, and fatigue; 23.1% experienced difficulty breathing; and 7.7% experienced rapid heartbeat and wheezing. Furthermore, the study concluded that workplace temperatures exceeded prescribed standards, and oxygen concentration levels is slightly higher than Occupational Safety and Health Administration (OSHA) standards. These findings should provide the intervention to address hazardous working conditions, including regulating temperature to safeguard worker health and well-being. Continuous monitoring and enforcement of safety standards are imperative to prevent future respiratory ailments and ensure a safe working environment conducive to optimal productivity and employee welfare within the Thung Yai Rubber Fund Cooperative.

Keywords : workplace environment; health effects; ribbed smoked sheet; total dust; CO_2; O_2

Introduction

Rubber production occupies a central position in Thailand's economy, supporting livelihoods, driving economic growth, and shaping social development [1, 2]. However, concerns arise regarding air pollution emissions from rubber sheet processes, particularly from the Ribbed Smoked Sheet process. The air pollution stemming from this process poses significant challenges, particularly for workers within the facilities and surrounding communities [1, 3]. Air pollution from Ribbed Smoked Sheet (RSS) factories can have significant health impacts due to the emissions generated during the rubber drying and smoking processes [3]. Toxic compounds are released into the air at nearly every stage of rubber processing, where heat is applied to mold its shape or incorporate additives. Because rubber requires heat to soften and react with these additives, emissions occur throughout the process. Studies have shown that the rubber industry emits significant amounts of hazardous substances. These emissions have a harmful impact on human health, particularly on workers in the industry [4]. These emissions include particulate matter, volatile organic compounds (VOCs), carbon monoxide (CO), sulfur dioxide (SO_2), and polycyclic aromatic hydrocarbons (PAHs). The pollutants have significant health implications [1-5].

Regarding Particulate matter (PM), consisting of fine particles like soot and ash produced during the smoking process, can be deeply inhaled into the lungs, causing respiratory and cardiovascular problems. VOCs, including chemicals like benzene, toluene, and xylene, are released during rubber processing and contribute to air pollution, leading to health issues such as headaches, dizziness, and long-term effects like liver and kidney damage [6]. Carbon monoxide, a toxic gas generated by incomplete combustion during smoking, can cause symptoms ranging from headaches and dizziness to potentially fatal outcomes at high concentrations. Sulfur dioxide, produced from burning sulfur-containing materials, can irritate the respiratory system, exacerbating conditions like bronchitis and asthma. PAHs, which are released during the incomplete combustion of organic materials, are known carcinogens, with prolonged exposure increasing the risk of cancer, particularly lung cancer [4-9]. Regarding, Mitigation measures to address pollution in RSS factories include improving ventilation and filtration systems, which can effectively lower the concentration of harmful pollutants inside the facility and safeguard workers' health. Implementing emission control technologies, such as scrubbers and electrostatic precipitators, can significantly cut down on the pollutants released from the factory. Additionally, conducting regular health check-ups and continuous air quality monitoring are essential practices for the early detection and prevention of pollution-related health issues among workers and nearby residents.

According to Thitiworn et al. (2010) [7], the production of RSS leads to significant environmental pollution, affecting both ambient air quality and workplace conditions in factories. While previous research on the environmental impact of Thailand's rubber industry [1-3, 5-7] has primarily concentrated on greenhouse gas emissions [8-10], other harmful emissions such as SOx, NOx, PAHs, and particulate matter (PM) from the primary para-rubber industry have not been adequately studied. Additionally, the overall environmental burden from Ribbed Smoked Sheet process has not been comprehensively evaluated. Regarding previous study relating to pollution from the rubber process has focused on intermediate products and their transportation in Thailand [1]. However, the data on the environmental impacts in work place of Ribbed Smoked Sheet productions are crucial to understand the issue and take measures to reduce the environmental issues.

This study presents a comprehensive examination of air pollution and its health effects originating from a Ribbed Smoked Sheet factory. The research includes an in-depth analysis of the factory's ventilation system, recognizing its critical role in mitigating indoor air pollution and safeguarding worker health. The study aims to provide valuable insights into the complex interplay between industrial air pollution and worker health. Through a multidisciplinary approach encompassing environmental science, occupational health, and public policy, we endeavor to inform evidence-based interventions aimed at minimizing pollution-related health risks and fostering a healthier, more sustainable working environment within the Ribbed Smoked Sheet Factory and similar industrial settings.

Methodology

This investigation encompasses multiple facets crucial to understanding the dynamics of working conditions and their ramifications on worker health. The Ribbed Smoked Sheet (RSS) factory which is Thung Yai Rubber Fund Cooperative located in Trang Province, Thailand was designated as a study area. We scrutinize the study area of the factory to contextualize our analysis within the operational environment. This involves assessing factors such as layout (Figure 1), infrastructure, working area temperature, and wind velocity, which can influence pollution dispersion and exposure pathways [5]. Figure 1 showed the schematic of smoking room and collecting area where V, G and TD is velocity, gas and total dust collecting point, respectively. Additionally, the study focusses on characterizing the air pollutants emitted by the factory, particularly Total dust, CO_2 levels [1, 2, 5], and oxygen (O_2) concentrations. Moreover, the Pollution Exposure is examined to elucidate its potential health implications.

Monitoring of environmental parameters

The working area temperature and wind velocity at two locations in the Ribbed Smoked Sheet factory were monitored to understand environmental variations. The hot wire anemometer (Tesco, model 425) was strategically placed for temperature and wind velocity measurements, respectively. Air quality parameters, including total dust, carbon dioxide (CO_2), and oxygen (O_2) levels, were examined. Total dust (airborne particulate) as per NIOSH 0500 sampling method was measured using gravimetric technique with personal pump (Gilian, model GilAir Plus) at flow rate of 2 L/min for 8 hour and 37 mm PVC filter cassette. The air sampling pump was calibrated with Soap bubble technique. Real-time CO_2 and O_2 measurements were conducted with gas detector equipment (model AS8900) every 2-hour for 8 hours working time.

The data for each parameter were collected every 2 hours during the 8-hour working time, resulting in four data sets for each parameter. The averages and standard deviations of the measured parameters are illustrated in Tables 1 and 2.

Health Effects

The experienced Pollution Exposure is examined by workers in various roles and departments within the factory. Through personal exposure monitoring and health assessments, we seek to quantify the magnitude of pollution exposure and elucidate its potential health implications. Respiratory ailments, cardiovascular disorders, and other adverse health effects associated with prolonged exposure to industrial pollutants are of particular concern.

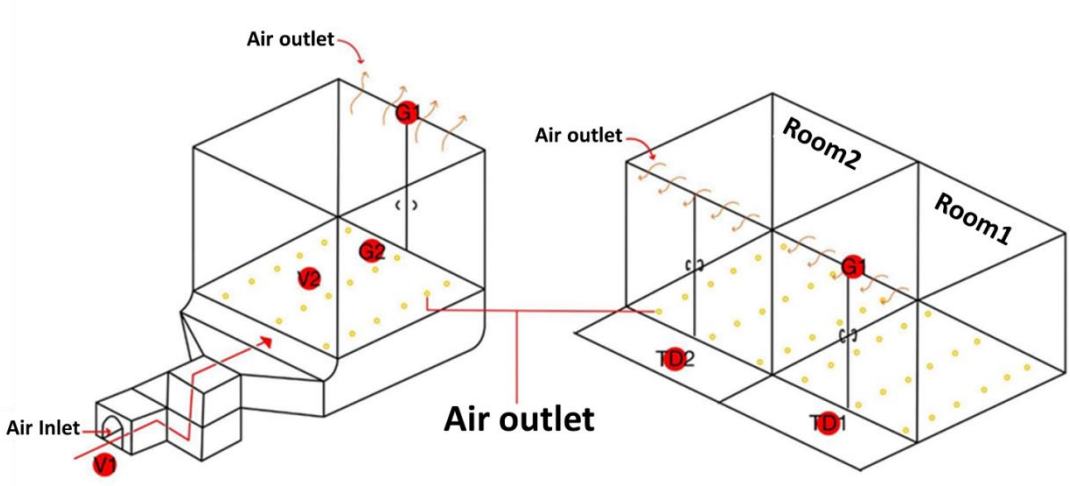

Figure 1 Schematic of Ribbed Smoked Sheet Room

A qualitative approach as questionnaire was employed to evaluate adverse health effects experienced by workers. The questionnaire was developed from the World Health Organization [11-12] and administered to collect health effects related to pollution exposure from work. The questionnaire presented factors including sociodemographic, medical history, symptoms, and perceived health effects related to work environment. Workers from various departments participated, providing informed consent. Comprehensive interviews were conducted to gather detailed insights into workers' health experiences concerning working conditions and air pollution exposure. The questionnaire was evaluated by three specialists, who focused on examining the Index of Congruence (IOC). The evaluation resulted in an IOC of 0.91 and a Cronbach's alpha coefficient of 0.87. The data analysis was conducted using descriptive statistics as frequency, mean, standard deviation, median, maximum, and minimum.

Results and Discussion

The environment of Thung Yai Rubber Fund Co-operative

By observation, it was noted that the environmental conditions, particularly within the working area of the Thung Yai Rubber Co-operative Development Fund, are excessively warm, humid, and stuffy, especially during rubber sheet smoking sessions. This is attributed to a poor ventilation system, characterized by limited natural ventilation, leading to inadequate air circulation within the building. The smoking rooms, totaling 11 in number, are constructed with steel doors and equipped with 8-24 drilled holes per room to facilitate smoke ventilation from the burning stoves situated outside the cooperative. The wind direction flowed upstream from holes to roof as can be seen the smoke direction in figure 2. However, the roof is not high so it caused the smoke still dispersion in the air around working area. The temperature during smoking sessions ranges from 55-60 degrees Celsius, spanning approximately 3 days and 3 nights, resulting in a substantial release of smoke particulates from the smoking rooms and subsequent accumulation within the cooperative building (See Figure 2).

Working environment and ventilation systems

Monitoring studies of the working environment at the Thung Yai Rubber Fund Cooperative were conducted in two locations: working room no. 1 and no. 2. The results in Table 1 showed average wind speeds ($\overline{x}$) of 0.46 and 0.97, with standard deviations (S.D.) of 0.032 and 0.067, in room no. 1 and no. 2, respectively. The temperature measurements yielded average values ($\overline{x}$) of 66.7°C and 58.7°C, with standard deviations (S.D.) of 0.984 and 1.752, in room no. 1 and no. 2, respectively (See Table 1). The temperature in 2 rooms was not much difference.

Assessments of the ventilation system at Thung Yai Rubber Fund Cooperative were conducted at various locations within the building for total dust, carbon dioxide (CO_2), and oxygen (O_2). Total dust measurements were taken at two locations adjacent to the smoking rooms. The measured total dust levels were found to meet the Safety in Working with the Environment (Chemicals) standard (15 mg/m^3) from Ministry of Interior with readings of 8.3 mg/m^3 and 1.6 mg/m^3 at locations 1 and 2, respectively. It can be seen that total dust concentration at location 1 was found higher than location 2. This might be due to high temperature from wood burning in smoking room 1 lead air and particulate matter spreading in environment.

Indoor CO_2 concentrations are typically managed to address general Indoor Air Quality (IAQ) concerns, with recommended limits generally below 1000 ppmv [13]. The American Society of Heating, Refrigerating, and Air Conditioning Engineers (ASHRAE) recommends that indoor CO_2 levels should not exceed the local outdoor air concentration by more than around 650 ppm. ASHRAE Standard 62-2001 sets indoor air quality standards intended to be acceptable to occupants and to reduce the potential for adverse health effects. Moreover, the Occupational Safety and Health Administration (OSHA) has specific guidelines regarding oxygen levels in the workplace. OSHA's respiratory protection standard (29 CFR 1910.134) outlines these requirements, defining

the minimum acceptable oxygen concentration for general industry as 19.5% [14].

CO_2 and O_2 concentrations were assessed at seven different locations: smoking room no. 1, smoke release point from room no. 1, one meter away from the smoking room no. 1, smoking room no. 2, smoke release point from room no. 2, one meter away from the smoking room no. 2, and the rubber sheet squeezing area. CO_2 and O_2 concentration levels met the standards for all measured locations. The result of total dust, CO_2 and O_2 concentrations at working area location were shown in Table 2.

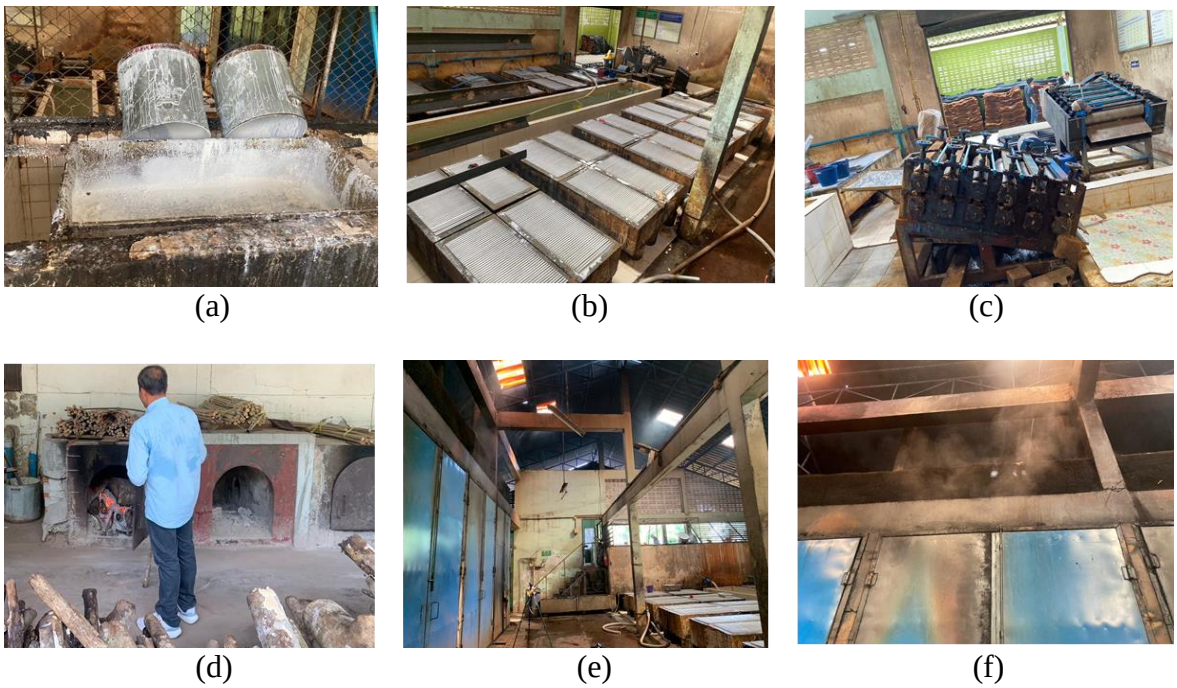

(a) (b) (c)

(d) (e) (f)

Figure 1 Rubber sheet production process and Working condition at Thung Yai Rubber Fund Cooperative; (a) Raw rubber loading, (b) Rubber slab formation, (c) Rubber sheet squeezing, (d) Wood burner, (e) Rubber sheet drying and (f) Particle matter and smoke from smoking room

Table 1 Temperature and wind velocity at 2 different smoking rooms

Parameter	$\bar{x}$	SD	Standard
Wind Velocity (m/s)			
Room 1	0.46	0.032	NA
Room 2	0.97	0.067	NA
Temperature (°C)			
Room 1	66.7	0.984	NA
Room 2	58.7	1.752	NA

Table 2 Total dust, CO_2 and O_2 concentrations at working area location

Parameter	Measured location	Measured Value	Standard
Total dust (mg/m^3)	Smoking room no.1	8.3	Regulations on Standards for Administration, Management and Operation of Safety, Occupational Health and Working Environment Regarding Heat, Light and Noise B.E. 2559
	Smoking room no.2	1.6	
CO_2 (ppm)	Smoking room no.1	515	ASHRAE Standard 62-2001
	Smoke release point from room no. 1	529	
	1.0 meter away from the smoking room no. 1	22	
	Smoking room no.2	505	
	Smoke release point from room no. 2	123	
	1.0 meter away from the smoking room no. 2	18	
	Rubber sheet squeezing area	10	
O_2 (%)	Smoking room no.1	20.1%	OSHA's respiratory protection standard (29 CFR 1910.134)
	Smoke release point from room no. 1	19.9%	
	1.0 meter away from the smoking room no. 1	20.9%	
	Smoking room no.2	20.2%	
	Smoke release point from room no. 2	20.9%	
	1.0 meter away from the smoking room no. 2	20.9%	
	Rubber sheet squeezing area	20.9%	

The result show difference in oxygen and CO_2 levels between Room No. 1 and Room No. 2. The CO_2 level was higher in Room No. 1, which is coherent with the lower oxygen level found there compared to Room No. 2. Thia can be attributed to several factors. Room No. 1 may have less effective ventilation, leading to inadequate fresh air exchange, which is critical in maintaining oxygen levels. Additionally, higher combustion activity in Room No. 1 could result in more significant oxygen consumption. The room's layout and airflow patterns might also contribute to localized oxygen depletion, particularly if air circulation is obstructed or uneven. Lastly, if Room No. 1 is closer to primary emission sources, this proximity could exacerbate oxygen depletion due to increased consumption of oxygen by combustion processes.

Worker health assessment

For the worker health assessment, there were a total of 13 workers participated in the study including 9 male workers and 4 female workers. Among them, one was under 20 years old, 4 workers were aged between 20-29, 1 worker was between 40-49, 4 workers were between 50-59, and 1 worker was over 60 years old. In terms of health conditions, it was found that 4 workers had chronic diseases (30.8%), while 9 workers did not (69.2%). Regarding respiratory diseases, 2 workers were affected

(15.4%), while 11 workers were not (84.6%). Concerning smoking frequency, 7 workers smoked (53.8%), while 6 workers did not (46.2%). As for exercise frequency, 6 workers exercised weekly (46.2%), while 7 workers did not (53.8%). In terms of personal protective equipment usage, 4 workers wore personal protective equipment (30.8%), while 9 workers did not (69.2%).

The assessment of adverse health effects experienced by workers exposed to total dust over the last three months is shown in Table 3. The study results revealed that 53.8% of workers experienced nose congestion and stuffy nose; 46.2% experienced runny nose; 30.8% experienced sore eyes, itchy eyes, body rash and body itching; 15.4% experienced red eyes; 38.5% experienced sore throat, coughing, mucus, and fatigue; 23.1% experienced difficult breathing; while 7.7% experienced rapid heartbeat and wheezing. None of the participants had experienced nosebleeds.

Table 3 Adverse health effects assessment

Adverse Health Effects	Worker	Percentage
1. Do you have symptoms of nasal congestion?		
Regularly	0	0
Often	1	7.7
Occasionally	5	38.5
Rarely	1	7.7
Never	6	46.2
total	**13**	**100**
2. Do you have a stuffy nose?		
Regularly	1	7.7
Often	2	15.4
Occasionally	3	23.1
Rarely	1	7.7
Never	6	46.2
total	**13**	**100**
3. Do you have symptoms of sore eyes?		
Regularly	0	0
Often	1	7.7
Occasionally	1	7.7
Rarely	2	15.2
Never	9	69.2
total	**13**	**100**
4. Do you have symptoms of itchy eyes?		
Regularly	0	0
Often	1	7.7
Occasionally	2	15.4
Rarely	1	7.7
Never	9	69.2
total	**13**	**100**
5. Do you have symptoms of red eyes?		
Regularly	1	7.7
Often	0	0
Occasionally	1	7.7
Rarely	0	0
Never	11	84.6
total	**13**	**100**

Adverse Health Effects	Worker	Percentage
6. Do you have symptoms of a sore throat?		
Regularly	0	0
Often	2	15.4
Occasionally	0	0
Rarely	3	23.1
Never	8	61.5
total	**13**	**100**
7. Do you have a runny nose?		
Regularly	0	0
Often	1	7.7
Occasionally	4	30.8
Rarely	1	7.7
Never	7	53.8
total	**13**	**100**
8. Do you have a rash appearing on your body?		
Regularly	1	7.7
Often	0	0
Occasionally	0	0
Rarely	3	23.1
Never	9	69.2
total	**13**	**100**
9. Do you have symptoms of itching on your body?		
Regularly	1	7.7
Often	0	0
Occasionally	0	0
Rarely	3	23.1
Never	9	69.2
total	**13**	**100**
10. Are you experiencing fatigue?		
Regularly	1	7.7
Often	1	7.7
Occasionally	1	7.7
Rarely	2	15.4
Never	8	61.5
total	**13**	**100**
11. Do you have symptoms of difficulty breathing?		
Regularly	0	0
Often	1	7.7
Occasionally	1	7.7
Rarely	1	7.7
Never	10	76.9
total	**13**	**100**
12. Do you have symptoms of coughing?"		
Regularly	0	0
Often	1	7.7
Occasionally	1	7.7
Rarely	3	23.1
Never	8	61.5
total	**13**	**100**

Adverse Health Effects	Worker	Percentage
13. Do you have symptoms of rapid heartbeat?		
Regularly	0	0
Often	0	0
Occasionally	1	7.7
Rarely	0	0
Never	12	92.3
total	**13**	**100**
14. Do you have symptoms of wheezing?		
Regularly	0	0
Often	0	0
Occasionally	0	0
Rarely	1	7.7
Never	12	92.3
total	**13**	**100**
15. Do you have mucus?		
Regularly	1	7.7
Often	1	7.7
Occasionally	1	7.7
Rarely	2	15.4
Never	8	61.5
total	**13**	**100**
16. Do you have nosebleeds?		
Regularly	0	0
Often	0	0
Occasionally	0	0
Rarely	0	0
Never	13	100
total	**13**	**100**

Conclusions

This study unveiled environmental conditions during the smoking room operating for RSS production for Thung Yai Rubber Co-operative Development Fund. The oxygen and carbon dioxide concentration level slightly exceeded the standard. The total dust was emitted from smoking room and its concentration is below the standard. Workers experienced health effects on nose congestion and stuffy nose, and a runny nose. The key findings underscore the pressing need for immediate intervention to address the working conditions identified in this study. Implementing measures to regulate temperature and improve carbon dioxide levels in the workplace is crucial to safeguarding the health and well-being of workers. Furthermore, ongoing monitoring and enforcement of safety standards are imperative to prevent future occurrences of respiratory ailments and ensure a safe working environment conducive to optimal productivity and employee welfare.

Acknowledgements

This study was supported by the Institute of Research and Innovation, Thaksin University: Pre-TSU Move for Industry (grant no. TSUPre-TMI66-08). The authors would like to thank the participants of Thung Yai Rubber Co-operative, Trang, Thailand, for providing information.

References

[1] Phairuang, W. Tekasakul, P. Hata, M. Tekasakul, S. Chomanee, J. Otani, Y. and Furuuchi, M. 2019. Estimation of air pollution from ribbed smoked sheet rubber in Thailand exports to Japan as a pre-product of tires. Atmospheric Pollution Research. 10(2): 642-650.

[2] Choosong, T. Furuuchi, M. Tekasakul, P. Tekasakul, S. Chomanee, J. Jinno, T. Hata, M. and Otani, Y. 2007. Working Environment in a Rubber Sheet Smoking Factory Polluted by Smoke from Biomass Fuel Burning and Health Influences to Workers. Journal of Ecotechnology Research. 13(2): 91-96.

[3] Tekasakul, P. and Tekasakul, S. 2006. Environmental Problems Related to Natural Rubber Production in Thailand. Journal of Aerosol Research, 21(2): 122-129.

[4] Machimontorn, P. and Tekasakul, P. 2007. CFD study of flow in natural rubber smoking-room: I. Validation with the present smoking-room. Applied Thermal Engineering. 27(11-12): 2113-2121.

[5] Machimontorn P., P. Tekasakul. 2007. CFD study of flow in natural rubber smoking-room: I. Validation with the present smoking-room. Applied Thermal Engineering. 27(11-12): 2113-2121.

[6] Purba, L.P. and Tekasakul, P. 2012. Computational Fluid Dynamics Study of Flow and Aerosol Concentration Patterns in a Ribbed Smoked Sheet Rubber Factory. Particulate Science and Technology, 30(3): 220-237.

[7] Choosong, T. Chomanee, J., Tekasakul, P. Tekasakul, S. Otani, Y. Hata, M. and Furuuchi, M. 2010. Workplace Environment and Personal Exposure of PM and PAHs to Workers in Natural Rubber Sheet Factories Contaminated by Wood Burning Smoke. Aerosol Air Qual. Res. 10(1): 8-21.

[8] Dejchanchaiwong, R. Kumar, A. Tekasakul, P. 2019. Performance and economic analysis of natural convection based rubber smoking room for rubber cooperatives in Thailand. Renewable Energy. 132: 233-242.

[9] Purba, L.P. 2009. Airflow and aerosol concentration in a ribbed smoked sheet rubber cooperative and improvement of ventilation. Master's Thesis. Prince of Songkla University.

[10] Musikavong, C. and Gheewala, S.H. 2017. Assessing ecological footprints of products from the rubber industry and palm oil mills in Thailand. Journal of Cleaner Production. 142: 1148-1157.

[11] World Health Organization (WHO). 2021. Screening questionnaire for selection of sampling sites for assessment of risks from combined exposure to multiple chemicals in indoor air. Retrieved from https://www.who.int/europe/publications/i/item/9789289055635

[12] World Health Organization (WHO). 2019. Health risk assessment of air pollution. Retrieved from https://iris.who.int/bitstream/handle/10665/329677/9789289051316- eng.pdf

[13] The American Society of Heating, Refrigerating and Air-Conditioning Engineers (ASHRAE). 2022. ASHRAE Position Document on Indoor Carbon Dioxide. Retrieved from https://www.ashrae.org/file%20library/about/position%20documents/pd_indoorcarbondioxide_2022.pdf

[14] The Occupational Safety and Health Administration (OSHA). 2022. The presence of oxygen in the workplace. Retrieved from https://www.osha.gov

Thai Environmental Engineering Journal Vol. 38 No. 3 (2024) : 55-63
www.eeat.or.th

Natural Attenuation of Arsenic in Natural Wetlands at Thung Kham Gold Mine Wang Saphung District, Loei Province

Apinya Tonguntang[1], Netnapid Tantemsapya[1*], Chatpet Yossapol[1] and Vanlop Thathong[2]

[1]School of Environmental Engineering, Institute of Engineering,
Suranaree University of Technology, Nakhon Ratchasima 30000, Thailand
[2]Environmental Science and Technology Program, Loei Rajabhat University 42000, Thailand
[*]E-mail : netnapid@sut.ac.th

Article History; *Received: 4 June 2024, Accepted: 11 December 2024, Published: 24 December 2024*

Abstract

The gold mining operations in Khao Luang Sub-district, Wang Saphung District, Loei Province, have had a significant impact on the surrounding environment, leading to arsenic contamination. The objective of this research was to examine the extent of arsenic contamination in the natural wetland area and Pu Leuk Creek, adjacent to the Thung Kam gold mine. The study focused on sediments samples taken from three points along the creek: upstream, middle, and downstream, at depths ranging from 0 to 150 cm. The findings revealed that concentrations of total arsenic in the sediment at the upstream, middle, and downstream points ranged from 160.1-1,112 mg/kg, 49.79-1,911 mg/kg, and 0.39-1,080 mg/kg, respectively. For As(III), the concentrations ranged from 28.63-320.40 mg/kg, 0-1,032 mg/kg, and 0-544.60 mg/kg, respectively. For As(V), the concentrations ranged from 115.49–853.70 mg/kg, 8.5-879 mg/kg, and 0–586.5 mg/kg, respectively. Most of these values exceed the standard threshold for soil quality for agricultural use (25.00 mg/kg) set by the National Environmental Board in 2021. The highest concentrations of arsenic were found at the middle point of the creek, possibly due to its proximity to the mineral waste pond in the gold mining area. Additionally, the highest concentrations of arsenic were found at depths of 0–40 cm, indicating that depth levels affect the accumulation of arsenic in the sediment. The analysis of the elemental composition in the sediment using the Energy Dispersive X-ray Fluorescence (EDXRF) technique revealed that the chemical constituents in the sediment include Al, Si, K, Ca, Ti, Mn, Fe, Cu, Zn, As, Rb, Zr, and Pb. The predominant mineralogical components in the sediment are quartz (SiO_2) and hematite (Fe_2O_3). Regarding the analysis of the forms of arsenic in the sediment, it was observed that the concentration of As(V) was higher than that of As(III). This suggests that As(V) may have been absorbed or precipitated along with other mineral elements in the sediments. The presence of arsenic exceeding the standard limits in this area, as mentioned above, may have adverse health effects on the people residing near the gold mining area.

Keywords : Arsenic; Gold mine; heavy metal; Loei

Introduction

In nature, arsenic is considered a highly toxic semimetal, primarily found in the forms of arsenite (As(III)) and arsenate (As(V)). Arsenic predominates in its +5-oxidation state, As(V), in the form of arsenate oxyanions ($H_2AsO_4^-$, $HAsO_4^{2-}$). The high affinity of As(V) for Fe(III) (oxyhydr) oxides may effectively immobilize aqueous its [1-4]. Arsenite (As(III)) is more toxic than arsenate (As(V)) due to its higher ability to penetrate cells and disrupt cellular processes. Both forms pose significant health risks, including cancer and organ damage, with arsenite being more mobile and readily absorbed by organisms. Effective treatment strategies, such as oxidation and adsorption, are necessary to manage both forms and reduce their harmful effects on health and the environment. In Thailand, arsenic occurs naturally throughout the country, mostly on the western side, such as in Suphan Buri Province, and has been discovered through excavation in provinces like Nakhon Si Thammarat, Phichit, and Loei. Arsenic contamination in the environment can stem from two main sources: natural resources and human activities. Natural contamination is associated with the weathering and degradation of rocks or minerals that store arsenic [5]. Human-induced contamination arises from activities such as mining, industrial waste disposal, leaching of arsenic-containing minerals, combustion of fossil fuels, and the use of arsenic in various products, such as pesticides [6]. Generally, naturally occurring arsenic is found within mineral pathways, often in conjunction with other compounds such as copper, iron, manganese, cobalt, nickel, silver, and gold. Therefore, mining activities may disperse arsenic into the surrounding areas [7]. In wetland environments, arsenic is retained mostly in sediments or media. Arsenic in wetlands can precipitate and form insoluble sulfide compounds or arsenopyrite (FeAsS) [8-11]. Coprecipitation processes can obtain high removal efficiency in the presence of sulfate, ferric chloride, and Iron oxide [11, 12].

The gold mining activities of Thung Kam Company in Wang Saphung District, Loei Province, have been identified as the root cause of arsenic contamination in the surrounding areas between the years 2014-2018. It was found that the highest accumulation of arsenic was in the soil samples and water sources near the gold mining area, resulting from leaching and absorption on the lateritic soil rich in iron and manganese. This situation has impacted the health of the residents living near the mining site. Investigations revealed that people's bodies were contaminated with arsenic, cadmium, lead, manganese, and cyanide. Moreover, elevated levels of arsenic were found in both water sources and soil samples, exceeding the standard limit of 0.01 mg/L. This conflict has led affected individuals to mobilize collectively through community-based governance, demanding government intervention to address the issue [13].

Additionally, assessments of water quality and heavy metal contamination in sediment, fish, and frogs, including the bioaccumulation factor (BAFs) observed in these aquatic organisms, have revealed concentrations surpassing regulatory limits [15]. Notably, arsenic in the sediment exists predominantly in the forms of arsenate (As(V)) and arsenite (As(III)), with arsenite being more mobile and toxic than As(V). Various soil elemental minerals have also been found to influence the transformation and species of Arsenic, as well as its storage and movement in the environment. Consequently, our research aims to investigate the extent of arsenic contamination in the natural wetlands and Phu Lek Creek adjacent to the Thung Kam gold mine. This investigation focused on analyzing dispersion patterns over distance and depth, as well as the chemical components influencing arsenic dispersion patterns.

Methodology

Study area

The natural wetland area is located along Phu Lek Creek adjacent to the mineral waste pond at the end of the gold mine (which is currently closed). The gold mine operated as an open-pit mine and ore-dressing plant from the year 2006 to 2013. Water from the Phu Lek Creek flows downstream from the area behind the mine, sometimes receiving wastewater from the waste pond. The natural wetland receives water from two sources: wastewater from the mine to the northwest and underground springs from the northeast. The wetland area extends approximately 643

meters in length, with a width ranging from 10 to 50 meters and a depth of 0.20 to 1.0 meters. The total study area is approximately 10,000 sq.m. (Figure 1).

Sampling and preparation of sediment samples

In this study, sediment core samples were collected at sampling points along the creek, as illustrated in Figure 2 (1-10 March 2023, dry season). The samples were collected at a depth of 150 cm., with 5 cm. intervals at three points along the distance: the upstream at 0 m., middle at 290 m., and the downstream at 640 m. They adjusted their conditions by air-drying them in a shaded area for 7-14 days, depending on the soil moisture content. After that, the samples were heated at 105 degrees Celsius for 24 hours. Subsequently, the dried samples were ground using a ceramic mortar and passed through a 2-millimeter sieve in preparation for further analysis.

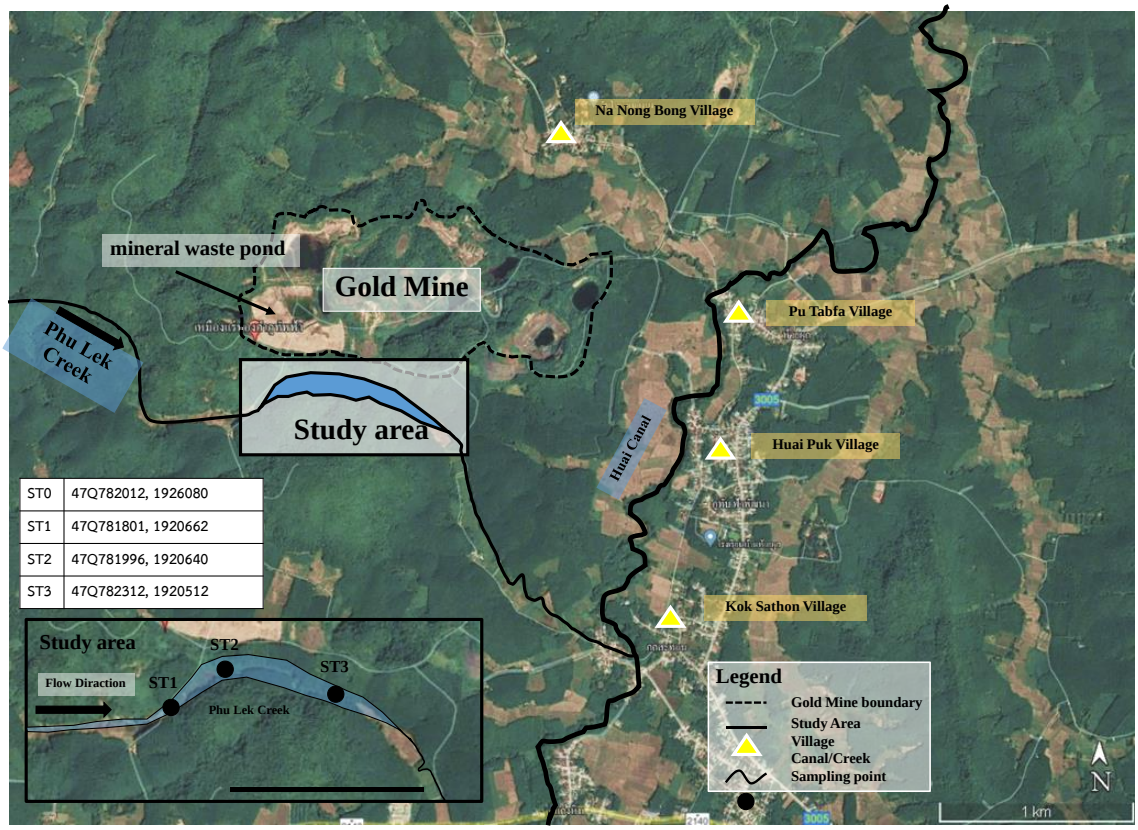

Figure 1 Map of the gold mine and Phu Lek Creek

Figure 2 Sampling point characteristics: (a) Upstream (b) Middle and (c) Downstream

Sediments preparation

Sediments were collected from 3 sampling points along Phu Lek Creek, where the location was illustrated in Figure 1. Samples were classified according to particle size by sieving (all sizes, < 2 mm and > 2.00 mm). After the sieve, the samples were air-dried at room temperature. Sediment was analyzed for chemical and physical properties as shown in Table 1.

Physical characteristics: The analysis of sediment texture by hydrometer shows that the sediment sample is composed of sand 33.78%, silt 23.22%, and clay 43%. The high percentage of clay appears as a fine texture with low permeability.

Chemical properties: Sediments are mainly composed of Quartz (SiO_2), Hematite (Fe_2O_3), and Bauxite ($Al_2O_3.H_2O$). The EDX study and the X-ray diffraction spectrum of sediments indicated that the elemental compositions are Mg, Al, Si, S, K, Ti, Fe, and As (Table 1). From these results, it can conclude that sediment is composed of a high level of aluminum ($Al_2O_3.H_2O$ and $AlSi_2O_6$ (OH_2)) and iron oxide (Hematite). Physical appearance studied by SEM indicated that all sediment samples had low porous and rough surfaces which occurred from a binding of a small particle on the surface soil to generate shallow porous.

The pH of all sediment samples is between 4.76-5.04 which is considered a weak acid (Land Development Department, 2010). The electrical conductivity of the samples is lower than 0.1 ds/m which is considered as non-saline soil. Organic matters in all samples were moderate (1.5-2.5). The amount of iron was found highest in soil size < 2 mm 134,300 mg/kg (Table 1).

Analysis of total arsenic, As(III) and As(V)

Sediment samples were prepared in accordance with US EPA test methods for solid waste evaluation. Physical/Chemical Method (SW-846). Initially, 0.15 g of each dried sample was placed in a beaker and digested using a hot plate with a mixed acid concentration of 10 mL of HNO_3 and 5 mL of HCl. After cooling to room temperature, the suspended material was filtered through 0.42-µm filters. The solution was then diluted with deionized water. The digested samples were determined for arsenic using inductively coupled plasma optical emission spectrometry (ICP-OES, Agilent 5800 series, Santa Clara, CA, USA). For the analysis of As(III) and As(V), the ion exchange resin technique was used according to the methods specified in the American Public Health Association standards (APHA, 2012).

Energy Dispersive X-Ray Fluorescence (EDXRF)

The middle-point sediment, which showed the highest concentration of arsenic, was dried at 105 degrees Celsius and finely ground to prepare for elemental analysis. The ground sediment samples, with three replicates, were analyzed using the EDXRF spectrometer technique (Horiba XGT-5200). The power specifications of the tube are 50 kV maximum and 1 mA. The selection of filters, tube voltage, sample position, and current were fully computer-controlled, with an energy range of 0–40 keV. Quantitative analysis was conducted using the built-in software.

Table 1 Sediment characteristics and analytical methods

Parameters;	Particle size			Methods/ reference
	All size	> 2 mm	< 2 mm	
Physical properties				
Particle size (mm)		0.002 – 2.00		Sieve analysis, SEM-EDX, Carter and Gregorich (2006)
Bulk density (g/cm^2)	2.01	2.55	1.75	Core method, Carter and Gregorich (2006)
Surface area (m^2/g)	17.03	18.15	16.00	BET analysis (2013)

Parameters;	All size	Particle size > 2 mm	< 2 mm	Methods/ reference
Chemical properties				
pH	5.10	4.76	5.04	1:5, Sediments:water mixture, pH meter, APHA (2012)
pH_{ZPC}	5.80	4.75	4.91	1:5, laterite:water mixture, pH meter, APHA (2012)
EC (ds/m)	0.025	0.036	0.021	1:5, Sediments:water mixture, EC meter, APHA (2012)
CEC (c mol(+)/kg)	25.14	23.36	33.45	Ammonium acetate extraction (1N) Land Development Department, (2010)
Organic matter (%)	2.08	2.17	1.96	UV254, APHA (2012)
Inorganic composition (by SEM-EDX)				SEM-EDX, model: ESM-5800, GEOL, Japan
Magnesium(Mg) (%)	0.44	0.39	0.15	
Aluminum(Al) (%)	24.84	22.54	24.47	
Silicon(Si) (%)	44.01	44.68	42.55	
Sulfur(S) (%)	0.14	0.17	0.43	
Potassium(K) (%)	2.76	2.72	2.56	
Titanium(Ti) (%)	1.44	1.41	1.41	
Iron(Fe) (%)	26.18	27.93	28.39	
Arsenic (As) (%)	0.19	0.16	0.05	
Metals (by ICP-OES)				Digestion with 1:3(HNO_3 : $HClO_4$)(v/v),
Iron(Fe) (mg/kg)	99,640	98,030	134,300	ICP-OES, Perkin Elmer, Optima 8000
Arsenic (As) (mg/kg)	0.17	0.13	0.16	APHA (1998)

Statistical analysis

Statistical analysis was performed by the SPSS statistics 17.0 for Windows software package program network Licensed in Suranaree University of Technology. Data was calculated by mean, minimum, maximum, and standard deviation for a result. The significance of the difference between depth and arsenic species was determined with a *t*-test (Significant at a level of 0.05). Quality assurance (QA) and quality control (QC) were used in planning, sampling, analysis, and reporting of data in all processes throughout the study. Pearson correlation coefficient (significant at a level of 0.05) was used to determine the correlation between date, sediment depth, and arsenic (total/As^{3+}/As^{5+}).

Results and Discussion

Sediment properties in the wetland

The results of the analysis of sediment properties are shown in Table 1, which found that most of the analysis results have values consistent with laterite soil properties [14], namely Particle size (0.025-2.00 mm.), Bulk density (1.98-2.32 g/cm^3), Surface area (15.52-18.35 m^2/g), Pore volume (0.011-0.020 ml/g), Organic Matter (0.56-2.08%), Iron (Fe) (27.93-28.39%) etc.

Study of total arsenic, As(III) and As(V)

The concentrations of total arsenic in sediment at the upstream, middle, and downstream at depths of 1-150 cm. ranges from 160.1-1,112 mg/kg, 49.79-1,911 mg/kg, and 0.39-1,080 mg/kg, respectively. (Table 2) For As(III), the concentrations range from 28.63-320.40 mg/kg, 0-1,032 mg/kg, and 0-544.60 mg/kg, respectively. As for As(V), the concentrations range from 115.49-853.70 mg/kg, 8.5-879 mg/kg, and 0-586.5 mg/kg, respectively. Most of the values exceed the standard threshold for soil quality for agricultural use (25.00 mg/kg) set by the National Environmental Board in 2021.

Figure 3, which illustrates the relationship between depth and the total amount of arsenic at the Upstream point, Middle, and Downstream, it is evident that as depth increases, the quantity of arsenic in the sediments decreases. Additionally, the highest concentration of arsenic was found at depths of 0-40 cm., indicating that depth levels influence the accumulation of arsenic in the sediments. Furthermore, at depths of 0-40 cm., conducive to root growth, arsenic tends to be trapped on plant roots and accumulates predominantly in the sediments. Moreover, the highest arsenic concentration was observed around the middle of the stream, possibly due to

its proximity to the mine tailings in the gold mining area.

Figure 4, which illustrates the relationship between As(III) and As(V), shows that at higher concentrations, particularly at depths of 0–40 cm, arsenic is predominantly found in the form of As(V) rather than As(III). This is because As(V) is more stable and exists in oxidizing environments. As the depth increases, arsenic is mainly present in the form of As(III) and is found at lower concentrations compared to As(V). At greater depths, arsenic in pore water diffuses into a reducing environment, leading to in-situ precipitation into stable forms, As(V) [16], resulting in higher concentrations of As(V) than As(III). In areas with a high amount of Fe(III) (ferric oxyhydroxide), arsenic may oxidize to form arsenopyrite (FeAsS) and accumulate in the soil [4, 14].

Table 1 Sediment properties

Properties	Quantitative value
Particle size (mm)	0.021-2.10
Bulk density (g/cm^3)	1.18-2.20
Surface area (m^2/g)	13.85-18.00
Pore volume (ml/g)	0.013-0.020
pH_{ZPC} (1:5, laterite: water mixture)	5.30-7.10
Conductivity (1:5, laterite: water mixture) (µS/cm)	40.00-52.60
Organic Matter (%)	0.86-2.080
Magnesium(Mg) (%)	0.17-0.40
Aluminum(Al) (%)	22.40-24.40
Silicon(Si) (%)	42.20-45.00
Sulfur(S) (%)	0.11-0.20
Potassium (K) (%)	1.06-2.00
Titanium (Ti) (%)	0.21-1.40
Iron(Fe) (%)	27.90-28.30

Table 2 Total arsenic, As(III) and As(V) content in natural wetlands

	Upstream			Middle			Downstream		
	Total As	**As(III)**	**As(V)**	**Total As**	**As(III)**	**As(V)**	**Total As**	**As(III)**	**As(V)**
count	30	30	30	30	30	30	30	30	30
Max (mg/kg)	1,112	320.4	853.7	1911	1032	879	1080	544.6	586.5
Min (mg/kg)	160.1	28.63	115.49	49.79	0	8.5	0.398	0	0

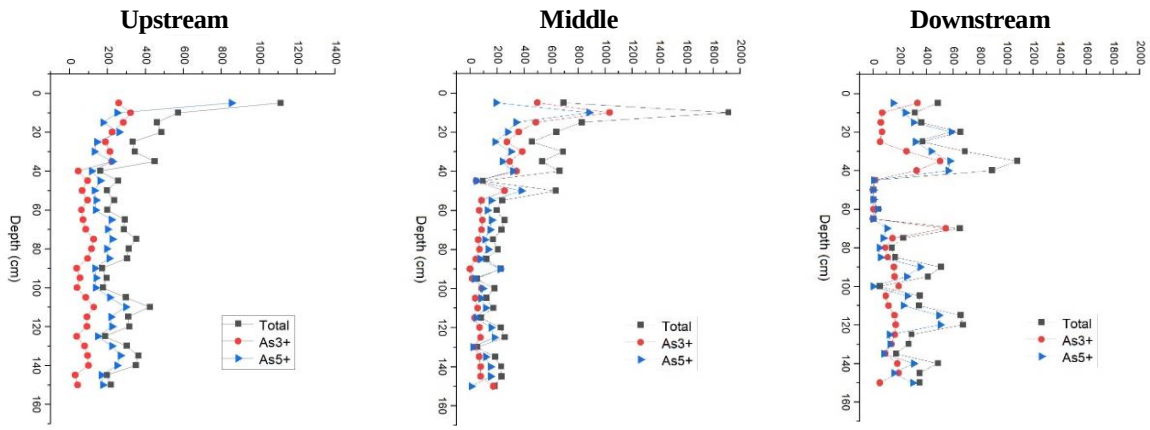

Figure 3 Concentration of total arsenic, As(III) and As(V) with depth

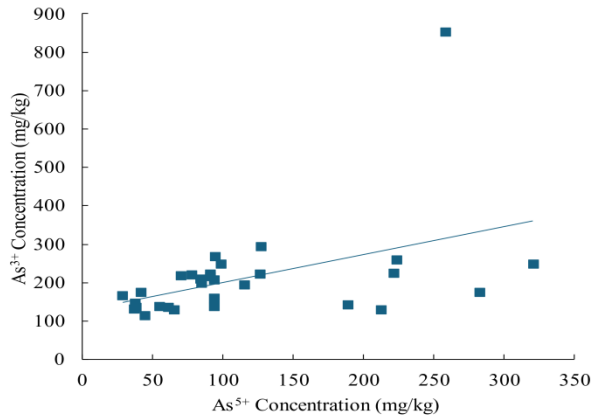

Figure 4 Difference between As(III) and As(V)

Results of the study of elemental composition in sediments

The analysis of elemental composition in the sediment using Energy Dispersive X-ray Fluorescence (EDXRF) technique revealed that the chemical constituents in the sediment consist of Al, Si, K, Ca, Ti, Mn, Fe, Cu, Zn, As, Rb, Zr, and Pb, as shown in Figure 5. The predominant mineralogical components in the soil sediment are quartz (SiO_2) and hematite (Fe_2O_3). Furthermore, Table 3 reveals that iron is found in higher quantities compared to other mineral elements in the sediments samples. This is attributed to the predominance of iron in the environmental conditions of the Thung Kam gold mine area [14].

Mechanisms of natural attenuation of arsenic in the wetland

In this study of the natural wetland area of the Thung Kam gold mine, the predominant mineralogical components in the sediment were quartz (SiO_2) and hematite (Fe_2O_3). The arsenic content accumulated in the sediments ranged from 0.39 to 1,080 mg/kg. In wetland environments, arsenic is primarily retained in sediments or media rather than accumulated in plants. Depending on redox conditions, arsenic in wetlands can precipitate and form insoluble sulfide compounds, such as arsenopyrite (FeAsS) [8-11]. Coprecipitation processes can achieve high removal efficiency in the presence of sulfate, ferric chloride, and iron oxides [11, 12].

In this study, the highest arsenic concentration was found at depths of 0–40 cm, where arsenic predominantly occurred in the form of As(V) rather than As(III). At greater depths, arsenic was mainly present in the form of As(III) and at lower concentrations compared to As(V). The sediment was rich in Fe(III) (ferric oxyhydroxide), which facilitated the oxidation of arsenic in water by Fe(III), leading to its adsorption or precipitation along with other mineral elements in the sediments. At depths less than 40 cm, which are conducive to root growth, arsenic tends to be trapped on plant roots and accumulates predominantly in the sediments.

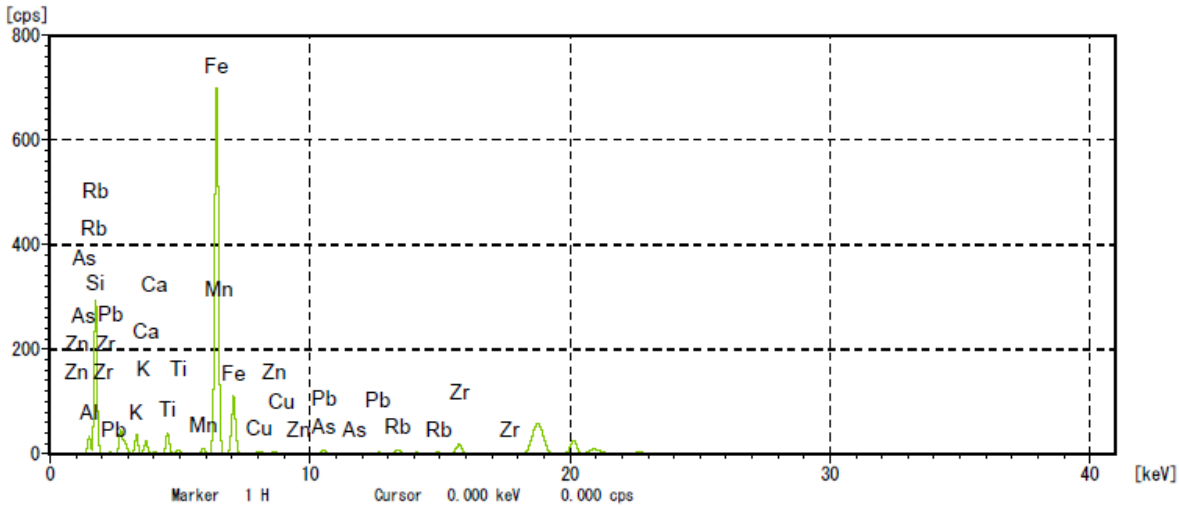

Figure 5 Chemical composition of sediments in natural wetlands

Table 3 Descriptive statistics of heavy metals in the sediment profiles in natural wetlands (%)

	Statistic	Fe	Al	Mn	Cr	Pb	As	P	Zn
Soil Profiles	Maximum	78.21	6.47	1.92	0.11	0.00	0.63	0.30	0.43
	minimum	31.61	0.00	0.35	0.03	0.00	0.21	0.00	0.10
	Mean	47.13±1.86	1.23±0.34	0.75±0.07	0.07±0.004	0.00	0.41±0.22	0.05±0.01	0.22±0.01
	SD	10.18	1.91	0.36	0.02	0.00	0.12	0.08	0.76

Conclusions

From the study of sediment at depths of 0-150 cm, it was found that the total arsenic, As(III), and As(V) concentrations exceeded soil quality standards for agricultural purposes. The depth level with the highest accumulation of arsenic was 0-40 cm, indicating that sediment depth influences arsenic accumulation. The main chemical constituents in the sediment in the wetland area are quartz (SiO_2) and hematite (Fe_2O_3). Regarding the analysis of the forms of arsenic in the sediment, it was observed that the concentration of As(V) was higher than As(III). This suggests that As(V) may have been absorbed or precipitated along with other mineral elements in the sediments.

The presence of arsenic exceeding standard limits in this area may pose significant health risks to residents near the gold mining site. The sediment in the Phu Lek wetland area is laterite, with iron oxides as its main component. This type of soil can remove arsenic from water with 50-93% efficiency [14]. The arsenic levels detected were far above standard, resulting in contamination of water, plants [17], and food [18] around the gold mining area. Therefore, mitigation and remediation measures for arsenic contamination, such as land improvement, soil rehabilitation, phytoremediation, and soil amendments, are recommended to reduce arsenic exposure. Furthermore, future research should focus on monitoring arsenic migration, assessing its bioavailability to crops, and exploring the health impacts on the local community to mitigate these risks more effectively.

Acknowledgements

This research was supported by the Thailand Science Research and Innovation (TSRI), contract number RSA6280078. The authors thank the National Research Council (NRCT) of Thailand, Synchrotron Light Research Institute (Public Organization) and Suranaree University of Technology (SUT) for the financial support of the Research Program. We would like to express our sincere thanks to Loei Rajabhat University, the Environmental Research Institute (ERIC) for their invaluable support in terms of facilities and scientific equipment.

References

[1] Blodau, C., Fulda, B., Bauer, M., and Knorr, K.H. 2008. Arsenic speciation and turnover in intact organic soil mesocosms during experimental drought and rewetting. Geochem et Cosmochim. Acta, 72(16): 3991-4007.

[2] Burton, E.D., Bush, R.T., Sullivan, L.A., Johnston, S.G., and Hocking, R.K. 2008. Mobility of arsenic and selected metals during re-flooding of iron- and organic-rich acidsulfate soil. Chemical Geology, 253(1-2): 64-73.

[3] Weber, F.-A., Hofacker, A.F., Voegelin, A., and Kretzschmar, R. 2010. Temperature dependence and coupling of iron and arsenic reduction and release during flooding of a contaminated soil. Environmental Science & Technology, 44(1): 116-122.

[4] Drahota, P., Peřestá, M., Trubač, J., Mihaljevič, M., and Vaněk, A. 2021. Arsenic fractionation and mobility in sulfidic wetland soils during experimental drying. Chemosphere, 277: 130306.

[5] Jain, C.K. and Ali, I. 2000. Arsenic: occurrence, toxicity and speciation techniques. Water Research, 34(17): 4304-4312.

[6] Hassan, M. M. 2017. Arsenic in groundwater: poisoning and risk assessment, 1st Edition. Boca Raton, FL: Taylor & Francis Group.

[7] Mensah, A.K., Marschner, B., Shaheen, S.M., Wang, J., Wang, S.-L., and Rinklebe, J. 2020. Arsenic contamination in abandoned and active gold mine spoils in Ghana: Geochemical fractionation, speciation, and assessment of the potential human health risk. Environmental Pollution, 261: 114116.

[8] Buddhawong, S., Kuschk, P., Mattusch, J., Wiessner, A., and Stottmeister, U. 2005. Removal of arsenic and zinc using different laboratory model wetland systems. Engineering in Life Sciences, 5(3): 247-252.

[9] Henke, K. 2009. Arsenic: environmental chemistry, health threats and waste treatment. John Wiley & Sons.

[10] Singhakant, C., Koottatep, T., and Satayavivad, J. 2009. Enhanced arsenic removals through plant interactions in subsurface-flow constructed wetlands. Environmental Science & Health Part A, 44(2): 163-169.

[11] Lizama A., K., Fletcher, T. D., and Sun, G. 2011. Removal processes for arsenic in constructed wetlands. Chemosphere, 84(8): 1032-1043.

[12] Su, C. and Puls, R. W. 2001. Arsenate and arsenite removal by zerovalent iron: kinetics, redox transformation, and implications for in situ groundwater remediation. Environmental Science & Technology, 35(7): 1487-1492.

[13] Watcharin, C. 2018. Gold mining problems in Loei Province. The Journal of Political Science, Kasetsart University, 5(2). July-December 2018.

[14] Thongkhan, W. and Tantemsap, N., 2016. Adsorption of arsenic on laterite soil from a gold mining area. The 40th National Graduate Research Conference, 20-21 October 2016, International Convention Center Commemorating the 60th Anniversary of His Majesty the King's Accession to the Throne, Prince of Songkla University, Hat Yai Campus.

[15] Intamat, S., Phoonaploy, U., Sriuttha, M., Tengjaroenkul, B., and Neeratanaphan, L. 2016. Heavy metal accumulation in aquatic animals around the gold mine area of Loei province, Thailand. Human and Ecological Risk Assessment: An International Journal, 22(6): 1418-1432.

[16] Van Den Berghe, M.D., Jamieson, H.E., and Palmer, M.P. 2018. Arsenic Mobility and Characterization in Lakes Impacted by Gold Ore Roasting, Yellowknife, NWT, Canada. Environmental Pollution, 234: 630-641.

[17] Thathong, V., Tantamsapya, N., Yossapol, C., Liao, C. H., and Wirojanagud, W. 2019. Role of Natural Wetlands in Arsenic Removal from Arsenic-Contaminated Runoff. Applied Environmental Research, 41(1): 8-21.

[18] Hasan, M. S. 2022. Health risk assessment for adult loei residents exposed to arsenic in water and food around an abandoned gold mine. Environmental and Toxicology Management, 2(3): 24-29.

Thai Environmental Engineering Journal Vol. 38 No. 3 (2024) : 65-73
www.eeat.or.th

Effects of an Electrokinetic Barrier to Inhibit Heavy Metal Absorption in *Rhizophora mucronata* Seedlings

Ivan de La Grange[1,2*], Jenyuk Lohwacharin[3] and Chadtip Rodtassana[4]

[1]International Program in Hazardous Substance and Environmental Management, Graduate School, Chulalongkorn University, Bangkok 10330, Thailand
[2]Center of Excellence on Hazardous Substance Management (HSM), Chulalongkorn University, Bangkok 10330, Thailand
[3]Department of Environmental Engineering, Faculty of Engineering, Chulalongkorn University, Bangkok 10330, Thailand
[4]Department of Botany, Faculty of Science, Chulalongkorn University, Bangkok 10330, Thailand
[*]E-mail : Ivan.de-La-Grange@fulbrightmail.org

Article History; *Received: 27 June 2024, Accepted: 11 December 2024, Published: 24 December 2024*

Abstract

Developing an electrokinetic barrier to hinder mangrove seedlings from heavy metal absorption is a novel technology for conducting mangrove reforestation within contaminated environments. In this study, the objectives were to discover a hydroponic solution that offers favorable plant responses for mangrove seedlings and to investigate this environment under a micro-electric field and/or a heavy metal (HM) presence. For 15 weeks, *Rhizophora mucronata* seedlings were grown hydroponically in containers encompassing unique conditions: the control, 1 ml nutrient solution (NS)/L, and 1.5 ml NS/L. Seedlings from 1.5 NS had the greatest mean regarding the number of roots ($p < 0.05$), but the 1 mL NS had the largest mean for root diameter ($p < 0.05$), along with thicker roots and more leaf development also observed. An electrokinetic experiment was performed to compare a direct current of 10 V/m and 20 V/m in a HM solution consisting of 1 ml NS/L with $ZnSO_4 \cdot 7H_2O$ (400 mg/L), $CrCl_3 \cdot 6H_2O$ (400 mg/L), and $CdCl_2 \cdot 2.5H_2O$ (1.5 mg/L). 10 V/m caused a statistically significant migration for Cd and Cr, whereas 20 V/m was required for Zn, respectfully. When comparing the nitrate to phosphate ratios and pH between HM and HM plus electric current (EC), the margins of difference were less substantial for 10 V/m than 20 V/m. It can be concluded that 1 ml NS/L and 10 V/m is preferable for future electrokinetic barrier design, but because HMs affect the pH values of hydroponic solution greater than natural soil conditions, the HM concentration must be reduced for mangrove tolerability accordingly.

Keywords : electrokinetic barrier; mangrove; heavy metal; hydroponics; ion migration

Introduction

Mangroves are a group of tropical-to-subtropical trees and shrubs that grow in intertidal regions due to their ability to withstand fluctuating salinities, as well as aerobic and anaerobic conditions. In developing countries alone, the ecological services and products provided by mangroves are equivalent to an economic value between 33,000-57,000 USD ha/year [1]. However, over the last 50 years, 20-35% of mangrove forests have been lost [2]. Anthro-pogenically, mangroves growing nearby urban areas are impacted by pollution and heavy metals [3, 4]. While mature trees that have been subjected to heavy metal encroachment are capable of impressive bioaccumulation and tolerance [5], germinating seeds and young plants lack fully developed defense systems [6, 7], which lowers their rate of survival and the success of conducting mangrove reforestation projects in similar regions. Plant absorption of heavy metals (HM) and excessive biometals can lead to damage at the cellular level, which inhibits enzyme function, photosynthesis, respiration, and encourage defense mechanisms

that heighten stress [8-11]. Moreover, exposure to multiple HMs simultaneously amplifies the toxic effect to mangrove plants in comparison with single-metal contamination [12, 13]. Therefore, attempting to conduct reforestation in these areas is problematic.

Developing an electrokinetic barrier to hinder mangrove seedlings the opportunity from absorbing HMs is a novel technology for conducting mangrove reforestation within contaminated environments. As a form of electrokinetics, which is a type of environmental remediation that utilizes electric current (EC) to remove chemical species from soil [14], the main advantages are that minimum soil disruption is required, low amounts of waste material are produced, and it can be used in heterogeneous, fine-grained media [15]. For marine application, its potential to inhibit saltwater intrusion into fresh water has been studied [16].

The aim of this study was to address two issues. First, to discover a hydroponic environment that offers favorable plant responses for mangrove seedlings by comparing diverse conditions**.** Second, to investigate the character-istics of an aqueous saline environment under the presence of micro-electric fields and the changes when exposed to a HM intermixture of cadmium (Cd), chromium III (Cr), and zinc (Zn). These results from this study provide fundamental components to developing an intricate electro-kinetic barrier experiment.

Materials and Methods

Growing Mangroves

Rhizophora mucronata seedlings of 35.0 cm ± 4.5 were procured from the Bangpu Nature Education Center (Samut Prakan Province, Thailand). The propagules collected were deemed mature yet absent of any signs of root development. The plants were then grown hydro-ponically in a ventilated greenhouse under natural conditions for 15 weeks that had an average temperature of 37 °C and 65% humidity. Three plastic containers having dimensions of 34 x 34 x 14 cm were selected as growing apparatuses for the mangrove propagules. Nine seedlings were grown per container, with each possessing a distinct solution for comparing morphology. The characteristics of each solution are presented in Table 1. Hydroponic experiments involving mangrove seedlings have been traditionally reliant on the Hoagland Solution for growing [17], which has to be prepared manually using fundamental chemicals. To reduce cost, time, and waste a commercially-made nutrient solution (NS) was purchased and used as an alternative (Sed Grow Tech, Thailand). Buoyant foam was utilized as a contraption to allow the seedlings to stand erect inside of the container while being elevated above the floor of the container, for accommodating root develop-ment. Pieces of foam were cut into sections to fit firmly inside of the container and holes were drilled through the foam to cradle the seedlings, which were then fastened into a stationary position using plastic cable ties (Figure 1). To reduce erroneous results, areas of the containers that were not blocked from sun exposure by the foam were covered with a non-transparent plastic bag to reduce both evaporation and algae growth. Tap water replenishments were added to maintain a consistent volume until a solution change was performed, which occurred once a week.

Morphological Growth Analysis

To reduce touching the plants, which lowers the risk of stress and damage, and ensure better accuracy, seedling growth was recorded once a week through photographic analysis. Pictures of the seedlings were taken using a 12 MP camera, from a smartphone. Every photograph included a ruler in the same plane of each component intended to be measured.

Table 1 Characteristics of the different hydroponic solutions

Parameters	Concentrations			Unit
	Control	1 mL NS	1.5 mL NS	
Volume of tap water	3.0	3.0	3.0	L
Sea salt	9.0	9.0	9.0	g/L
Nutrient solution (NS)	N/A	1.0	1.5	mL/L
Electrical conductivity	12.77	13.13	13.40	mS/cm

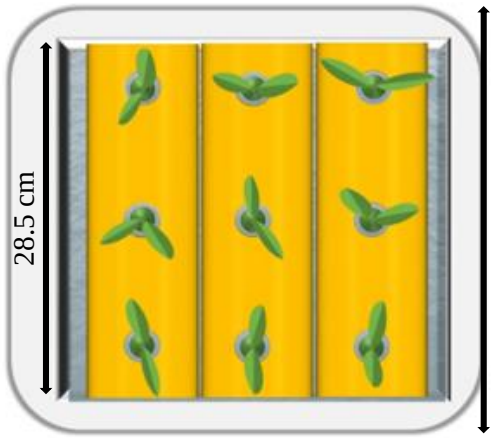

Figure 1 An illustration of the growing phase setup for the seedlings showing the buoyant foam inside of the container. Note that the sides of the container have a solution that is highly exposed to sunlight, which is where a plastic bag was used for covering

ImageJ software was used for calibrating the pixels from the photos into measurements of length, which then allowed the morphological changes of the seedlings to be recordable. The morphology of interest was the number of roots (and fine roots those < 2mm thick), root system diameter, and the number, length (L) and width (W) of the leaves. Additionally, any notable signs of stress for the seedlings were also recorded. To provide the most accurate results, the seedlings were left undisturbed apart from the routine morphology recordings, water replenishments, and solution changes. The data from each seedling was then compiled over a timeline to provide evidence pertaining to which NS would be most favorable for future applications.

Electrokinetic barrier

Electric current was assessed to see how it would affect NS, both with and without the presence of HMs. To carry similar variables to that of the plant growth experiment, the same size containers and volume of solution (3 L) for each setup was used. For the electrokinetic barrier setup, the containers consisted of graphite electrodes (10 x 3 cm) for the anode and cathode, with the attached wiring hung securely over a dowel in order to suspend them above the floor of the container, and a constant direct current (DC) of either 10 V/m or 20 V/m applied (PeakTech 6225 A PeakTech®, Germany), as shown in Figure 2. Due to results of the earlier tests, 1 mL NS/L saline water was used as the control, seedlings omitted, with a HM mixture of $ZnSO_4 \cdot 7H_2O$ (400 mg/L), $CrCl_3 \cdot 6H_2O$ (400 mg/L), and $CdCl_2 \cdot 2.5H_2O$ (1.5 mg/L) to provide the contamination parameters. The HM concentrations selected are reflective of samples collected from the Chao Phraya River and the Upper Gulf of Thailand [18], which has been the regional focus for mangrove reforestation in this study. The six distinct conditions that were explored are presented in Table 2. Each trial lasted for 24 hours followed by sampling at the surface region to prevent mixing and analysis done in triplicates to verify consistency in the results. Cd, Cr, K, and Zn were sampled at the anodic, middle, and cathodic region separately, but nitrate (NO_3^-), phosphate (PO_4^{3-}), and pH were sampled as a composite because the earlier sampling led to solution disruption and inevitable mixing. The metals mentioned were analyzed by ICP-OES; (NO_3^-) and (PO_4^{3-}) values were obtained by using a spectrophotometer (Hach, DR900, United States); and the pH was able to be determined with a pH/Ion/Conductivity probe (SevenGo Duo pro, Mettler Toledo, Switzerland).

Statistics

Data in the figures and tables includes mean values ± SD (standard deviation). The statistical differences of plant morphology grown under distinct hydroponic solutions were analyzed using the Kruskal-Wallis test. Non-parametric Dunn's test was used to provide a pairwise comparison between the three treatments. Findings for metals in the electrokinetic portion of the experiment used one-way ANOVA with Fisher's LSD test. All tests that had the significance determined utilized p-value < 0.05, respectively.

Table 2 Conditions of the six solutions. The plus and minus sign indicate the addition or omittance, respectively

Conditions	Solution 1 mL NS/ L saline water	N: 17.4 mg/L P: 4.2 mg/L K: 85.7 mg/L	Zn: 400 mg/L Cr :400 mg/L Cd: 1.5 mg/L	Electric Current (EC)
Control	+	+	-	-
Control HM	+	+	+	-
10 V/m	+	+	-	+
10 V/m HM	+	+	+	+
20 V/m	+	+	-	+
20 V/m HM	+	+	+	+

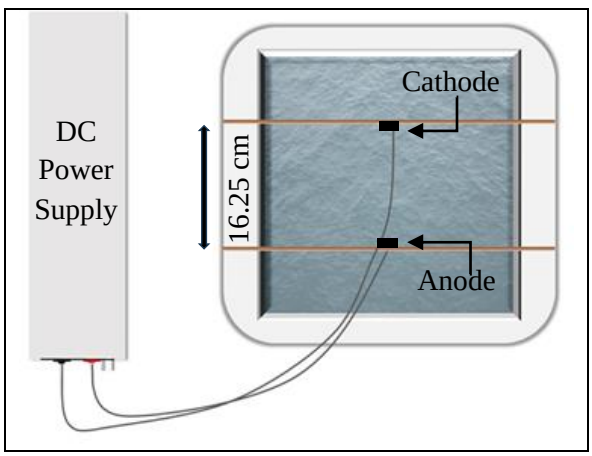

Figure 2 An illustration of the electrokinetic barrier experiment that has applied EC

Results and Discussion

Seedling Morphology

All hydroponic setups induced growth for the *Rhizophora mucronata* seedlings (Table 3). Furthermore, no signs of stress that would have been associated from either the buoyant foam or cable ties were displayed, indicating that the design is suitable for future studies. Despite all this, seedling death was still unavoidable for all the setups, but the cause was independent from the methodology used, for the seedlings never established roots whatsoever. Starting with nine seedlings per container, the final number was 6 for the control, 7 for the 1 mL NS, and 7 for the 1.5 mL NS, respectively.

The average number of roots for the seedlings was 17.5 (control), 27.6 (1 mL NS), and 38.1 (1.5 mL NS). The difference between the control and 1.5 mL NS was significant ($p < 0.05$), but not between the 1 mL NS and 1.5 mL NS. In terms of the number of fine roots (< 2mm), no prominent variations between the 1 mL and 1.5 mL NS solutions were found ($p > 0.05$). For the diameter of the roots, the averages were 4.0 (control), 8.1 (1 mL NS), and 6.6 cm (1.5 mL NS).

The roots of the 1 mL NS group appeared thicker. Mangrove plants do not require aeration in the roots, but rather absorb oxygen in the lenticels and pneumatophores of the stems and leaves which are then delivered to the sub-merged roots. Oxygen can escape through the aerenchyma in the submerged roots in a process known as radial oxygen loss ROL. Longer and thicker roots are a good sign that the plant is delivering oxygen to the root tips in an efficient manner, as thin roots may be more prone to releasing oxygen due to having a higher surface area to volume ratio [19].

The difference in root length between the control and 1 mL NS was significant ($p < 0.05$), but not between the 1 mL NS and 1.5 mL NS. Regarding leaf development, the container of 1 mL NS had five plants with leaf manifestations (3 of which having fully developed leaves) and whose average leaf dimension was (L x W) 3.78 x 1.77 cm, while the 1.5 NS had two plants with leaf appearances (both having fully developed leaves), and whose average leaf dimension (L x W) was 3.60 x 1.40 cm. Leaves were absent in the control. While the ratio of leaf growth between the two nutrient solutions was not significant, the number of leaves was significant (Mann-Whitney test). However, one of the mangrove seedlings from the 1.5 NS group developed yellowish-green leaves with burnt spots, which may indicate that the stronger concentration causes stress or harm to the plants [20]. In connection, it could also explain why lower algae growth were detected (albeit unwanted) with 1.5 mL NS compared with the 1 mL NS solution.

Table 3 Results of the seedling morphology for the different hydroponic solutions (mean ± SD), the different letters represent significant difference by the Kruskal-Wallis test and post-hoc Dunn's test ($p < 0.05$)

Recording Metrics	Control	1 mL NS	1.5 mL NS
Number of Plants	6	7	7
Total number of roots	17.5 ± 4.4^{b}	27.6 ± 5.7^{a}	38.1 ± 10.2^{a}
Number of roots (< 2mm)	5.0 ± 3.9^{b}	11.3 ± 4.8^{a}	13.4 ± 4.9^{a}
Root system diameter (cm)	4.0 ± 0.6^{b}	7.8 ± 1.5^{a}	6.2 ± 1.2^{a}
Number of Plants with leaves	0	5	2
Leaf Length (cm)	-*	3.8 ± 0.3^{a}	3.6 ± 0.5^{a}
Leaf Width (cm)	-*	1.8 ± 0.3^{a}	1.4 ± 0.5^{a}

* No developed leaf observed.

Electrokinetics

Comparisons between the four different metals are presented in Figure 3. Detection of Cr was notably less than the other metals in the Control HM ($p < 0.05$) but inaccurately represented the actual concentration. Due to its semi solubility, the majority of oxidized Cr(III) settled to the bottom of the container, where sampling could not be realized.

For 10 V/m HM, Cd having low hydration properties were advantageous in migrating to the cathode region swiftly ($p < 0.05$), prior to competitive absorption by Zn and Cr [21, 22], but K was more likely grounded by the charges from copious Cl^-. As the activation energy was met to mobilize a larger share of Cr, a significant increase was observed at the cathode ($p < 0.05$), Moreover, their competition for absorption at the cathode repulsed a high number of Zn ions [23], which caused its concentration to rise modestly at the anode ($p > 0.05$). As Cd reached the cathode first, Cr barricaded the ions from escaping, thus forming an inward repulsion that localized the concentration [24], but if failed to migrate in time before mass Cr mobilization, they then followed suit to that of Zn ($p > 0.05$), respectively.

20 V/m HM achieved the highest Cr detection ($p < 0.05$), while also altering some Cr(III) ions into Cr(VI). This was observed as the color of the solution changed from a light green (associated with Cr(III)) to an orange (associated with Cr(VI). The most common Cr(VI) species in low pH is predominantly $HCrO_4^-$ [23]. Being negatively charged, a portion of Cr ions once attracted to the cathode, began reverse migration. This, along with heterogenous Cr reduction offered Zn^{2+} migration opportunity, and the charge density near the cathode freed-up to expectedly permit Cd and K repulsion.

An immense buildup occurred on the cathode in both HM setups, qualitatively signifying that metal migration took place. Although K^+ does not easily precipitate, this phenomenon may also explain the reduced concentration as graphite released from it caused flocculation. As 20 V/m generated a larger buildup, the fixation of K and other metals was assumingly more prominent.

Indeed, the creation of Cr(VI) is concerning due to its greater health risk to the environment than Cr(III). Additionally, its justification for practicality is less pursuant based on the notion that a charge of 20 V/m has been shown to start affecting aquatic life through electrotaxis, whereas 10 V/m is considered to cause minimal impact [25, 26].

EC reduced nitrate and phosphate in all electrokinetic experiments when compared to the control (Figure 4). In terms of nitrogen to phosphate ratio (based on mg/L), the values are as follows: 4.12:1 (control), 12.50:1 (HM), 2.11:1 (10 V/m), 36.15:1 (10 V/m HM), 7.66:1 (20 V/m), and 186.17:1 (20 V/m HM), respectively. While 10 V/m caused a decline, due to the ions conditionally reacting and forming nitrogen gas products at the anode region [27], 20 V/m was less dramatic, as the high amount of hydroxide precipitates may have contributed to NO_3^- stabilization [28]. Interestingly, setups containing HMs showed higher concentrations of NO_3^- than its counterparts without it, which advocates that pH is not a determining factor in concentration decline [29]. In the HM setup, NO_3^- were attracted to the highly polarizing Cr ions (despite reduction from available OH ions) and migrated downward towards the bottom of the container, which caused a low concentration in similarity to

Cr(III) mentioned. The polarity of Cr in the 10 V/m HM hindered the rate of NO_3^- migration to the anode, which extended the time and concentration near the surface region. NO_3^- was more abundant for 20 V/m HM because of the combined effects of enhanced Cr mobility and negatively-charged Cr(VI) engaged in competition for anode access. Moreover, the immense buildup occurred on the cathodes previously mentioned likely also dampened its polarity repulsion of NO_3^- as well.

Phosphate reduction was more apparent. 20 V/m caused a reduction greater than 10 V/m, as the higher pH stabilized PO_4^{3-} for precipitation by the bioessential metals found in the hydroponic solution, but the concentration was still less impacted than being spiked with HMs only. This was mainly contributed to Cr(III) capability of binding to phosphorus ions that exist at lower pH values than that of phosphate, which further reduced in concentration upon experiencing higher Cr mobilization by EC.

The high reduction of both ions are due to the fast migration capability from the hydroponic environment. The depletion of nitrogen and phosphorus would not have been as significant in soil because the ions would had been attracted to soil particles (causing binding) and the byzantine patterns involved with migration [30]. Furthermore, seawater contains traces of both ions [31], which in abundance can provide a source of ion replenishment to help compensate for the deficiency.

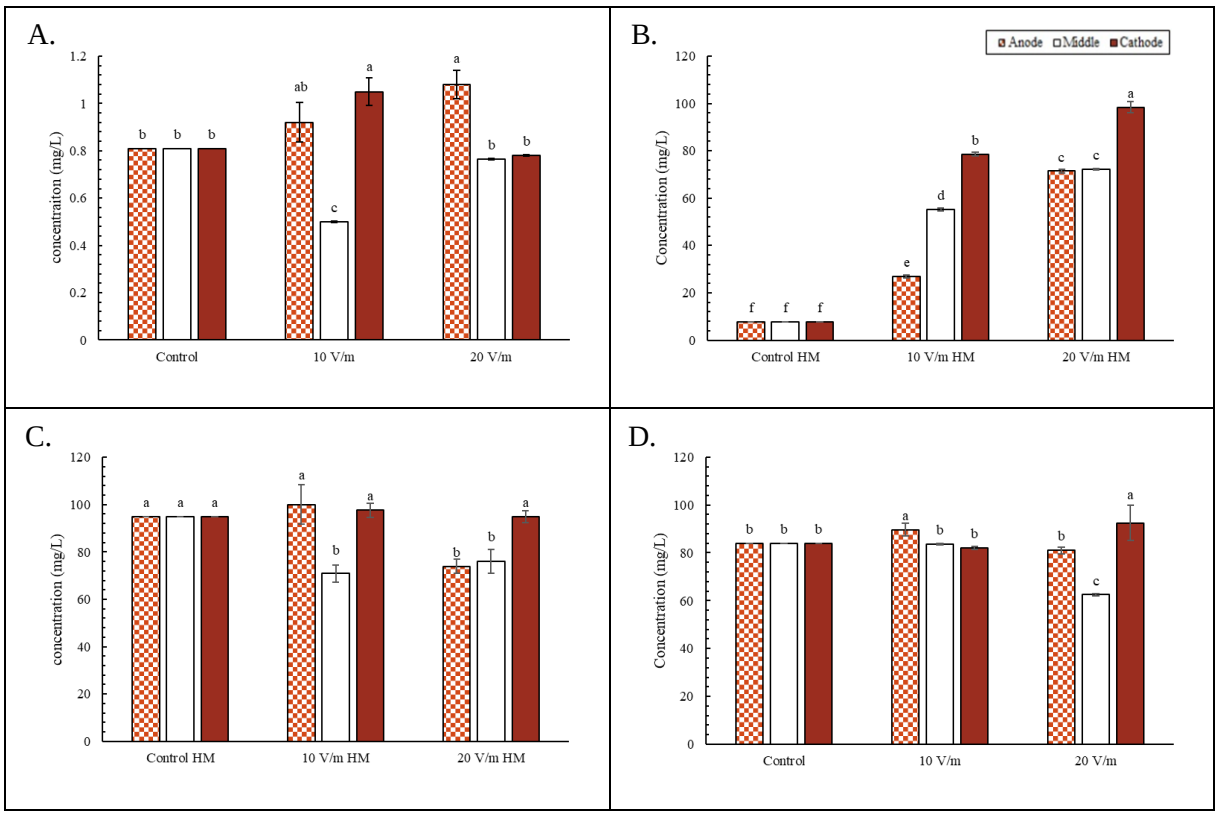

Figure 3 The migration of metals for (A) Cd, (B) Cr, (C) K, and (D) Zn after 24 hours. Error bars display the standard deviation. Columns with different letter symbolize statistical significance as per Fisher's LSD test ($p < 0.05$)

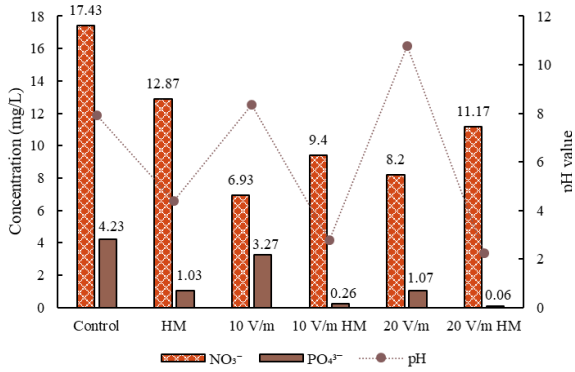

Figure 4 The concentrations of nitrate and phosphate (bars) and pH values (line) of the different setups

HMs and EC were both responsible for fluctuations in pH. A correlation was observed between the pH value of a solution and how it shifted after EC implementation. Essentially, EC exposure heightened alkalinity in the control, whereas the HM solution, which had a lower pH than the initial control, became even more acidic. While both outcomes consisted of OH^- and H^+ being generated from the electrodes, the difference stemmed from hydrogen gas being emitted out of the EC setups (leaving behind OH^-), whereas hydroxide precipitation from HM reduction was stabilizing the dissolved H^+ from volatilization. This margin of dichotomy was consistent for all the setups utilizing EC, with results being more profound for 20 V/m than 10 V/m in both setups. Moreover, the highest and lowest values in the pH range for 20 V/m tend to exceed the tolerability for mangroves [32]. Adding several types of bases was attempted to raise the pH, but this warranted ion precipitation and hindered ion migration.

These findings may not necessarily depict that of soil, for it has a complex buffering capacity and particle heterogeneity which are of absence in the studied hydroponic solution. But it is likely that soil conditions would still adhere to similar trends, even if not as severe, and therefore should be noted for in soil applications.

Conclusions

Despite the larger number of roots observed from the mangrove seedlings in the 1.5 mL NS solution, the 1 mL NS solution was selected for future experiments as the average root diameter was longer and thicker along with the leaf development being more prominent. 10 V/m caused a significant migration of ions for Cd, and Cr in the 1 mL NS/L, while 20 V/m was required for Zn, and K was ambivalent, respectively. While pH values are sensitive to both HM presence and EC, the setups incorporating 10 V/m provided an overall pH margin range less substantial than 20 V/m. Moreover, the ratio of nitrogen to phosphate for 10 V/m is also less than that of 20 V/m in all setups. Being that future investigation will involve *R. mucronata* seedlings being exposed to a HM hydroponic environment with EC applied, 10 V/m will be selected for future study in the electrokinetic barrier design. However, HM concentrations affect pH acidity more sensitively for a hydroponic solution than a soil, which has led to values too low for mangrove tolerability. Therefore, advisement is focused on raising the pH through a reduction in the initial HM concentration prior to starting the experiment. Additionally, the durability and placement of the electrodes (due to buildup) along with the avoidance of unintended electrokinetic phytoremediation requires further investigation prior to experiments beginning to incorporate live plants.

Acknowledgements

This research is supported by the Rachadapisek Sompote Endowment Fund (2022), Chulalongkorn University (765007-RES02) and the IP-HSM research grant, Graduate School, Chulalongkorn University. The first author would like to express gratitude to the Faculty of Engineering, Chulalongkorn University for providing the facilitation and resources to conduct this study. Recognition and appreciation are also to be given to the personnel at Bangpu Nature Education Center for their propagule contribution.

References

[1] UNEP. 2014. The Importance of Mangroves to People: A Call to Action. van Bochove, J., Sullivan, E., Nakamura, T. (Eds). United Nations Environment Programme World Conservation Monitoring Centre, Cambridge. 128 pp.

[2] Polidoro, B. A., Carpenter, K. E., Collins, L., Duke, N. C., Ellison, A. M. et al. 2010. The Loss of Species: Mangrove Extinction Risk and Geographic Areas of Global Concern. PLOS ONE, 5(4): e10095.

[3] Dwivedi, S. N. and Padmakumar, K. G. 1983. Ecology of a Mangrove Swamp near Juhu Beach, Bombay with Reference to Sewage Pollution. In H. J. Teas (Ed.), Biology and ecology of mangroves. Springer Netherlands. 163-170.

[4] Tam, N. F. Y. and Wong, Y. S. 2000. Spatial Variation of Heavy Metals in Surface Sediments of Hong Kong Mangrove Swamps. Environmental Pollution. 110(2): 195-205.

[5] Peters, E.C., Gassman, N.J., Firman, J.C., Richmond, R.H. and Power, E.A. 1997. Ecotoxicology of Tropical Marine Ecosystems. Environmental Toxicology and Chemistry. 16(1): 12-40.

[6] Liu, X.L., Zhang, S.Z., Shan, X.Q. and Zhu, Y.G. 2005. Toxicity of Arsenate and Arsenite on Germination, Seedling Growth and Amylolytic Activity of Wheat. Chemosphere. 61: 293-301.

[7] Wang, W. 1987. Factors Affecting Metal Toxicity to (and Accumulation by) Aquatic Organisms - Overview. Environ Int. 13: 437-57.

[8] Huang, G-Y. and Wang, Y-S. 2010. Physiological and Biochemical Responses in the Leaves of Two Mangrove Plant Seedlings (*Kandelia candel* and *Bruguiera gymnorrhiza*) Exposed to Multiple Heavy Metals. Journal of Hazardous Materials. 182: 848-854.

[9] Vangronsveld, J. and Clijsters, H. Toxic Effects of Metals. In: Farago, M.E. (Ed.), Plants and The Chemical Elements-Biochemistry, Uptake, Tolerance and Toxicity, VCH Publishers; 149-177.

[10] Yadav, A., Ram, A., Majithiya, D., Salvi, S., Sonavane, S., Kamble, A. et al. 2015. Effect of Heavy Metals on the Carbon and Nitrogen Ratio in *Avicennia marina* from Polluted and Unpolluted Regions. Marine Pollution Bulletin. 101: 359-365.

[11] Yadav, K.K., Gupta, N., Prasad, S., Malav, L.C., Bhutto, J.K., Ahmad, A. et al. 2023. An Eco-Sustainable Approach towards Heavy Metals Remediation by Mangroves from the Coastal Environment: A Critical Review. Marine Pollution Bulletin. 188: 114569.

[12] Liu, Y., Tam, N.F.Y., Yang. J.X., Pi, N., Wong, M.H. and Ye, Z.H. 2009. Mixed Heavy Metals Tolerance and Radial Oxygen Loss in Mangrove Seedlings. Marine Pollution Bulletin. 58: 1843-1849.

[13] MacFarlane G.R. and Burchett, M.D. 2002. Toxicity, Growth and Accumulation Relationships of Copper, Lead and Zinc in the Grey Mangrove *Avicennia marina* (Forsk.) Vierh. Marine Environmental Research. 54(1): 65-84.

[14] Acar, Y.B. and Alshawabkeh, A.N. 1993. Principles of Electrokinetic Remediation. Environmental Science and Technology. 27(13): 2638-2647.

[15] Alshawabkeh, A.N. 2009. Electrokinetic Soil Remediation: Challenges and Opportunities. Separation Science and Technology. 44(10): 2171-2187.

[16] Sutar, A.A. and Rotte, V.M. 2023. Performance Evaluation of One Dimensional Electrokinetic Barrier Subjected to Saltwater Intrusion: A Laboratory Scale Study. Materials Today: Proceedings. 80: 972-980.

[17] Hoagland, D.R. and Arnon, D.I. 1950. The Water-Culture Method for Growing Plants Without Soil. California Agricultural Experiment Station. Circular 347.

[18] Qiao, S., Shi, X., Fang, X., Liu, S., Kornkanitnan, N., Gao, J. et al. 2015. Heavy Metal and Clay Mineral Analyses in the Sediments of Upper Gulf of Thailand and their Implications on Sedimentary Provenance and Dispersion Pattern. Journal of Asian Earth Sciences. 114: 488-496.

[19] Ogorek, L.L.P., Pellegrini, E. and Pederson, O. 2021. Novel Functions of the Root Barrier to Radial Oxygen Loss – Radial Diffusion Resistance to H_2 and Water Vapour. New Phytologist. 231: 1365-1376.

[20] Sarkadi, L. S. 2019. Effects of Fertilizer on Food Supply. In Chemistry's Role in Food Production and Sustainability: Past and Present; American Chemical Society, 1314; 129-145.

[21] Wang, T., Liu, W., Xiong, L., Xu, N. and Ni, J. 2013. Influence of pH, Ionic

Strength and Humic Acid on Competitive Absorption of Pb(II), Cd(II), and Cr(III) onto Titanate Nanotubes. Chemical Engineering Journal. 215-216: 366-374.

[22] Mahmood, T., Saddique, M.T., Naeem, A., Mustafa, S., Zeb, N., Shan, K.H. and Waseem, M. 2011. Kinetic and Thermodynamic Study of Cd(II), Co(II), and Zn(II) Adsorption from Aqueous Solution by NiO. Chemical Engineering Journal. 171: 935-940.

[23] Blázquez, G., Hernáinz, F., Calero, M., Martín-Lara, M.A. and Tenorio, G. 2009. The Effect of pH on the Biosorption of Cr (III) and Cr (VI) with Olive Stone. Chemical Engineering Journal. 148: 473-479.

[24] Yang, S., Yan, B., Lu, L. and Zeng, K. 2016. Grain Boundary Effects of Li-Ion Diffusion in a $Li_{1.2}Co_{0.13}Ni_{0.13}Mn_{0.54}O_2$ Thin Film Cathode Studied by Scanning Probe Microscopy Techniques. The Royal Society of Chemistry. 6: 94000-94009.

[25] Chew, C.C. and Zhang, T.C. 1999. Abiotic Degradation of Nitrates Using Zero-Valent Iron and Electrokinetic Processes. Environmental Engineering Science. 16(5): 389-401.

[26] Bary, B.M. 1956. The Effect of Electric Fields on Marine Fishes. Marine Research Scotland. 1: 1-32.

[27] Breen, M., Howell, T., Copland, P. 2011. A Report on Electrical Fishing for Razor Clams (*Ensis Sp*.) and its Likely Effects on the Marine Environment. Marine Scotland Science Report. 2(3): 1-120.

[28] Choe, S., Liljestrand, H.M. and Khim, J. 2004. Nitrate Reduction by Zero-Valent Iron under Different pH Regimes. Applied Geochemistry. 19: 335-342.

[29] Delfino, J.J. 1979. The Stability of Nitrate in Unpreserved Potable Water Samples. Journal - American Water Works Association. 71(10): 584-586.

[30] Yeung, A.T. 2006. Contaminant Extractability by Electrokinetics. Environmental Engineering Science. 23(1): 202-224.

[31] Pawlowicz, R. 2013. Key Physical Variables in the Ocean: Temperature, Salinity, and Density. 4(4): 1-13.

[32] Kathiresan, K., Moorthy, P. and Ravikumar, S. 1996. A Note of the Influence of Salinity and pH on Rooting of *Rhizophora mucronata* Lamk. Seedlings. The Indian Forester. 122(8): 763-764.

Thai Environmental Engineering Journal Vol. 38 No. 3 (2024) : 75-85
www.eeat.or.th

Performance of Pilot-scale Constructed Wetlands for Treating Paper Mill Effluent

Netnapid Tantemsapya[1*], Patcharin Racho[1] and Chatpet Yossapol[1]

[1]School of Environmental Engineering, Institute of Engineering,
Suranaree University of Technology, Nakhon Ratchasima, 30000, Thailand
[*]E-mail : netnapid@sut.ac.th

Article History; *Received: 30 May 2024, Accepted: 23 December 2024, Published: 24 December 2024*

Abstract

Wastewater discharged from the paper industry generates substantial volumes, ranging between 75 and 225 m³ per ton of product, containing high levels of organic content (COD 480-4450 mg/L), chloride (80-980 mg/L), and a variety of volatile fatty acids (approx. 950 mg/L), cellulose (approx. 1,200 mg/L). The objective of this study was to investigate the efficiency and reaction coefficients of the free water surface flow constructed wetlands (FWS CWs) for removing pollutants such as color, dissolved solids, suspended solids, chemical oxygen demand (COD), biochemical oxygen demand (BOD_5), and nitrogen (TKN). Three pilot-scale units were established, each containing sand as the media and planted with (1) Narrowleaf cattail (*Typha angustifolia* L.), (2) Loop-root mangrove (*Rhizophora mucronata* Lam.), and (3) Unplanted control. Upon evaluating the system's performance, it was observed that the FWS CWs effectively reduced contaminants in the factory effluent, particularly color, COD and TKN. The color removal efficiency ranged from 31.15-93.55% (56.86$\pm$18.31), 17.86-89.25% (54.30$\pm$21.39%), and 27.87-91.40% (58.11$\pm$18.84%) for control, cattail, and mangrove unit, respectively. Regarding COD removal, the efficiencies ranged from 31.15-93.55% (56.86$\pm$18.31), 17.86-89.25% (54.30$\pm$21.39%), and 27.87-91.40% (58.11$\pm$18.84%) for control, cattail, and mangrove unit, respectively. Both COD and color removal efficiency presented no statistically significant differences observed among the three units ($P > 0.05$). The removal efficiency of TKN was 40.00 and 85.74%, 20.00 and 85.71%, and 80.00% and 85.71% for control, cattail, and mangrove unit, respectively. The reaction kinetics of color removal appear to align with both Plug Flow Reactor (PFR) and Continuous Stirred Tank Reactor (CSTR) models. Rate constants for color removal were calculated for the control and mangrove units, as no color removal was observed in the cattail unit. For the mangrove unit, the first-order reaction rate constants were 0.021 d^{-1} for the PFR model and 0.023 d^{-1} for the CSTR model, while for the control unit, they were 0.030 d^{-1} for the PFR model and 0.035 d^{-1} for the CSTR model. COD reduction can be described by the CSTR model, with first-order reaction rate constants of 0.140 d^{-1} for the control unit, 0.131 d^{-1} for the cattail unit, and 0.143 d^{-1} for the mangrove unit.

Keywords : free water surface flow, paper mill wastewater, Narrowleaf cattail (*Typha angustifolia* L.), Loop-root mangrove (*Rhizophora mucronata* Lam.)

Introduction

The paper industry plays a significant role in global economy by providing essential products for various sectors. However, the paper production often generates substantial volumes of wastewater, between 75 and 225 m^3 per ton of product [1], with effluent containing high levels of chemical oxygen demand (COD) (480-4450 mg/L), chloride (80-980 mg/L), total dissolved solids (395-2500 mg/L), volatile fatty acids (approx.950 mg/L), and cellulose (approx.1,200 mg/L). Adsorbable organic halides (AOX) are also commonly presented [2]. Effluent of the paper mills can pose serious environmental challenges if it is not properly treated before discharge.

Constructed wetlands have emerged as a promising eco-friendly solution for tertiary treatment of wastewater from various sources, including the effluent generated by pulp and paper mills. These engineered systems mimic the natural processes occurring in wetlands, utilizing the combined mechanisms of physical, chemical, and biological processes to remove pollutants from wastewater [3]. Numerous studies have demonstrated the effectiveness of constructed wetlands in treating pulp and paper mill effluent. For example, the research conducted by Abira et al. [4] evaluated the performance of a pilot-scale constructed wetland system in removing phenols from pre-treated pulp and paper mill wastewater. The study reported significant reductions in phenols by 60% at 5-day hydraulic retention time (HRT) and 77% at 3-day hydraulic retention time (HRT) on average. Similarly, investigations by Rani et al. [5] documented the successful treatment of pulp and paper mill effluent using a small wetland system planted with cattail and canna. The study revealed high removal efficiencies for color, TS, BOD and COD, highlighting the potential of constructed wetlands for addressing the specific challenges associated with pulp and paper mill wastewater.

The study paper factory, located in central Thailand, specializes in producing corrugated paper from recycled materials. It discharges 30,000 m^3/day of effluent with total suspended solids (TSS) of 11.0 to 127.0 mg/L, chemical oxygen demand (COD) of 90.0 to 352.0 mg/L, biochemical oxygen demand (BOD_5) of 7.0 to 33.0 mg/L, and ammonia nitrogen (NH_3-N) of 70.4 to 22.8 mg/L. To improve the water quality of the effluent before discharging it into the nearby river, a low-cost and sustainable constructed wetland system was proposed as a tertiary wastewater treatment solution.

This paper aims to explore the application of constructed wetlands for the treatment of paper mill effluent. It will delve into the principles behind constructed wetlands, their design considerations, and the mechanisms by which they effectively remove contaminants from wastewater. The significance of this study lies in addressing the persistent need for sustainable and efficient wastewater treatment methods in the pulp and paper industry. By evaluating the feasibility and effectiveness of constructed wetlands, this paper seeks to contribute to the development of environmentally sound practices for mitigating the environmental impact of pulp and paper production.

Methodology

Paper mill wastewater characteristics

The paper factory, located in the central Thailand, specializes in producing corrugated paper derived from recycled materials. For the study, the paper mill effluent (PME) was sourced from the secondary clarifier of the factory's wastewater treatment plant. Table 1 presents the wastewater characteristics observed over a one-year period (2023); indicating TSS ranged from 11.0 to 127.0 mg/L (41.30±24.3), COD ranged from 90.0 to 352.0 mg/L (187.73±48.6), BOD_5 ranged from 7.0 to 33.0 mg/L (15.31±4.7) and NH_3-N ranged from 0.4 to 22.8 mg/L (10.1±3.3). Most of the time, effluent complied with Thai standards.

Pilot scale unit setup

The pilot study was conducted within the area of Suranaree University of Technology, where a small-scale constructed wetland system was set up using a fiberglass tank with the size of 2.30 m (length) x 0.80 m (width) x 0.55 m (height). The tank's full capacity was 1,012 liters, with a total working volume of 552 liters and a void volume of 300 liters. A layer of sand, less than 2.00 mm in size and 0.20 meters thick, was placed within the tank. The pilot-scale constructed wetland tank was equipped with a piping system comprising an inlet pipe (∅ 1/2 inch), an outlet pipe (∅ 1/2 inch), and a sampling

Table 1 Wastewater characteristic of paper mill effluent

Parameter	Unit	Ranges	Average ±SD	Industrial Eff. standard[1/]
pH	-	7.1-8.1	7.1±0.8	-
TSS	mg/L	11.0-127.0	41.30±24.3	40
Turbidity	NTU	5.3-92.1	21.77±18.9	-
COD	mg/L	90.0-352.0	187.73±48.6	270
BOD_5	mg/L	7.0-33.0	15.31±4.7	30
NH_3-N	mg/L	0.4-22.8	10.1±3.3	10 (TKN)
Phosphorus	mg/L	0.2-12.3	1.3±0.7	-

[1/]Ministerial Notifications on the requirements on the characteristic of discharge wastewater from pulp and paper industry, 2018. (B.E. 2562) issued by Department of Industrial Works

[2/] Data obtained from paper factory (2023)

pipe (∅ 4 inch). Three sampling pipes were positioned eventually within a perforated plastic basket filled with 3/8-inch crushed stone to facilitate water passage. Figure 1 illustrates the setup of the FWS CWs system and the positioning of the sampling pipe.

Cultivated-plant species

Narrowleaf cattail (*Typha angustifolia* L.) had exhibited promising efficacy in the removal of contaminants from wastewater in Subsurface Flow Constructed Wetlands (SFCW) [6, 7]. Additionally, the Loop-root mangrove (*Rhizophora mucronata* Lam.), a macrophyte commonly found in the vicinity of the factory and demonstrated to be effective in treating wastewater in the Laem Phak Bia development and environment research project under the Royal Projects demonstration site, was selected for inclusion in this study. In the pilot-scale units, Narrowleaf cattail shoots were carefully separated from the main rhizome, retaining only the supportive rhizome and root portions to promote initial growth. Two to three shoots were then planted directly into the media at a depth of 0.20 m, spaced 0.2 m apart (9 plants m^{-2}). For the loop-root mangrove, nursery-raised seedlings approximately 30 cm tall were planted at a depth of 0.20 m and spaced 0.12 m apart (9 plants m^{-2}) [8]. Before the application of the PME load, the plants underwent a nurturing period of 4 weeks in a nursery setting.

Pilot scale experiment operation

The experimental units were operated as continuous plug flow reactors. Initially, they were filled with clean water for a period of four weeks after planting, followed by a gradual increase in the supply of paper mill effluent (PME) over the subsequent four weeks. PME was collected weekly from the factory. The hydraulic retention time was set at 7 days, with the flow rate of PME into the experimental units controlled by inlet and outlet valves. Samples were collected from 5 points: the inlet, 3 sampling pipes, and the outlet of the system. These samples were then analyzed for pH, EC, TDS, color, TSS, BOD_5, and COD, following the methods outlined in APHA 2022.

The water quality was monitored at weekly intervals over a period of 2 months. The performance of pollutant removal in the pilot-scale constructed wetland was determined using the percentage removal equation (1):

$$\text{Percentage of removal, \%} = \frac{C_{in}-C_{out}}{C_{in}} x\ 100 \quad (1)$$

where C_{in} and C_{out} are the concentration of influent and effluent of the constructed wetland cell.

Two kinetic models, incorporating first-order biological degradation kinetics with plug-flow (PFR) and Continuous Stirred Tank Reactor (CSTR) flow patterns, were employed to calculate the constant rate for color and COD removal [9, 10].

The PFR first order reaction coefficient was determined using equation (2):

$$C_t = C_0 e^{-kt} \quad (2)$$

where C_t and C_o are the concentration at time t and influent of the constructed wetland cell.

The CSTR first order reaction coefficient was determined using equation (3):

$$C_t = \frac{C_0}{1+kt} \quad (3)$$

where C_t and C_o are the concentration at time t and influent of the constructed wetland cell.

Statistical analysis

Statistical analysis was performed by the SPSS statistics 17.0 for windows software package program network Licensed in Suranaree University of Technology. Data was calculated by mean, minimum, maximum and standard deviation for a result. Significance of different was determined with *t*-test (Significant at level of 0.05). Pearson correlation coefficient (significant at level of 0.05) was used to determine correlation.

Results and Discussion

Performance of treatment system

The pilot-scale of FWS CW units was planted with Loop-root mangrove (*Rhizophora mucronata* Lam.) and Narrowleaf cattail (*Typha angustifolia* L.) and supplied with the effluent of the paper factory. Additionally, the control system without plants was conducted for comparison, aiming to assess the potential of the units as tertiary treatment system and to serve as a control. Data collection was conducted at 8-13 different times to ensure the comprehensive data coverage. The results are depicted in Figure 3 and summarized in Table 2.

1) pH: The influent pH ranged from 7.60 to 8.16. After treatment, the pH increased slightly, with average values of 8.29 ± 0.16 for the control unit, 8.28 ± 0.12 for the cattail unit and 8.23±0.16 for the mangrove unit. The pH of the treated PME across all three units showed no statistically significant differences (P > 0.05).

2) EC: The EC of the PME ranged from 2.89-3.43 mS/cm. After treatment, all three units exhibited a slight reduction in EC compared to the influent values. The average EC values were 2.95 ± 0.11 mS/cm for the control unit, 3.01 ± 0.32 mS/cm for the cattail unit, and 2.91 ± 0.10 mS/cm for the mangrove unit. No statistically significant differences were observed among the three units (P > 0.05).

3) Total dissolved solids (TDS): All three FWS CWs units exhibited some reduction of TDS compared to its original state. Prior to treatment, the TDS levels contained in the paper mill effluent (PME) ranged from 1,422 to 1,688 mg/L. After treatment, the reduction of TDS levels ranged from 0.00-14.22% (6.00±5.39%), 0.00-11.49% (6.67± 5.19%) and 0.00-16.29% (7.32±6.31%) for control, cattail, and mangrove units, respectively. When comparing the TDS levels of the treated PME from all three units, no statistically significant differences were observed (P > 0.05). Moreover, TDS reduction of such 3 units was relatively low as not exceeding 16.29%. The TDS levels contained in PME primarily consist of highly soluble inorganic pollutants, such as Cl^- (459.05 ± 83.75 mg/L), which are resistant to biodegradation. Consequently, these pollutants cannot be easily reduced through chemical precipitation, ion exchange, or plant absorption in constructed wetlands, resulting in low overall removal efficiency.

4) Color: All three FWS CWs units exhibited a reduction of color in PME. Prior to treatment, color levels contained in PME ranged from 118.20 to 174.71 ADMI. After treatment, the reduction of color levels ranged from 0.00-29.39% (16.47±9.86%), 0.00-10.69% (3.56 ±3.90%), and 1.74-22.26% (14.06±6.95%) for control, cattail, and mangrove units, respectively. The color contained in the paper and pulp manufacturing process is generated by lignin compounded in the plants used as raw material for paper production. It exhibits a three-dimensional network structure of polymers, composed of units of phenylpropane. In its normal state, lignin is a complex polymer embedded within the cell structure of wood tissue and is insoluble in typical solvents. In the papermaking process, lignin is separated out during the pulp bleaching process [11]. Generally, soil infiltration systems have good color removal capabilities because of the slow flow of wastewater through the medium within the treatment system, allowing lignin to be filtered out by the medium, such as rocks, gravel, sand, and plant roots. Additionally, mechanisms

such as sedimentation and settling to the bottom, as well as decomposition within the system, also contribute to color removal [12, 13]. When comparing the color removal efficiency of the treated paper mill effluent across all three units, the control unit and the unit planted with mangrove demonstrated better treatment performance than the unit planted with cattail ($P > 0.05$). However, no significant difference in color removal was observed between the control unit and the unit planted with mangrove ($P > 0.05$). This finding suggests that the presence of mangrove in the FWS CWs does not substantially influence color reduction during the experimental period. Soil filtration appears to play a dominant role in color removal. This might be due to the constraint faced by any phytoremediation process that requires longer time for full contamination. Similar results were reported by Md Yusoff et al. [14], where no significant difference in color removal was observed between an SSF system planted with *S. grossus* and a control.

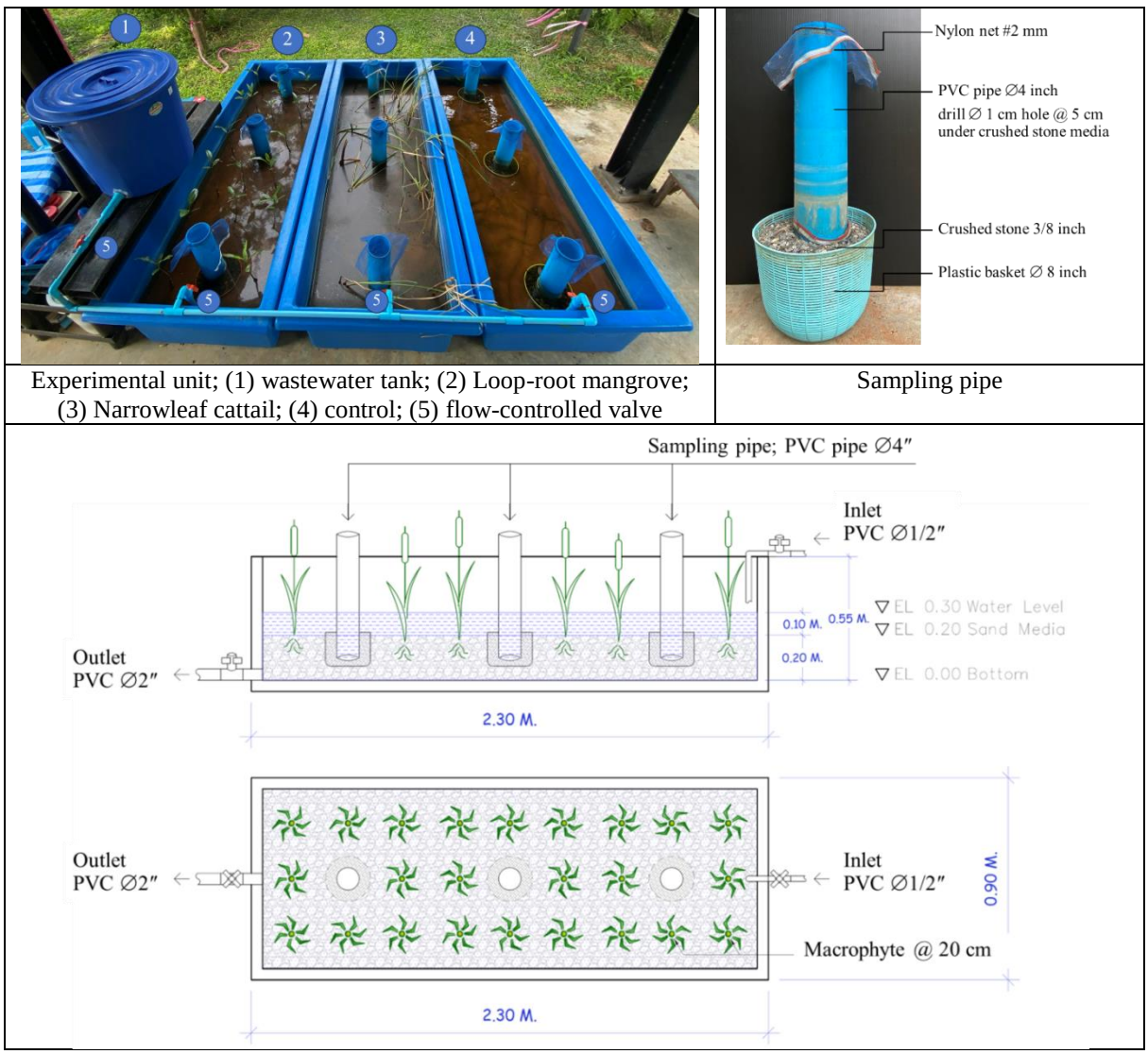

Experimental unit; (1) wastewater tank; (2) Loop-root mangrove; (3) Narrowleaf cattail; (4) control; (5) flow-controlled valve

Sampling pipe

Figure 1 The pilot-scale of FWS constructed wetland


Narrowleaf cattail (10.05.2023)


Narrowleaf cattail (10.08.2023)


Loop-root mangrove (10.05.2023)


Loop-root mangrove (10.08.2023)

Figure 2 Photo of plants in the pilot-scale constructed wetland at the beginning and at the end of the experiments

Table 2 Experimental results and removals (in %) of pH, EC, TDS, Color, BOD_5 and COD

Parameter		Inlet	Eff-Control	Eff-cattail	Eff-mangrove
pH (mg/L)	Ranges	7.60-8.16	8.04-8.54	8.15-8.54	8.03-8.47
	Avg. ±SD	7.87±0.19	8.29±0.16	8.28±0.12	8.23±0.16
EC (mS/cm)	Ranges	2.89-3.43	2.77-3.17	2.61-3.67	2.74-3.11
	Avg. ±SD	3.12±0.20	2.95±0.11	3.01±0.32	2.91±0.10
TDS (mg/L)	Ranges	1,422-1,688	1,392-1,509	1,318-1,526	1,376-1,480
	Avg. ±SD	1,533.67±100.56	1,451.63±32.50	1,449.38±75.66	1,425.88±32.07
	% removal	-	0.00-14.22	0.00-11.49	0.00-16.29
	% removal	-	6.00±5.39	6.67±5.19	7.32±6.31
Color (ADMI)	Ranges	118.2-174.7	119.0-132.3	145.3-187.0	94.3-139.3
	Avg. ±SD	151.2±17.4	123.2±4.5	158.1±13.7	127.3±16.5
	% removal	-	0.00-29.39	0.00-10.69	1.74-22.26
	% removal	-	16.47+9.86	3.56±3.90	14.06±6.95
BOD_5 (mg/L)	Ranges	9.0-14.0	74.5-143.9	19.3-171.7	22.0-149.9
	Avg. ±SD	11.0±9.0	106.1±27.9	119.4±53.6	87.0±50.3
	% removal	-	-	-	-
	% removal	-	-	-	-
COD (mg/L)	Ranges	112.0-186.0	12.0-84.0	20.0-92.0	16.00-88.00
	Avg. ±SD	150.08±22.29	61.54±21.33	64.77±23.77	59.69±21.63
	% removal	-	31.15-93.55	17.86-89.25	27.87-91.40
	% removal	-	56.86±18.31	54.30±21.39	58.11±18.84
NH_3-N (mg/L)	Ranges	0.7-1.0			
TKN (mg/L)	Ranges	5-10	1.0-4.0	1.0-3.0	1.0-1.0
Nitrate (mg/L)	Ranges	1.0-9.0			
	% removal	-	40-85.74	20.00-85.71	80.00-85.71

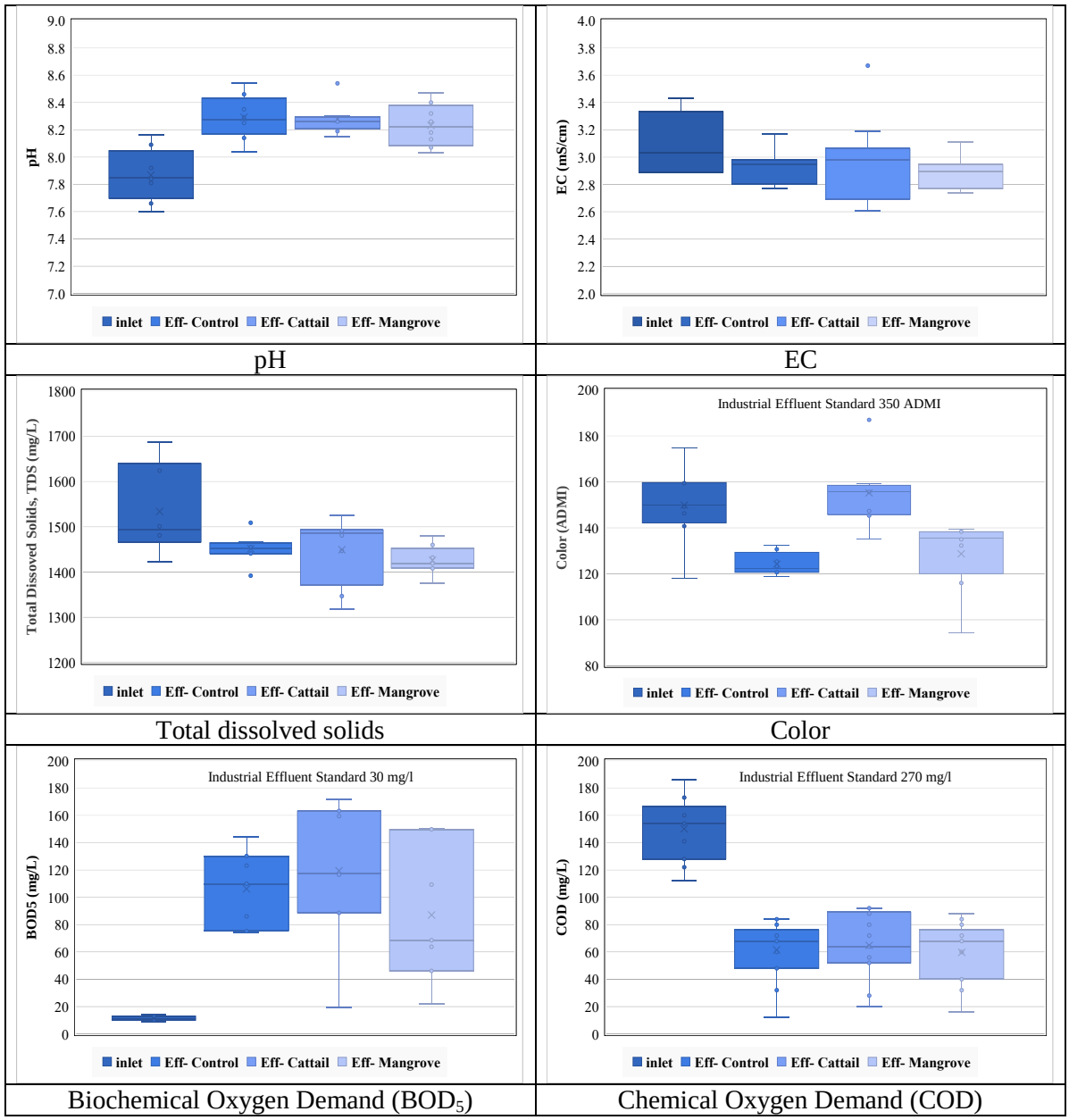

Figure 3 Graphical representation of pH, EC, TDS, Color, BOD_5 and COD at the inlet and outlet of FWS CWs units

5) Biochemical Oxygen Demand (BOD_5): The effluent of all three experimental units exhibited an increase in BOD_5 compared to its original state. Initially, the BOD_5 level contained in PME ranged from 9.0 to 14.0 mg/L. After treatment, the BOD_5 levels varied, ranging from 74.5 to 143.9 mg/L (106.15±27.89) for the control unit, 19.3 to 171.7 mg/L (119.43±53.61) for the cattail unit, and 22.0 to 149.9 mg/L (87.04±50.26) for the mangrove unit. However, upon the treatment with FWS CWs, it was observed that the BOD_5 levels contained in the effluent from all three units exceeded the standard limit of 20 mg/L set by the National Standard (Ministerial Notifications on the requirements on the characteristic of discharge wastewater from pulp and paper industry, 2018. (B.E. 2562)). It is worth noting that the paper mill effluent (PME) used in the experiment had a relatively low BOD_5 concentration of

9.0-14.0 mg/L. Upon passing through the experimental units placing with plants, the plant leaves undergone with microbial decomposition, which is a primary process in reducing organic matter. This decomposition occurred under both aerobic and anaerobic conditions, resulting in an increase in BOD_5 levels. Additionally, the wastewater contained nitrogen derived from the decomposition of proteins in paper tissue (ammonia nitrogen levels contained in PME ranged from 0.4 to 22.8 mg/L), as well as phosphorus (phosphorus levels in PME ranged from 0.2 to 12.3 mg/L). Nitrogen serves as a nutrient that stimulates algal and plant growth, increasing nutrient loads in the system and ultimately causing a rise in BOD_5.

6) Chemical Oxygen Demand (COD): The effluent of all three experimental units exhibited a decrease in COD compared to its original state. Prior to treatment, the COD levels contained in PME ranged from 112.0 to 186.0 mg/L. After treatment, the reduction in COD ranged from 31.15-93.55% (56.86$\pm$ 18.31), 17.86-89.25% (54.30$\pm$21.39%), and 27.87-91.40% (58.11$\pm$18.84%) for control, cattail, and mangrove unit, respectively. After treatment, the COD levels varied, ranging from 12 to 84 mg/L for the control unit, 20 to 92 mg/L for the cattail unit, and 16 to 88 mg/L for the mangrove unit. No statistically significant differences in COD levels were observed among the treated effluents from the three units ($P > 0.05$). The BOD_5/COD ratio, an indicator of organic matter biodegradability, revealed a low ratio for the PME before treatment (15.31:187.73 = 0.081), indicating low biodegradability. Post-treatment, the BOD_5/ COD ratios increased to 1.45 ± 0.54, 1.56 ± 1.03, and 1.24 ± 0.76 for the control, cattail, and mangrove units, respectively. A BOD_5/COD ratio greater than 1 suggests the activity of an aerobic nitrifying bacteria, which consume oxygen to convert ammonia (NH_3-N) into nitrate (NO_3-N). High ammonia levels contained in wastewater can increase oxygen demand, resulting in a higher BOD relative to COD [15].

7) Nitrogen: Nitrogen transformation and treatment efficiency were assessed through two sampling events. The results showed that the system effectively removed nitrogen. The treatment efficiency of TKN was 40 and 85.74% in the control unit, 20 and 85.71% in the cattail unit, and 80% and 85.71% in the mangrove unit. Nitrogen in the effluent was primarily in the form of NH_3–N, with concentrations ranging from 0.4 to 22.8 mg/L (Table 1). Upon entering the constructed wetland unit, NH_3–N was transformed into nitrite (NO_2-N) and subsequently nitrate (NO_3-N), with nitrate concentrations of 9.0 mg/L (Table 2). After treatment in the constructed wetland, nitrogen concentrations decreased significantly to 1.0-4.0 mg/L. Within the wetland, nitrogen transformation occurred simultaneously through nitrification, denitrification, and assimilation by plants and microorganisms [16]. This process resulted in a noticeable reduction in total Kjeldahl nitrogen (TKN) across all three units. Additionally, low TKN levels contained in the effluent reveal that the intermediate nitrification and denitrification products (e.g., NO_2–N) did not accumulate within the system [17]. CWs have demonstrated high nitrogen removal efficiency in various applications, including municipal wastewater, industrial effluents, and agricultural runoff [18].

First-order rate constant

From the experiment, it was observed that the system effectively reduced only color and chemical oxygen demand (COD) from the paper mill effluent (PME). From Table 3, no color removal was shown for cattail unit, only control unit and mangrove unit showed color removal. Thus, the coefficients of the system were specifically analyzed for color (control unit and mangrove unit) and COD using the first-order PFR kinetics equation (2) and first-order CSTR kinetics equation (2) as outlined above.

1) Color: The variation in color over time across all eight experimental runs is illustrated in Figure 4. The concentration-time (or distance-from-inlet) plot demonstrates a gradual decrease in pollutant levels over time in the control and mangrove units. This trend suggests that the reaction kinetics may conform to both Plug Flow Reactor (PFR) and Continuous Stirred Tank Reactor (CSTR) models. The first-order reaction rate constants for color treatment, derived from the PFR and CSTR kinetic equations, are summarized in Table 3.

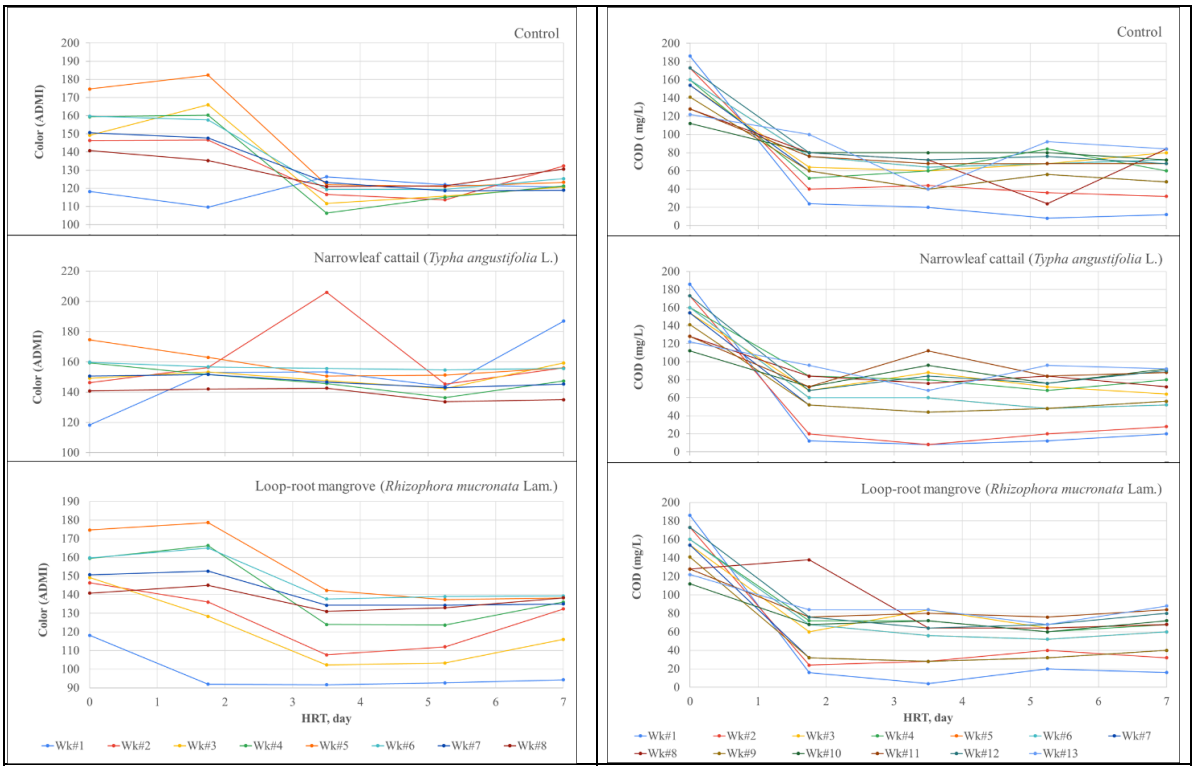

Color | Chemical oxygen demand (COD)

Figure 4 The relationship between color/COD and the hydraulic residence time of water within the system

Table 3 Rate constants for according to the first-order plug-flow kinetics

Parameter		Control	Cattail	Mangrove
Color (ADMI)	Influent (mg/L)	118.2-174.7	118.2-174.7	118.2-174.7
	Effluent (mg/L)	119.0-132.3	145.3-187.0	94.3-139.3
	HRT (days)	7	7	7
	K_{PFR} range (d^{-1})	0.011-0.050	-	0.003-0.036
	K_{PFR} avg (d^{-1})	0.030	-	0.021
	K_{CSTR} range (d^{-1})	0.011-0.059	-	0.003-0.038
	K_{CSTR} avg (d^{-1})	0.035	-	0.023
COD (mg/L)	Influent (mg/L)	112.0-186.0	112.0-186.0	112.0-186.0
	Effluent (mg/L)	12.0-84.0	20.0-92.0	16.00-88.00
	HRT (days)	7	7	7
	K_{PFR} range (d^{-1})	0.053-0.167	0.028-0.319	0.047-0.350
	K_{PFR} avg (d^{-1})	0.140	0.131	0.143
	K_{CSTR} range (d^{-1})	0.038-2.071	0.024-1.186	0.032-1.518
	K_{CSTR} avg (d^{-1})	0.248	0.278	0.291

2) Chemical oxygen demand (COD): The variation in COD over time for all 13 experimental runs is depicted in Figure 4. The concentration-time plot shows a notable reduction in COD at the beginning of the tank, characteristic of the CSTR process. The calculated rate constants are presented in Table 3, with average CSTR first-order rate constants of 0.248 d^{-1} for the control unit, 0.278 d^{-1} for the cattail unit, and 0.291 d^{-1} for the mangrove unit.

For vertical flow constructed wetlands (CWs), reaction rate constants reported in literature exhibit significant variation: total nitrogen removal k = 0.048-0.19 d^{-1}, and BOD_5 removal k = 0.071-6.11 d^{-1}. These fluctuations likely reflect variations in factors such as bed

matrix composition, porosity, and flow rate, which influence the efficiency of individual processes [19].

Conclusions

The system effectively reduced some specific pollutants contained in the factory effluent, specifically targeting color (only for the unit planted with mangrove) and COD for such study units. It's somewhat revealed that the system aiding in breaking down complex substances like lignin and nitrogen into more easily degradable forms, thereby increasing organic matter levels as BOD_5.

Regarding color removal efficiency, the control unit exhibited a range of 0.00-29.39% (16.47 ± 9.86%), the cattail unit showed 0.00-10.69% (3.56 ± 3.90%), and the mangrove unit demonstrated 1.74-22.26% (14.06 ± 6.95%). The control unit and the unit planted with mangrove exhibited better treatment performance than the unit planted with cattail ($P > 0.05$). However, no significant difference in color removal was observed between the control unit and the mangrove unit ($P > 0.05$).

In terms of COD removal efficiency, the control unit ranged from 31.1-93.5% (56.9 ± 18.31%), the cattail unit ranged from 17.9-89.2% (54.3 ± 21.39%), and the mangrove unit ranged from 1.7-22.3% (14.1 ± 6.95%). Both the control and mangrove units demonstrated somewhat higher performance compared to the cattail unit, with statistical significance ($P > 0.05$).

For the first-order rate constant calculation, it was found that.

1) Color: The concentration-time plot demonstrates a gradual decrease in pollutant levels over time, suggesting that the reaction kinetics may conform to both Plug Flow Reactor (PFR) and Continuous Stirred Tank Reactor (CSTR) models. Since no color removal was observed in the cattail unit, reaction rate constants were calculated exclusively for the control and mangrove units. For the mangrove unit, the first-order reaction rate constants were 0.021 d^{-1} for the PFR model and 0.023 d^{-1} for the CSTR model. For the control unit, the first-order reaction rate constants were 0.030 d^{-1} for the PFR model and 0.035 d^{-1} for the CSTR model.

2) Chemical Oxygen Demand (COD): The CSTR first-order reaction rate constants for the control unit were 0.140 d^{-1}, for the cattail unit was 0.131 d^{-1}, and for the mangrove unit was 0.143 d^{-1}. In terms of the CSTR first-order reaction rate constants derived by COD removal. For any units the CSTR first-order reaction rate constants are similar. Constructed wetland, therefore, exhibited significant COD removal and some color removal in the mangrove unit.

Acknowledgements

This work was supported by Suranaree University of Technology, Thailand Science Research and Innovation (TSRI), and National Science, Research and Innovation Fund (NSRF) (Code number 179348).

References

[1] Stefanakis AI. Introduction to constructed wetland technology. In: John Wiley & Sons; 2018; 1-21.

[2] Toczyłowska-Mamińska R. Limits and perspectives of pulp and paper industry wastewater treatment–A review. Renewable and Sustainable Energy Reviews. 2017; 78: 764-772.

[3] Wu S, Wallace S, Brix H, Kuschk P, Kirui WK, Masi F, Dong R. Treatment of industrial effluents in constructed wetlands: challenges, operational strategies and overall performance. Environmental Pollution. 2015; 201: 107-120.

[4] Abira MA, Van Bruggen JJA, Denny P. Potential of a tropical subsurface constructed wetland to remove phenol from pre-treated pulp and papermill wastewater. Water Science and Technology. 2005; 51(9): 173-176.

[5] Rani N, Singh B, Kumar V. Feasibility of Typha and Canna for pulp and paper mill wastewater treatment through small wetlands. International Journal of Environmental Sciences. 2015; 6(3): 388-395.

[6] Gaballah MS, Abdelwahab O, Barakat KM, Aboagye D. A novel horizontal subsurface flow constructed wetland planted with Typha angustifolia for treatment of polluted water. Environmental Science and Pollution Research. 2020; 27: 28449-28462.

[7] Jesus JM, Calheiros CSC, Castro PML, Borges MT. Feasibility of Typha latifolia for high salinity effluent treatment in constructed wetlands for integration in resource management systems. International Journal of Phytoremediation. 2014; 16(4): 334-346.
[8] Ahuja S. Comprehensive water quality and purification. Elsevier; 2013.
[9] Weerakoon GMPR, Jinadasa KBSN, Manatunge J, Wijesiri B, Goonetilleke A. Kinetic modelling and performance evaluation of vertical subsurface flow constructed wetlands in tropics. Journal of Water Process Engineering. 2020; 38: 101539.
[10] Tchobanoglous G, Crites R, Gearheart B, Reed W. A review of treatment kinetics for constructed wetlands. In: Disinfection and Reuse Symposium 2000. 2000; 723-734.
[11] Samudro G, Mangkoedihardjo S. Review on BOD, COD and BOD/COD ratio: A triangle zone for toxic, biodegradable and stable levels. International Journal of Academic Research. 2010; 2(4).
[12] Yusoff MFM, Rozaimah SAS, Hassimi AH, Hawati J, Habibah A. Performance of continuous pilot subsurface constructed wetland using Scirpus grossus for removal of COD, colour and suspended solid in recycled pulp and paper effluent. Environmental Technology & Innovation. 2019; 13: 346-352.
[13] Thunga M, Chen K, Grewell D, Kessler MR. Bio-renewable precursor fibers from lignin/polylactide blends for conversion to carbon fibers. Carbon. 2014; 68: 159-166.
[14] Md Yusoff MF, Abdullah SRS, Hasan HA. Performance of continuous pilot subsurface constructed wetland using Scirpus grossus for removal of COD, colour and suspended solid in recycled pulp and paper effluent. Environ Technol Innov. 2019. doi:10.1016/j.eti.2018.12.008.
[15] Parlakidis P, Mavropoulos T, Vryzas Z, Gikas GD. Fluopyram removal from agricultural equipment rinsing water using HSF pilot-scale constructed wetlands. Environmental Science and Pollution Research. 2021; 1-13.
[16] Tanner CC. Nitrogen removal processes in constructed wetlands. In: Wetlands ecosystems in Asia. Elsevier; 2004. 331-346.
[17] Chen TY, Kao CM, Yeh TY, Chien HY, Chao AC. Application of a constructed wetland for industrial wastewater treatment: A pilot-scale study. Chemosphere. 2006; 64(3): 497-502.
[18] Vymazal J, Zhao Y, Mander Ü. Recent research challenges in constructed wetlands for wastewater treatment: A review. Ecological Engineering. 2021; 169: 106318.
[19] Gajewska M, Skrzypiec K, Jóźwiakowski K, Mucha Z, Wójcik W, Karczmarczyk A, Bugajski P. Kinetics of pollutants removal in vertical and horizontal flow constructed wetlands in temperate climate. Science of the Total Environment. 2020; 718: 137371.

Thai Environmental Engineering Journal

Aims and Scope

Thai Environmental Engineering Journal is published 3 times a year by Environmental Engineering Association of Thailand in aims of provide an interdisciplinary platform for the disseminating recent research work in Environmental field. The journal's scope includes:

- Treatment Processes for Water and Wastewater
- Air Pollution and Control
- Solids and Hazardous Wastes Management
- Site Remediation Technology
- Water Resource Management; Surface water and Groundwater
- Environmental Management Protection and Conservation
- Impact Assessment of Pollution and Pollutants
- All areas of Environmental Engineering and Sciences

Frequency; 3 issues per year, every four months at April, August and December

Information for Authors

Manuscript submitted for publication should be of high academic merit and have never before, in whole or in part, been published elsewhere and will not be published elsewhere, except in abstract form. Manuscripts, parts of which have been previously published in conference proceeding, may be accepted if they contain additional material not previously published and not currently under consideration for publication elsewhere.

Submission of Manuscripts

All manuscripts should be submitted in https://www.tci-thaijo.org/index.php/teej/index

Manuscript Format and Style

Text format

Manuscript should be prepared using a text processing software such as Microsoft Word for windows. A4 size paper is conventionally accepted. Margins set up (in Page set up Menu) are outlined as follow.

Top Margin 3.0 cm., Bottom Margin 3.0 cm.
Left margin 2.5 cm., Right Margin 2.5 cm.

Title, author co-authors, address of correspondence and abstract are included in the first section while the remainder of paper is to appear in the second section. The total pages including figures, tables and references should not exceed 10 pages.

Font, font size & typeface

Times New Roman font type is required for Thai text and English text. Font size [Pica] for various text function are tabulated as follow.

Text functions	Font = Times New Roman	
	Pica Size**	Typeface
Title [English]	16 [CT]	Bold
Author & Co-authors	11 [CT]	Bold
Address of correspondence	11 [CT]	Normal
Abstract heading	12 [LRJ]	Bold
Abstract & Main Texts	11 [LJ]	Normal
Section Heading & Number*	12 [LJ]	Bold
Subsection Heading & Number	11 [LJ]	Bold

* Including "Abstract" "Acknowledgement" and "References"

** CT = Centre Text, LJ = Left Justified, LRJ = Left & Right Justified

Title

All titles of manuscript should be short and precise; long title should be condensed whenever possible (not more than 42 characters). Title should be printed with every first letter of every word capitalized, excluding prepositions and articles. Directly below the title, author should print their full names (first name then family name), address and institution. E-mail of corresponding author and between 3-5 key words should also be provided.

Abstract

Abstract should be provided on separate sheets and be not more than 300 words. International contributor who are unable to provide an abstract in Thai may submit an English abstract alone.

Style Guidelines

Units of measurement should be indicated in SI units throughout.

Tables

Tables and figures should be numbered with Arabic numerals, in order in which they are cited in the text. The table's titular heading should concisely detail the content of the table and include units of measure for all numerical data.

Format of Research Paper

The format of research paper is listed as follows:

1) Title
2) Author
3) Abstract
4) Introduction
5) Materials and Methods
6) Results and Discussion
7) Conclusions
8) References

References

The references section at the end of the manuscript should list all and only the references cited in the text in numberical order, with references given in Thai first and those in English following. In this section, the names of all authors should be provided if more than six, or the first three followed by *et. al.*

Reference to a journal article:

List all authors when six or fewer; when seven or more list only the first three (3) and add *et. al.* Titles of articles from academic journals should be listed in full and begin with a capital letter.

[1] Inthorn, D., Sidtitoon, N., Silapanuntakul, S. and Incharoensakdi, A. 2002. Sorption of mercury, cadmium and lead in aqueous solution by the use of microalgae. Science Asia. 28(3): 253-261.

Reference to article or abstract in a conference proceedings:

[1] Inthorn, D., Singhakarn, C. and Khan, E. Decolorization of reactive dyes by pre-treated Flute reed (phargmites karka (Retz)). At 34th Mid-Atlantic Industrial & Hazardous Conference, Annual Mid Atlantic Industrial and Hazardous Waste Conference at Rugers University, New Jersey, USA on September 20-21, 2002.

Reference to a book:

[1] Polprasert, C. 1996. Organic Waste Recycles. John Wiley & Sons Inc., New York.

Reference to article in a conference proceedings:

[1] Inthorn, D. Heavy metal removal. In: Kojima, H. and Lee, Y.K. Photosynthetic Microorganisms in Environmental Biotechnology, Springer-Verlag, 2001; 111-135.

Reference to an electronic data source:

Use the above format and supply the complete URL as well as the access date.

Subscription Form
Thai Environmental Engineering Journal

Date_____

Name_____

Address_____

_____

_____

_____

_____

Tel:_____ Fax:_____E-mail:_____

A subscription to the Thai Environmental Engineering Journal is request for_____year
(1,000 Baht/year for 3 Volume)

Signature_____

(_____)

Payment by "Environmental Engineering Association of Thailand"

- ❍ Bank Transfer: Savings Account No. 053-1-24040-3, Bank of Ayudhya Plc., Klong Prapa Branch
- ❍ Bank Transfer: Savings Account No. 056-2-32298-0, Siam Commercial Bank Plc., Aree Sampan Branch

Environmental Engineering Association of Thailand
122/4 Soi Rawadee, Rama VI Rd., Phayathai,
Phayathai, Bangkok 10400
Tel: +66 (0) 2617-1530-1 Fax: +66 (0) 2279-9720
E-mail: teej@eeat.or.th Website: http://www.eeat.or.th

THAI
ENVIRONMENTAL ENGINEERING JOURNAL
Environmental Engineering Association of Thailand (EEAT)

ISSN (PRINT) : 1686 - 2961
ISSN (ONLINE) : 2673 - 0359

Vol. 38 No. 3 September – December 2024